Probing the energy production of Galaxies in the Infrared

Βασίλης Χαρμανδάρης
(Πανεπιστήμιο Κρήτης & Ίδρυμα Τεχνολογίας και Έρευνας)

Several Collaborators
(U)LIRG work: Lee Armus (Caltech)
Seyfert work: Yanling Wu (Cornell/Caltech)

Outline of the talk

- Topics:
  - Background on the Spectral Energy Distribution (SED) of a galaxy
  - Major sources of energy: stars and accreting supermassive black holes
  - The role of dust
  - Polycyclic Aromatic Hydrocarbons and star formation
  - Current IR astronomical facilities
  - Mid-IR spectroscopy of (Ultra)Luminous Infrared Galaxy
  - Present some IR diagnostics for the presence of an active nucleus
  - Application to the 12micron Seyfert Sample

Measuring the EM Spectrum

Basic observed quantity is the flux (f):

- *Flux is the energy incident per unit time within a defined EM band per unit surface area (cross section of our detector)*
- *Usually quote "Bolometric" flux, implying all frequencies =>IMPOSSIBLE TO MEASURE*
- *Practically we measure incident flux within finite bands, engulfing typically 1-20% of the total flux. (ie Flux in the U,B,V,K, filters or "IR" and "soft/hard X-ray" fluxes)*
- *We also quote "Monochromatic" fluxes : within infinitesimal intervals*

  f_ν : flux within the frequency interval v and v+dv

  f_λ : flux within the wavelength interval λ and λ+dλ
- *Since $f_\nu\, d\nu = f_\lambda\, d\lambda$ and $\lambda\, \nu = c$, then $\nu f_\nu = \lambda f_\lambda$*
- *Typical Units*

  $[f_\nu]$ = erg s^{-1} cm^{-2} Hz^{-1} ; $[f_\lambda]$ = erg s^{-1} cm^{-2} $Angstrom^{-1}$

  1 Jy = 10^{-26} Wm^{-2} Hz^{-1} = 10^{-23} erg s^{-1} cm^{-2} Hz^{-1}

If we know the distance (d) to the source we can estimate the Luminosity

$L = 4\pi d^2 * f$ (Power)

Units: W or erg s^{-1} or Solar Bolometric luminosities Lsun=3.9 $x10^{33}$ erg s^{-1}

NGC 6240: IR luminous & interacting system

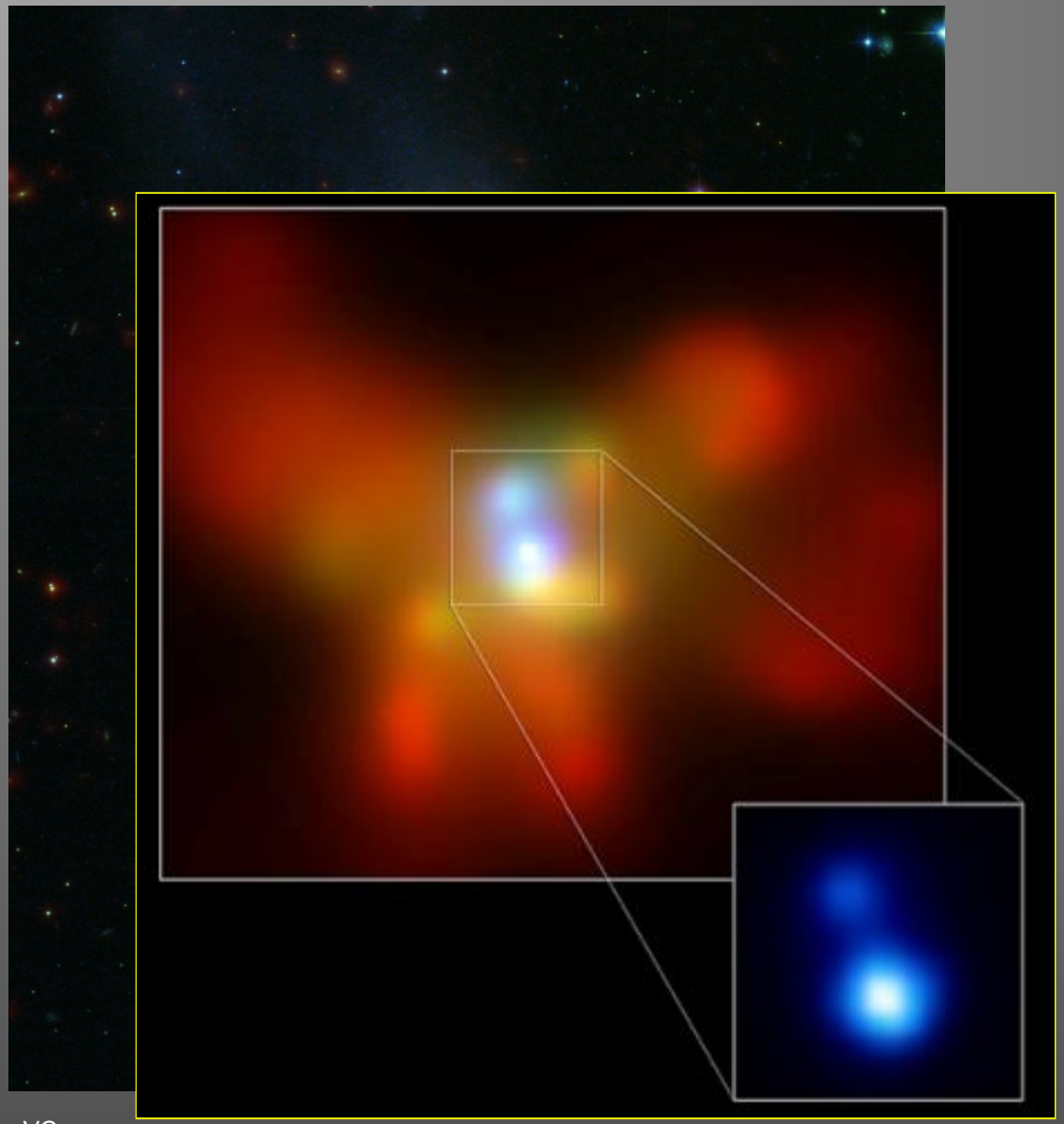

L(IR)~ 6×10^{11} Lsun

Two nuclei harboring accreting supermassive black holes

The SED of NGC 6240

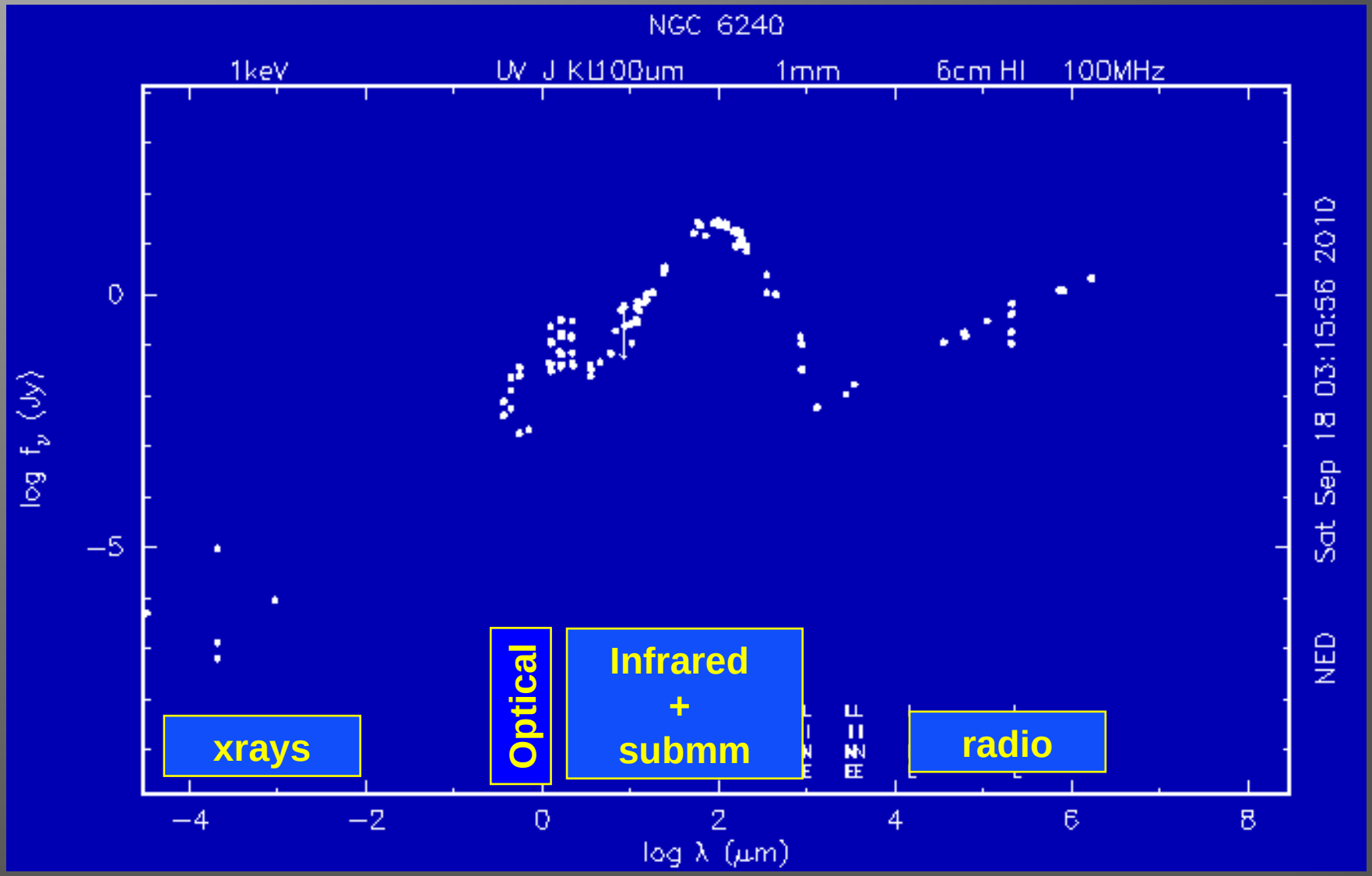

Energy / (time * freq * surface)

wavelength

The SED of NGC 6240

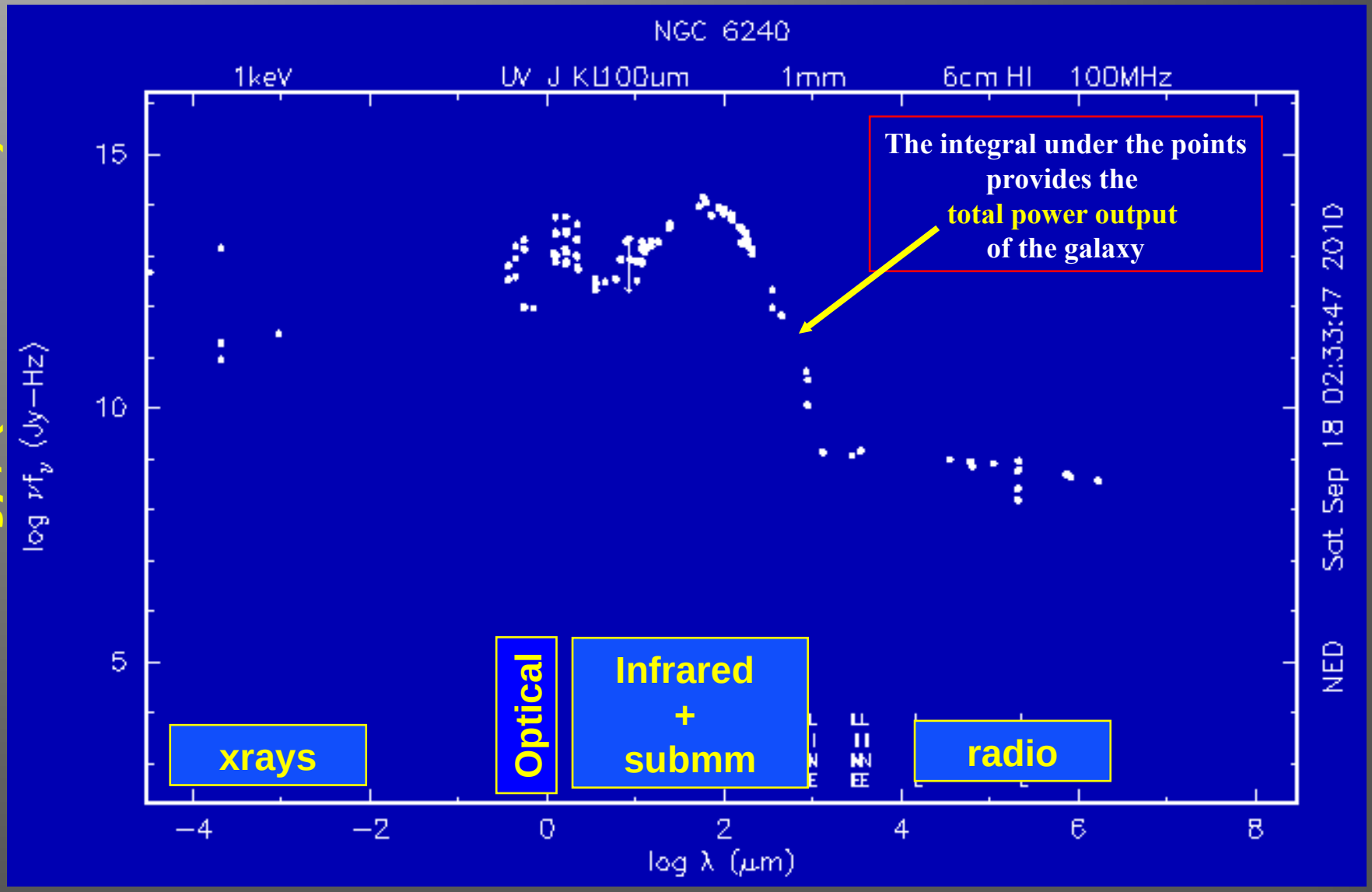

Energy / (time * surface)

wavelength

Sources of Observed EM Emission

- There are many distinct types of astrophysical sources which produce photons: stars, AGN, HII regions, jets, hot intercluster gas, shocked gas etc.

- These produce photons with various rates as a function of wavelength/ frequency due to the different physical mechanisms taking place at the same type on the source.

- Those mechanisms are usually “broad-band” emit across large ranges in wavelengths (continuum emission), but also emit in specific wavelengths (feature emission: ie atomic, molecular lines)

- We can also distinguish the mechanisms in “thermal” and “non-thermal”
  - *Thermal: Emitters/absorbers are close to Boltzmann distribution (Thermal equilibrium)*

    In most cases the radiation field in close to the Planck function (black body)
  - *Non-thermal: Emitters/absorbers/radiation far from thermal equilibrium*

    Examples are synchrotron jets where electrons with non-Maxwellian energy distribution move in magnetic fields and radiate ($f_\nu \sim \nu^{-\alpha}$, where: $\alpha \sim 0.7$)

Compare Star and AGN Structure

Structure of Stars

- Dense spheres r ~ $10^{11\text{-}13}$ cm
- Stars are dynamically stable, apart from convection and surface phenomena, throughout most of their lifetimes
- Isotropic radiators.
- Nuclear reactions maintain high-temperature (>10^7 K) core.
- X-ray and gamma-ray radiation transferred slowly through high optical depth envelope. Degraded to UV, Optical near-IR band.
- Observed radiation escapes from a very thin (300 km in Sun) layer = "photosphere"

  (NB: photospheres have 10^{17} particles/cm^3 so they are DENSE by the standards of AGN emitting regions
- Subsidiary processes (e.g. driven by magnetic fields) radiate small amounts in non-UV, optical, near-IR bands.

Credit: B. O'Connell

Compare Star and AGN Structure

Structure of Active Galactic Nuclei (AGN)

- Supermassive black hole ($M \sim 10^{7\text{-}9}\ M_{sun}$; $R_{Schw} \sim 3 \times 10^{13}\ M_8$ cm) at center of an accretion disk with $r > 10^{16}$ cm.
- Accretion disk is fed by infalling material; matter is continuously transported through a disk
- Dissipation and magnetic processes near center of disk generate relativistic particles.These can generate relativistic jets.
- Observed radiation emerges from a large volume with non uniform properties
- Relativistic jets and disk confinement produce anisotropic radiation.
- Relativistic particles produce broad-band non-thermal synchrotron radiation, directly observed at radio wavelengths.
- Direct thermal radiation from denser, hot inner disk (UV).
- Photon boosting of low-energy photons by inverse Compton scattering to UV/X-ray bands. (Compton boost: $v_2 \sim v_1\ \gamma^2$)
- Hard radiation field produces strong ionization of gas in a large, low-density volume around disk, ===> UV, Optical , near-IR, X-ray emission lines.
- Strong heating of surrounding dust grains ===> IR continuum & emission lines (3-500microns). (But grains sublimate=vaporized near center.)
- Star-formation regions often associated with AGN in disk galaxies

An AGN Schematic

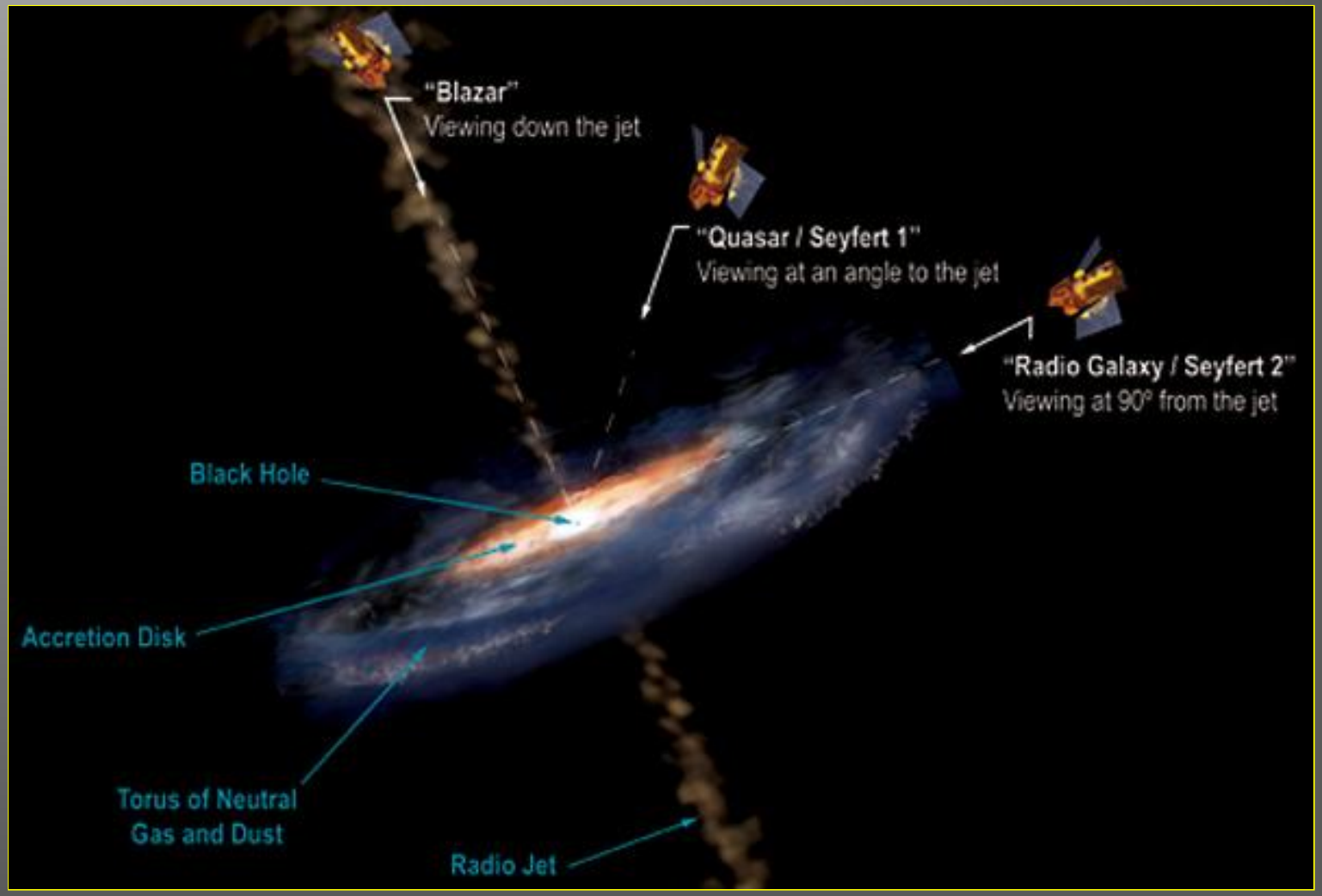

Compare Star and AGN Continuum Emission

Continuum Emission of Stars

- Primary component is UV, Optical, near-IR radiation from photosphere
- Thermal source; emergent spectrum ~Planck function
- Small spread of T around characteristic effective T_e of photosphere, approximately from where $\tau \sim 1$ at any wavelength
- Peak emission defined by Wien's law at ~ (2900 / T) microns if T in Kelvin
- Photospheric temperatures 1000-100000 K.
- Strong time variation only in minority of cases
- Strong concentration to UV Optical, near-IR, with rise $\nu f_\nu \sim \nu^3$, to peak, then dropoff.
- Spectral slope at higher ν allows estimate of mean T_e.
- Major absorption discontinuities from ionization edges of abundant ions (e.g. H: Lyman edge 912 A, Balmer edge 3646 A).
- Low level radiation in other bands from high temperature corona, synchrotron radiation, etc.

Compare Star and AGN Continuum Emission

Continuum Emission of AGN

- Primary component is very broad-band, nonthermal radiation extending from radio to X-rays
- Shape: no simple parameterization.
- Thermal components in IR (dust grains) & UV ("UV bump" from inner accretion disk).
- Continuum spectrum depends on viewing angle because of thick obscuring tori
- Strong time variation common

Compare Star and AGN Line Features

Line Features of Stars

- Complex, narrow, absorption lines
- Produced by transitions in those atoms, ions, and molecules which are prevalent at characteristic T_e and pressure.
- Originates from thin layers of cooler gas projected against higher T continuum of inner photosphere.
- Doppler widths small (thermal), ~ few km s^{-1}
- Line spectrum reflects physical state (composition, temperature, pressure) of photosphere
- Lines and local continuum usually coupled (imply ~ same T)
- Since nearly all features are due to electronic transitions of low A atoms (A= number of protons in the nucleus: H, He, O, C,) the energies of the lines involved are in the “eV” range which corresponds to photons in the optical/UV range.

Compare Star and AGN Line Features

Line Features of AGN

- Lines in emission since generally not viewed against continuum source.
- Wide range of ionizations (e.g. neutral to Fe XIV)
- Wide range of Doppler widths in different galaxies, to $>10^4$ km s^{-1}
- Lines and local continuum decoupled since originate in different volumes
- Doppler widths reflect kinematic motions of gas clouds
- "Broad" lines from r< 1 pc
- "Narrow" lines to r > 100 pc from the central black hole
- Line spectrum depends on viewing angle (inner regions concealed by thick tori, dust clouds). Polarization.
- Due to high energy of the ionizing source nearly some features are due to electronic

The emission of stars change with time

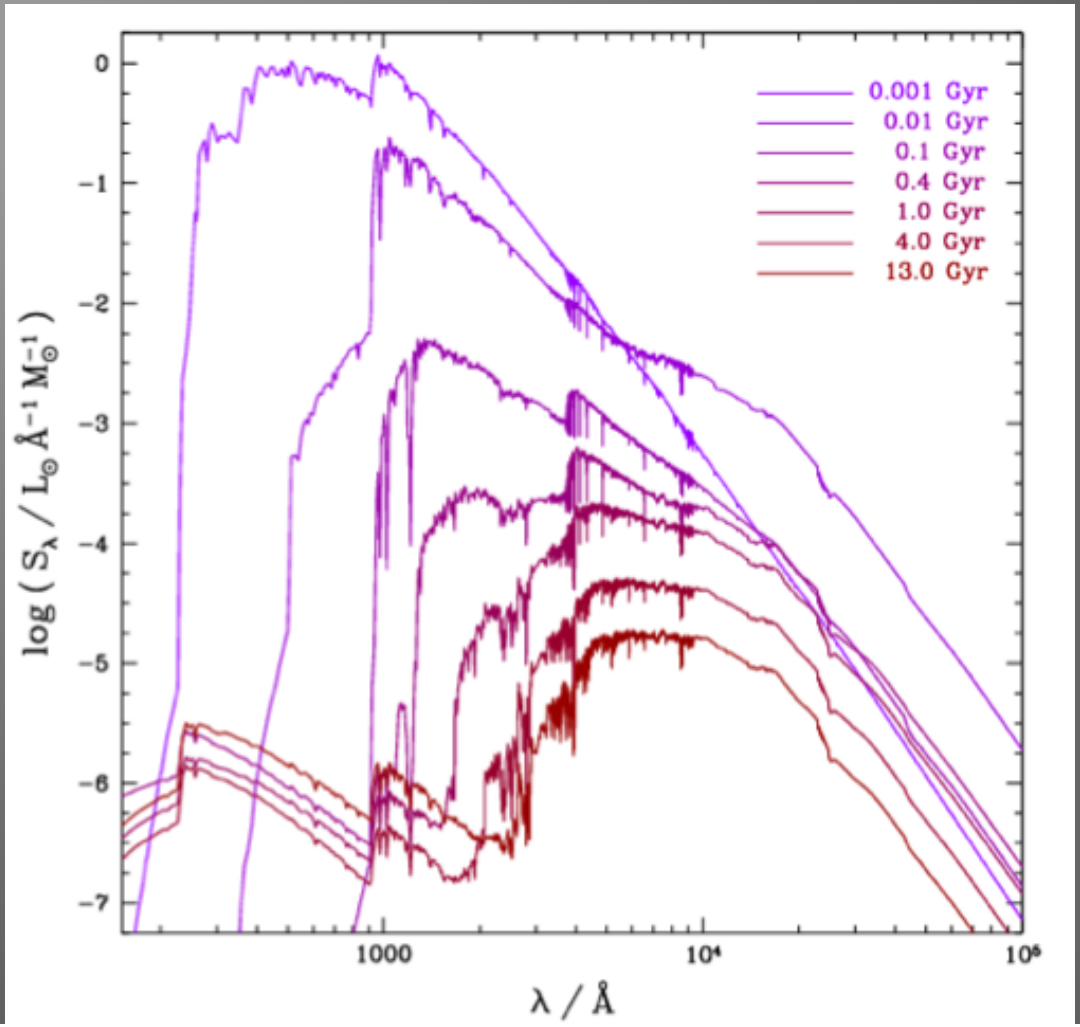

da Cunha 2008

Figure 1.7: Spectral evolution of a simple stellar population with solar metallicity and with the distribution of stellar masses following a Chabrier (2003) IMF, computed using the latest version of Bruzual & Charlot (2003) models, with ages indicated on the top right corner. Figure adapted from Bruzual & Charlot (2003).

Stellar spectrum of galaxies

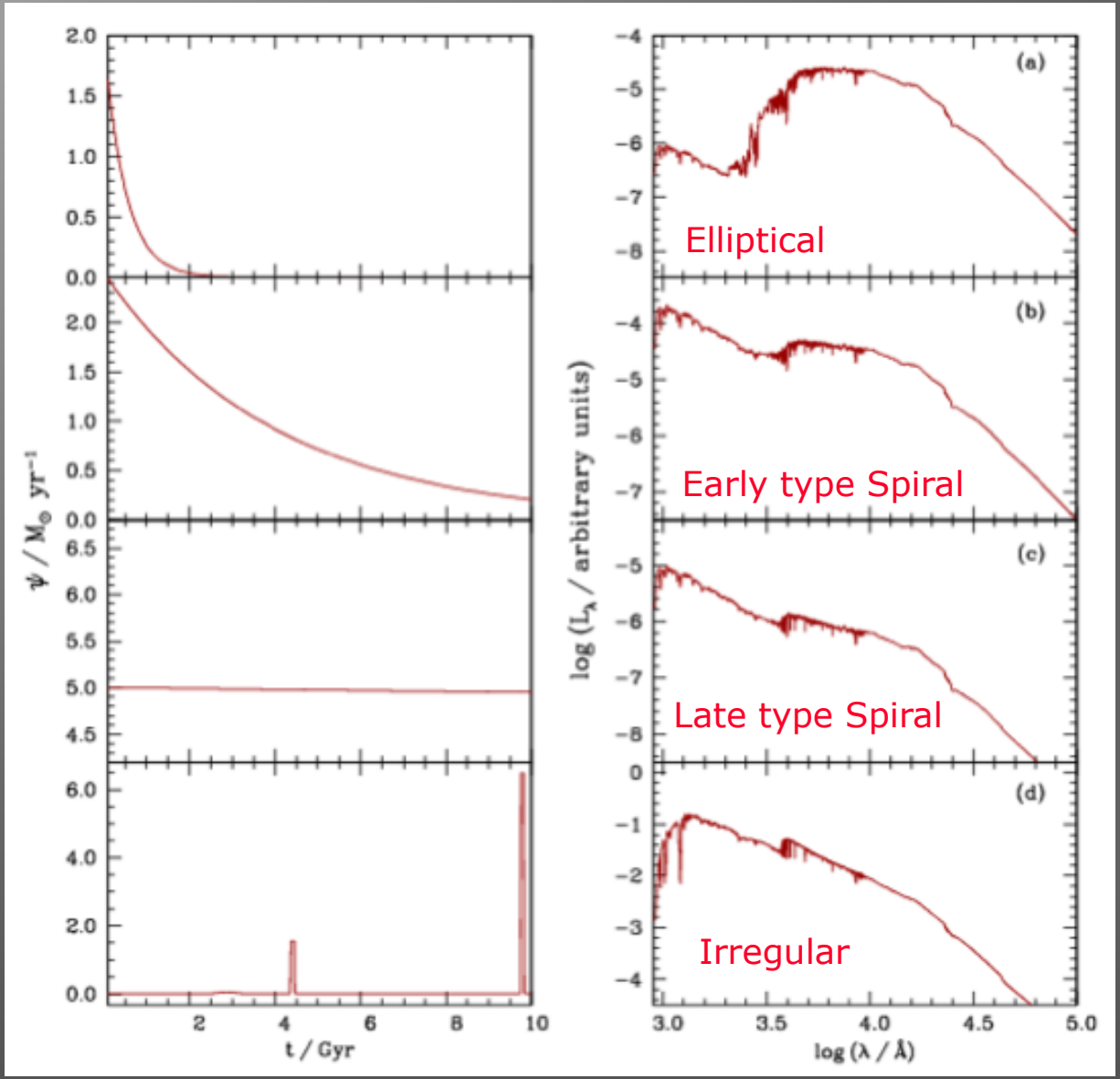

da Cunha 2008

The Role of Dust

- Dust is produced during the late stages of stellar evolution. It is directly coupled to regions star formation and regions of high (molecular) gas content such as galactic nuclei.
- Dust mass is typically 1% of the total atomic and molecular gas mass.
- The dust is responsible for wavelength selective absorption of the incident radiation and remission at longer wavelengths. This is also known as “reddening” and it is quantified by the so called “extinction curve” (talk by M. Xilouris)

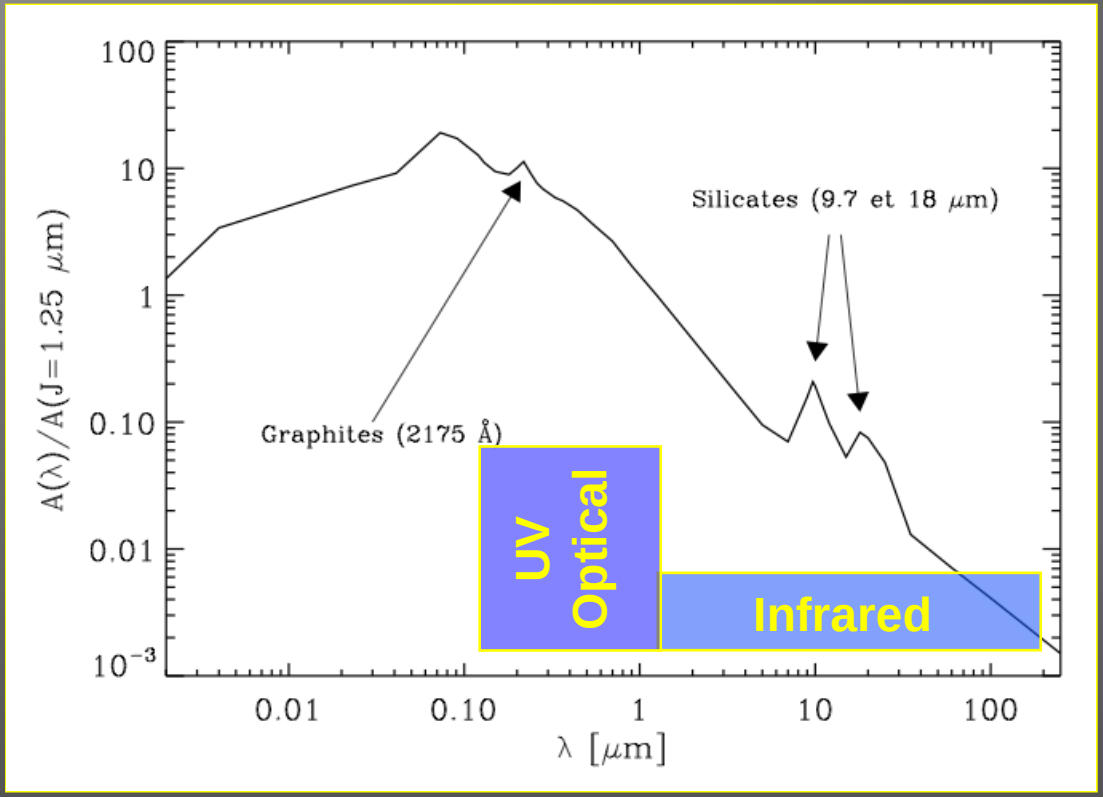

Dust - Types

Dust grains range in size from a few hundred Å to a few μ m. They are composed mainly of elements such as carbon and silicate compounds, and various kinds of ices.

"classical" dust grains → 0.1 μ m in size, containing ≥ 10000 atoms
responsible for the FIR, sub-mm emission

very small grains → containing ≤ 100 atoms (less than10nm in size)
responsible for a rising continuum ~10μ m

PAHs (Polycyclic Aromatic Hydrocarbons) → Groups of benzene rings contain N ~ 50 atoms trace photodissociation regions.

Due to the size distribution of grains & variations in the underlying radiation field the dust temperature varies (cold, warm, hot dust)

Spectra of different dust components are fitted by modified Planck curves

$$I_\nu \propto \varepsilon_\nu B_\nu (T)$$

Power-law emissivity: $\varepsilon_\nu \propto \nu^{\beta}$ (β~1-2: is the emissivity index see Dale et al, ApJ, 2001)

Really hot dust (~200-1500K) in a equilibrium is observed via a near/mid-IR "bump" close to tori of AGNs.

A day in the life of a dust grain

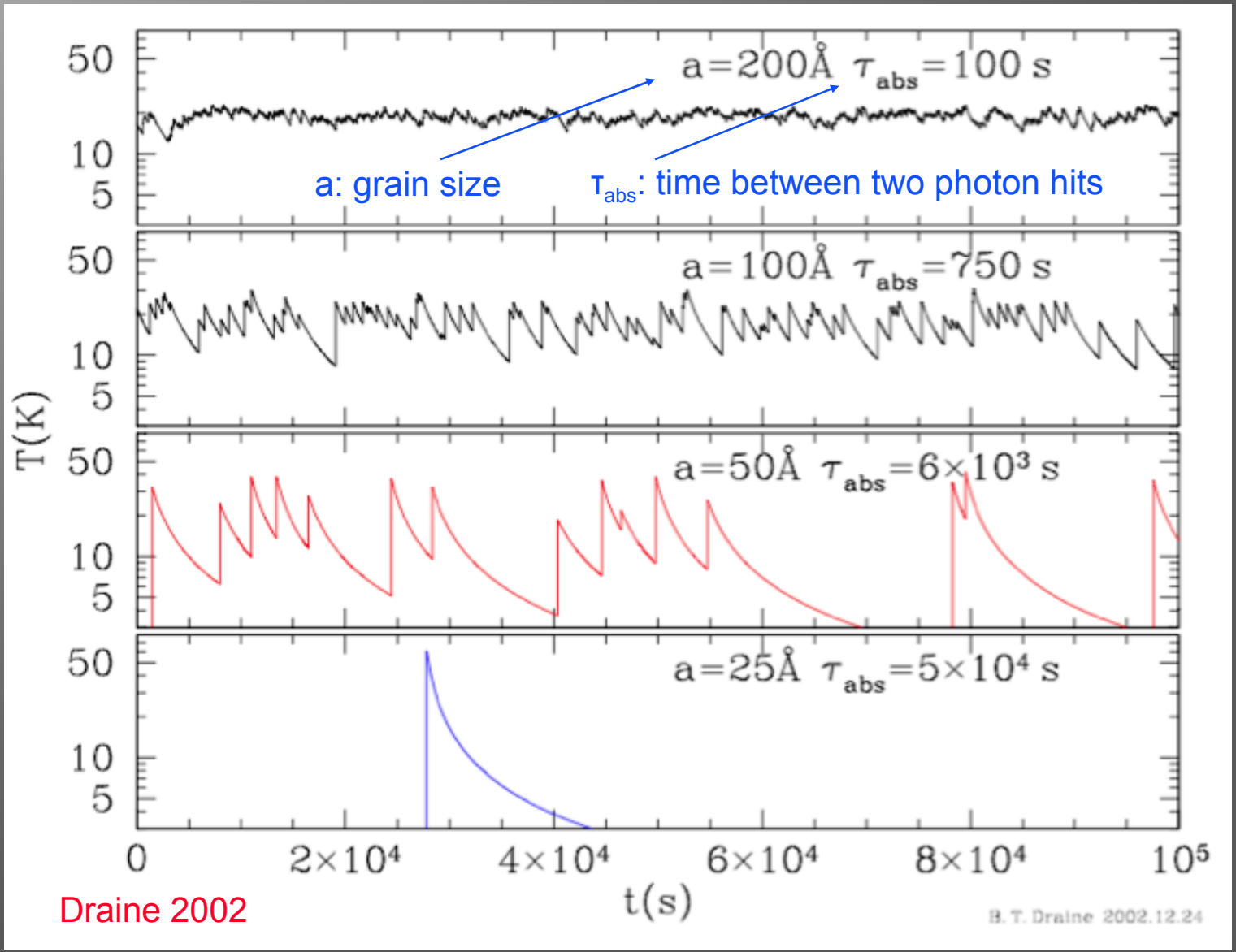

Draine 2002

NGC 4038/39: The Antennae

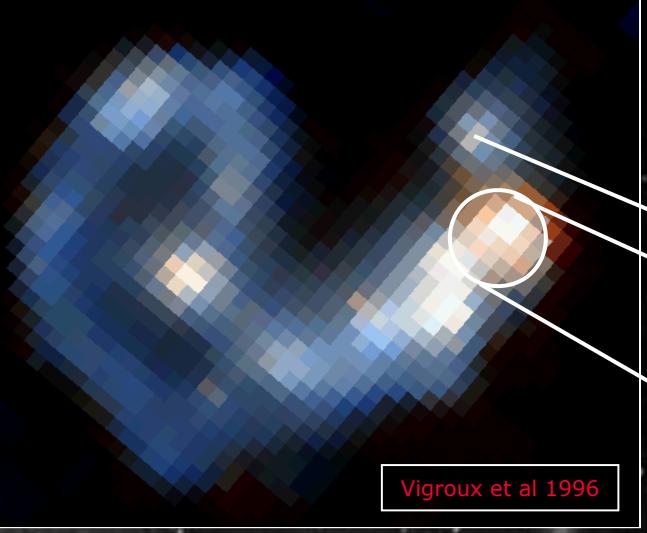

Whitmore & Schweizer, AJ,1995

UV/mid-IR comparison of two LIRGs

Images: HST/STIS UV - Contours: ISO/CAM 7um

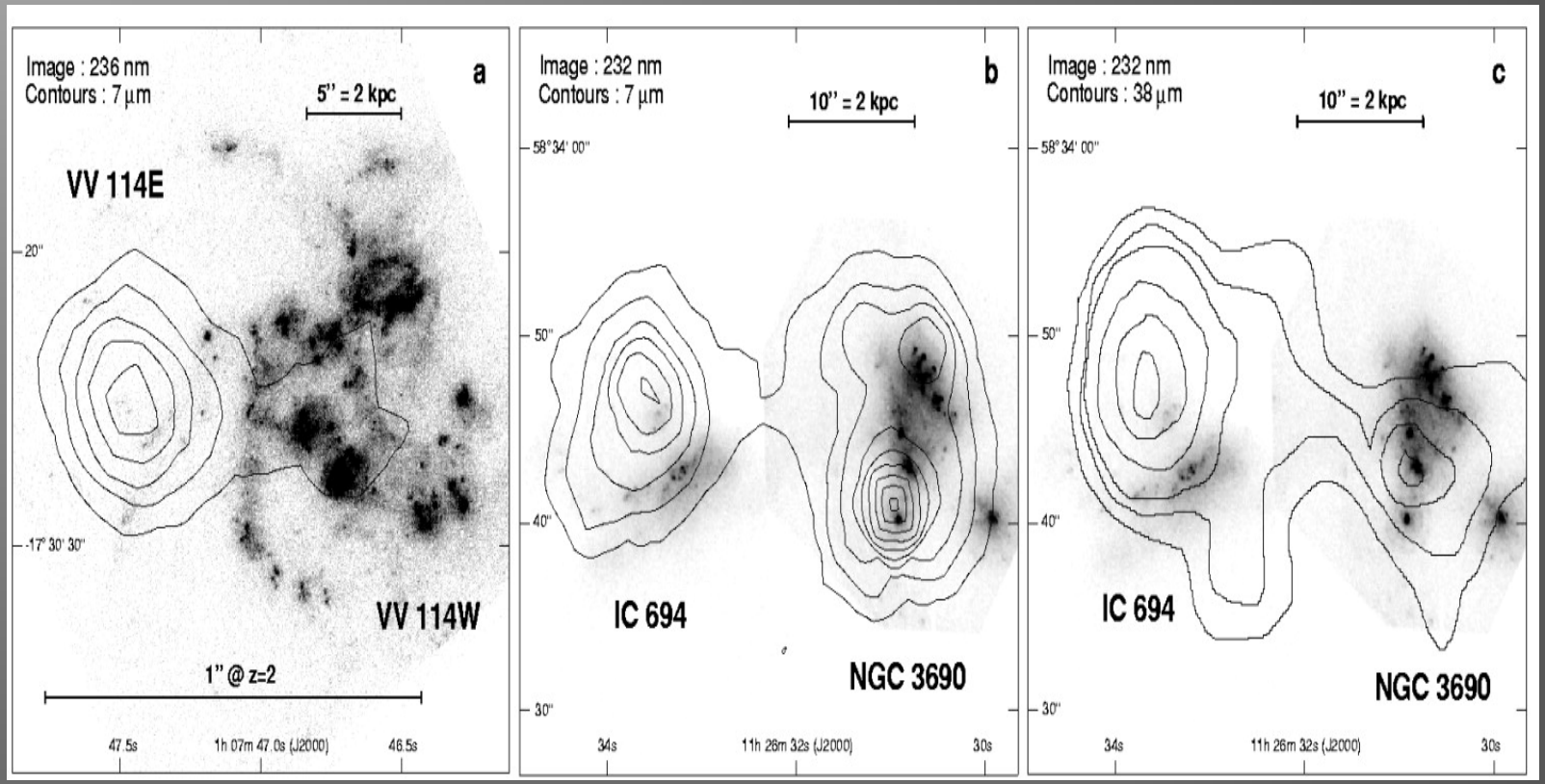

7μm/UV ~ 800:10:35 **7μm/UV ~ 330:160:190**

The spatial resolution of ground & Spitzer/MIPS24 surveys of LIRGs at z~2 will result in blending of the emission from the unresolved interacting components leading to a systematic underestimation of their dust content.

UV data: Goldader et al. 2002
Charmandaris et, al 2004

NGC4038/39 – Mid-IR spectroscopy

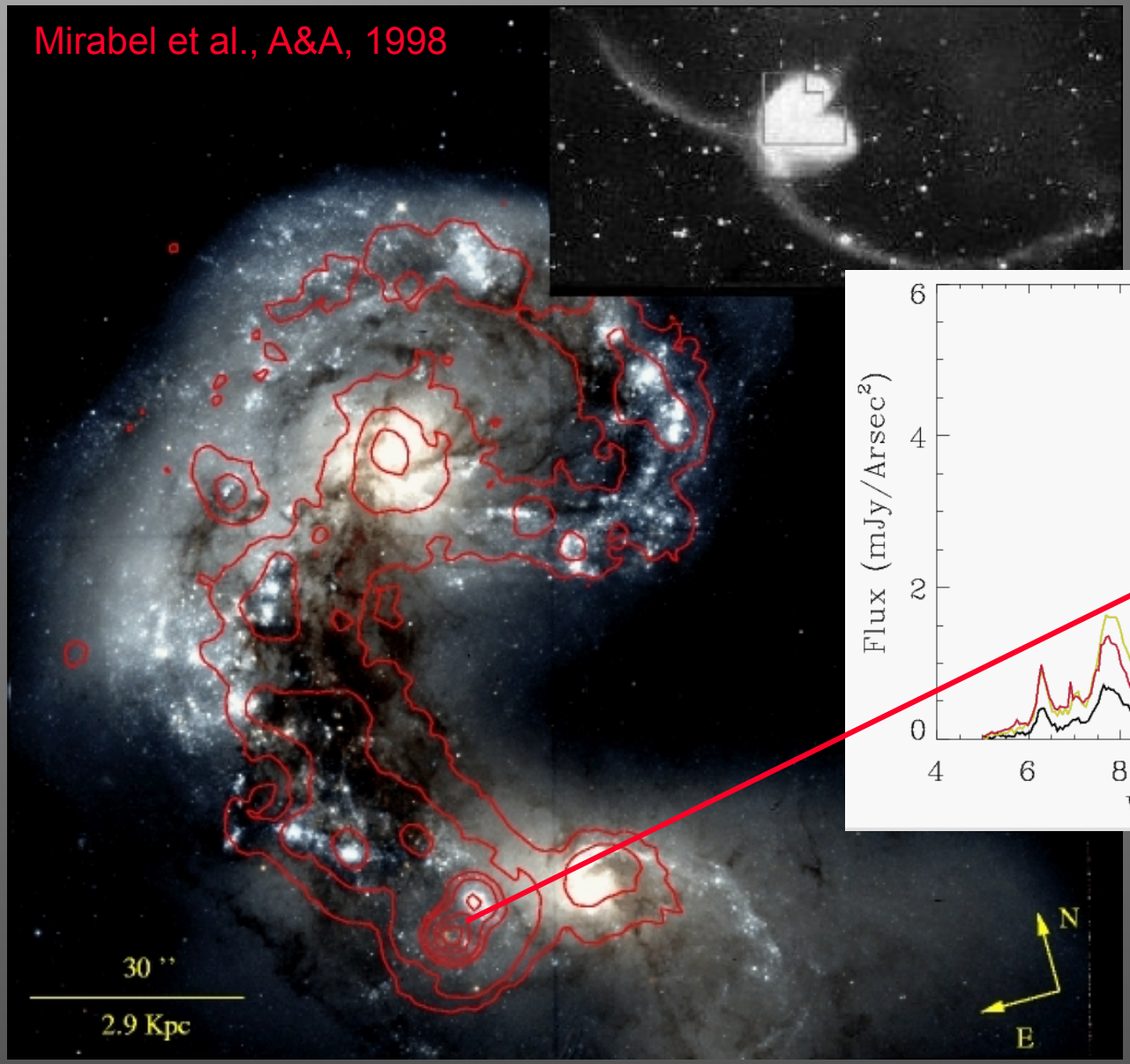

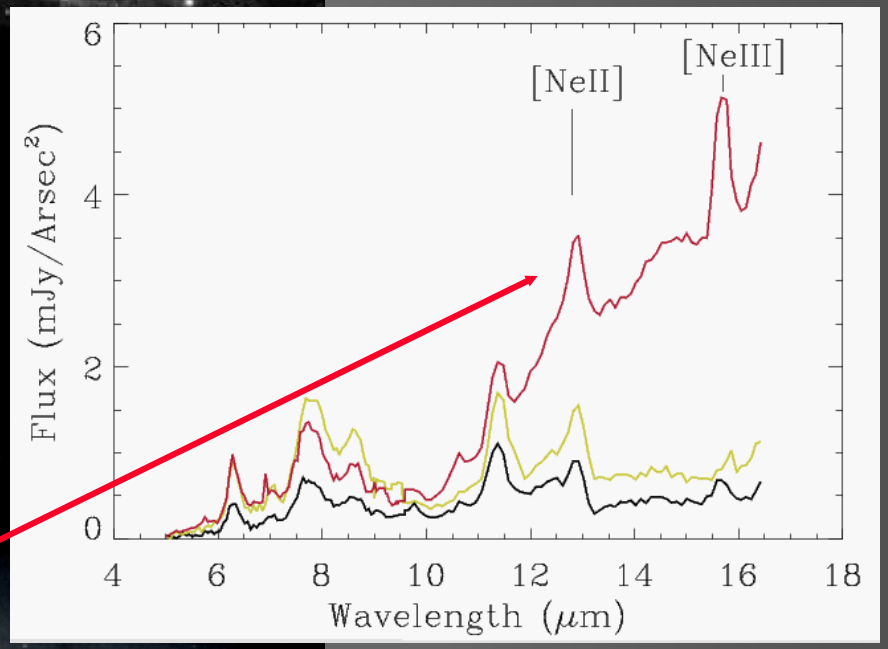

L(IR)~5x10¹⁰ Lsun

SED Decomposition of a Galaxy

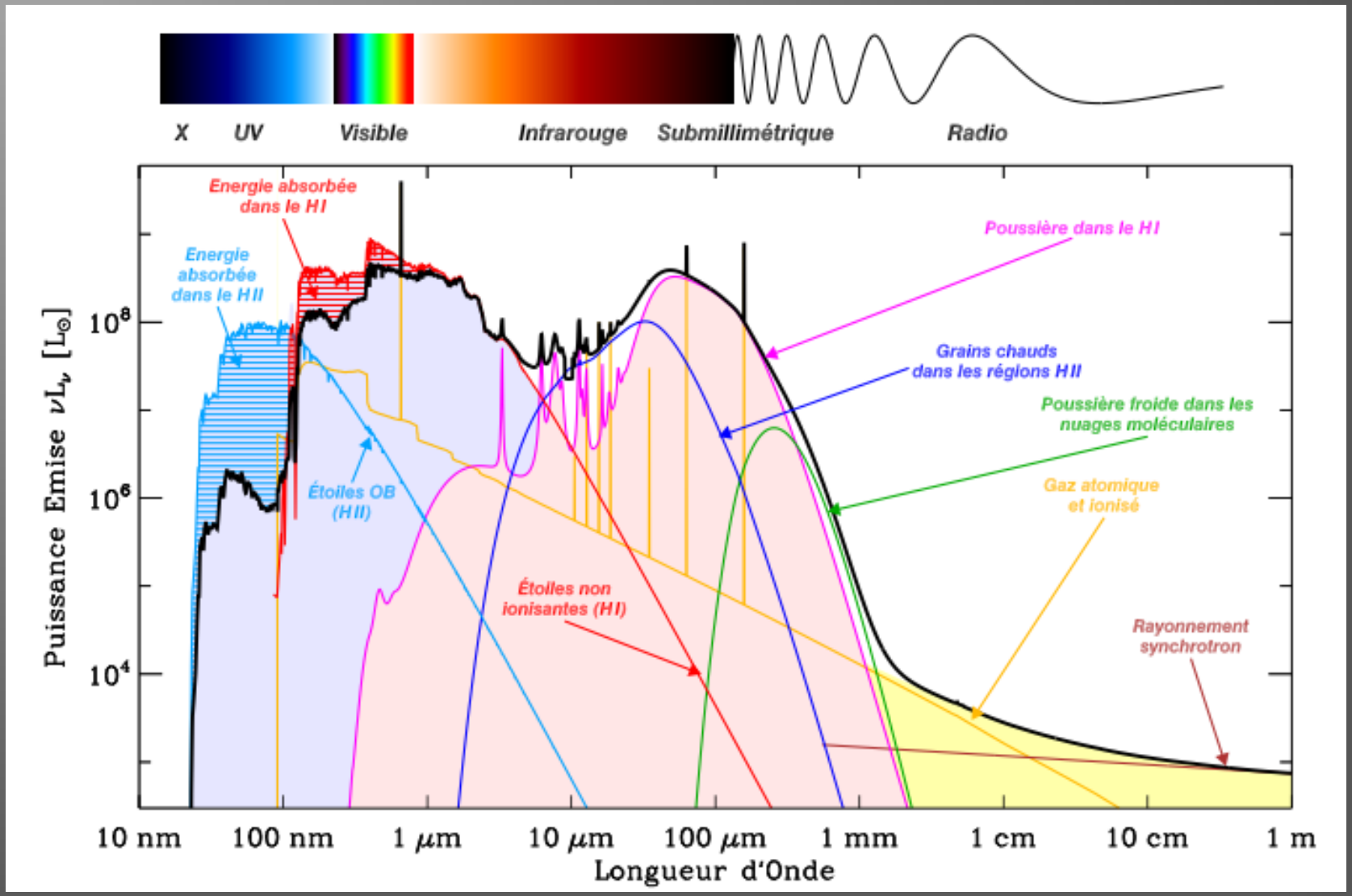

Credit: F. Galliano

History of Star-Formation in the Universe

- Optical surveys indicate that the mean SFR in the Universe was much greater at z > 1 (e.g. Madau et al. 1996)
- COBE revealed a cosmic far-IR background with energy > the integrated UV/optical light ⇒ dust extinction is important in the early Universe!
- IR/sub-mm surveys indicate even greater rates of star formation than seen in optical.
-

⇒ To accurately determine the "SFR" requires both optical and far-IR/sub-mm surveys.

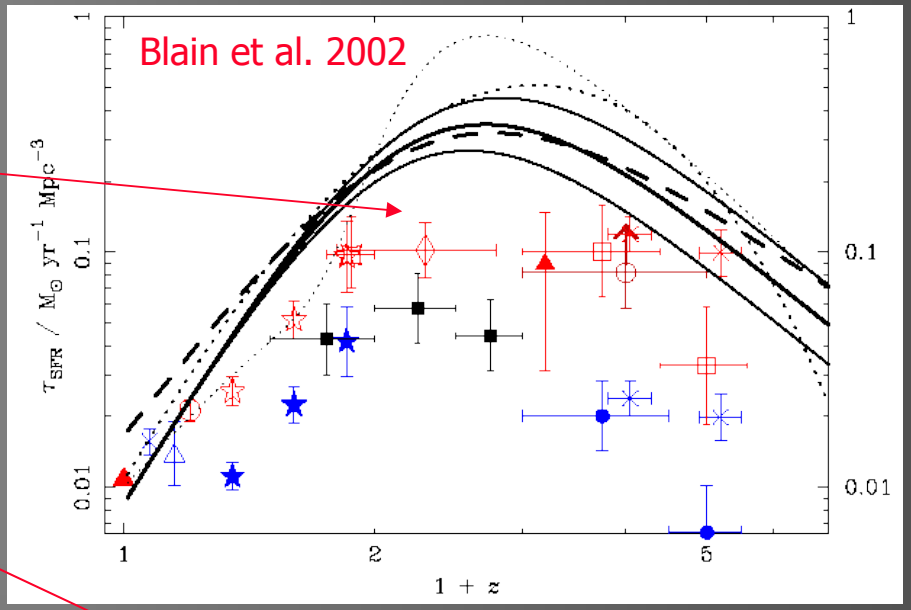

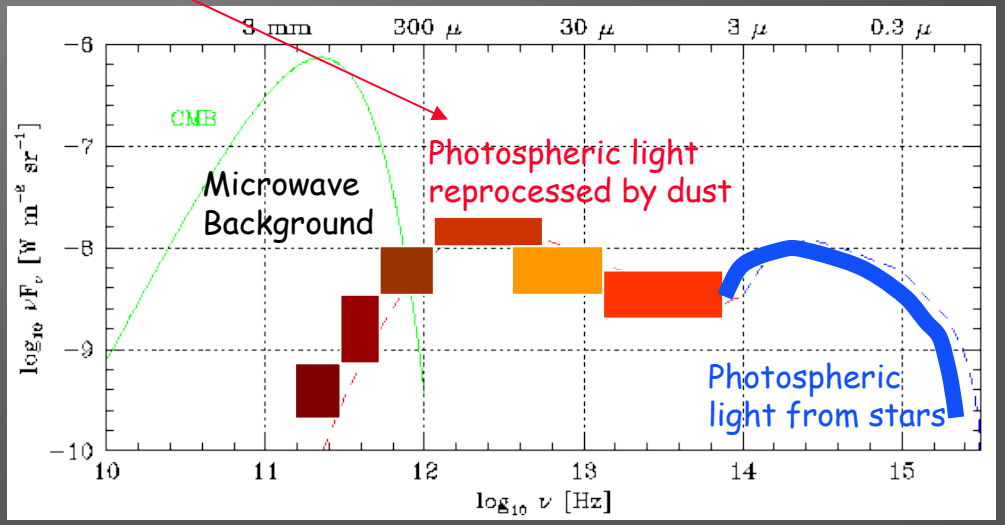

Why Select Seyferts at 12μm?

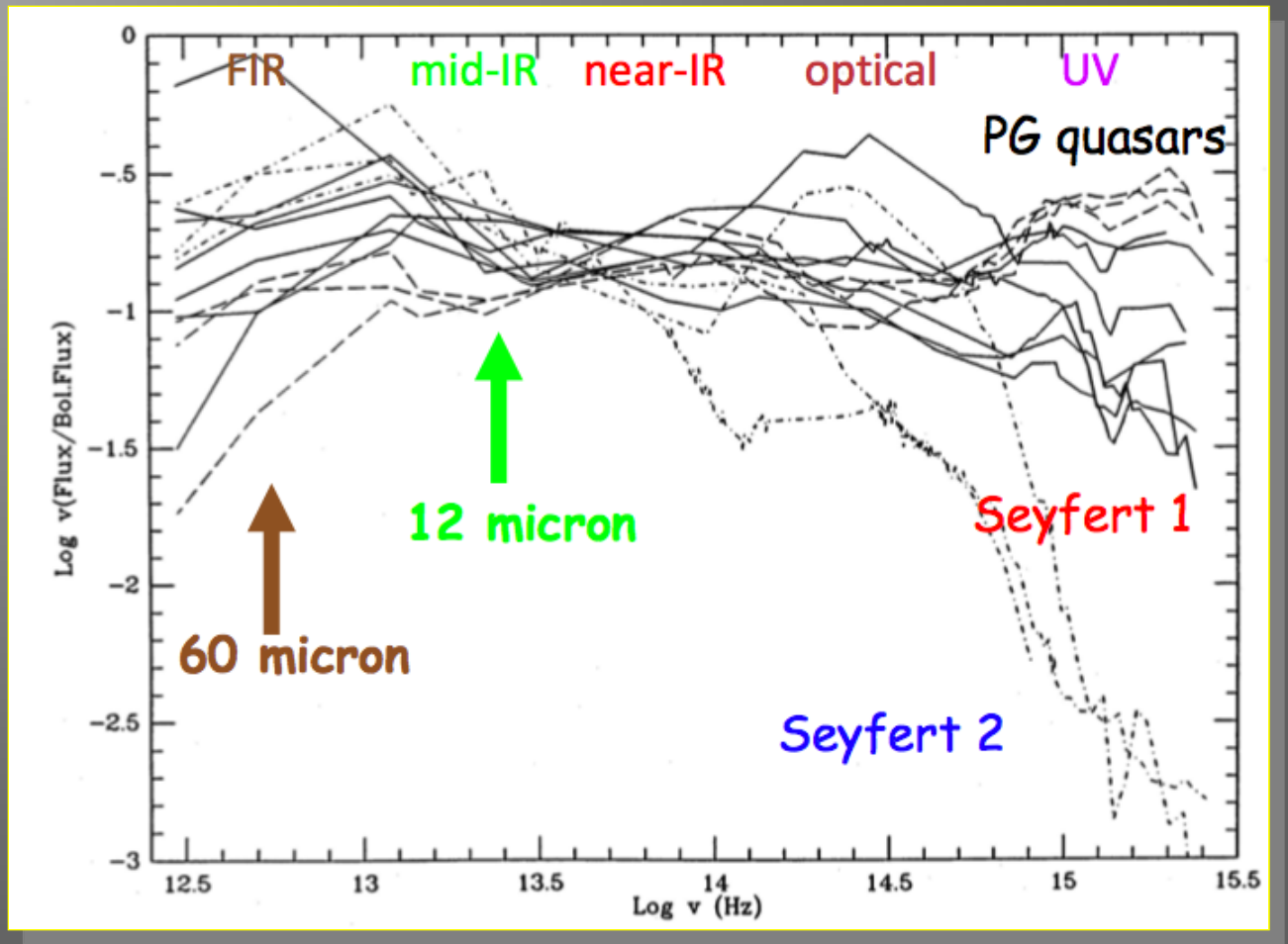

$F_{12\mu m} \sim 0.2\ F_{bol}$ for all types of AGN (Spinoglio et al. 1995)

Better sample definition for a statistical study

LIRGs dominate the IR/SFR at z~1

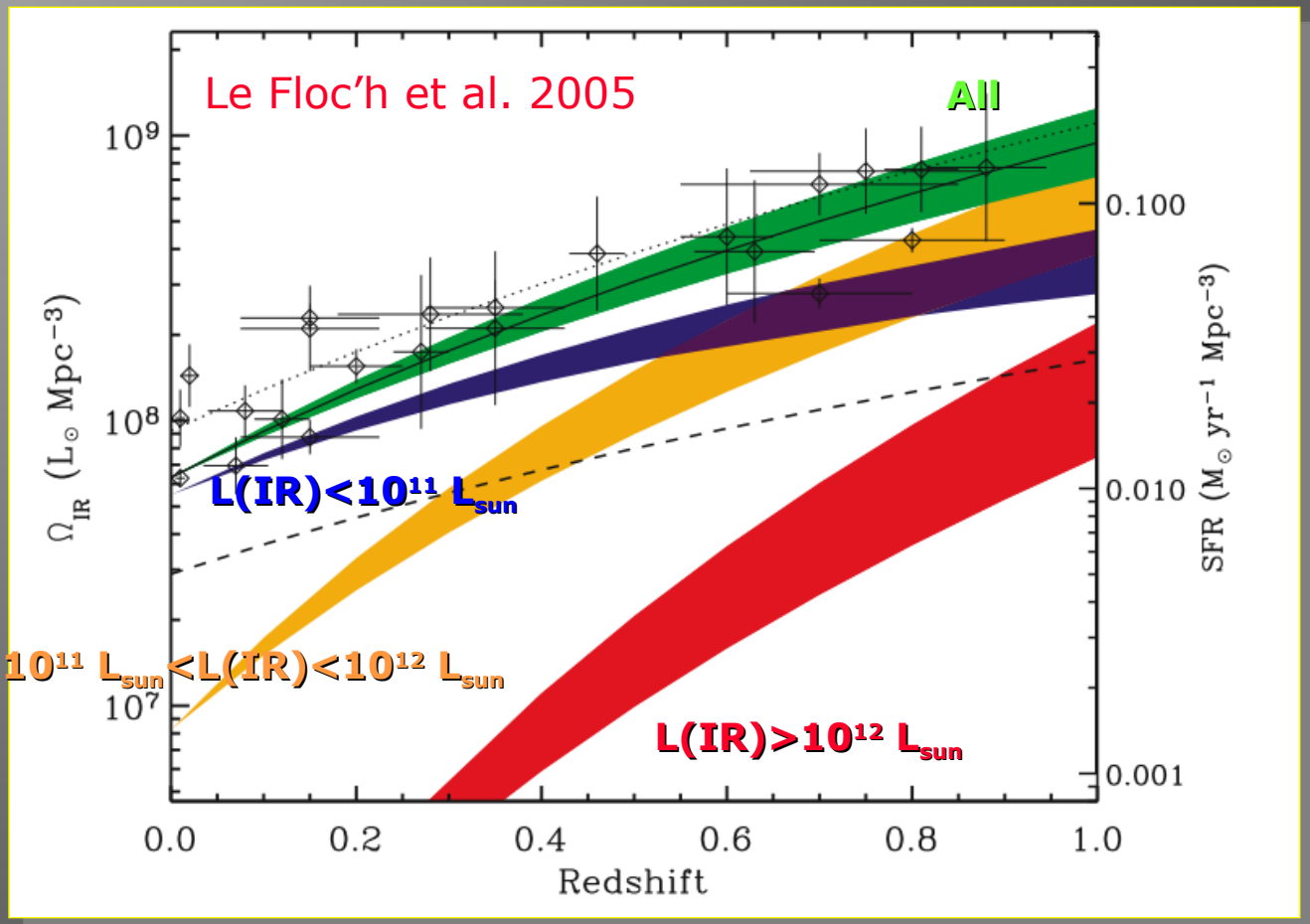

Most near-by 12μm selected Seyferts are LIRGs

Also CXR background/number counts due to (obscured) Seyferts at z~0.7 (Hasinger et al. 2005; Worsley et al. 2005; Gilly et al. 2007)

Why measure SF and accretion together?

- On cosmic scale the evolution of SBMH appears tied to the evolution of SFR (Merloni et al. 2004)
- Low-z SDSS emission-line AGN indicate the SMBH growth and bulge growth via SF are related (Heckman et al. 2004)
- Locally it appears that SF and nuclear activity are linked:

  HII -> Seyfert 2

  (ie Storchie-Bergmann et al. 2001)

  HII -> Seyfert 2 -> Seyfert 1

  (ie. Hunt & Malkan 1999)

- Using the infrared to study this issue offers a number of advantages the more important of which is…

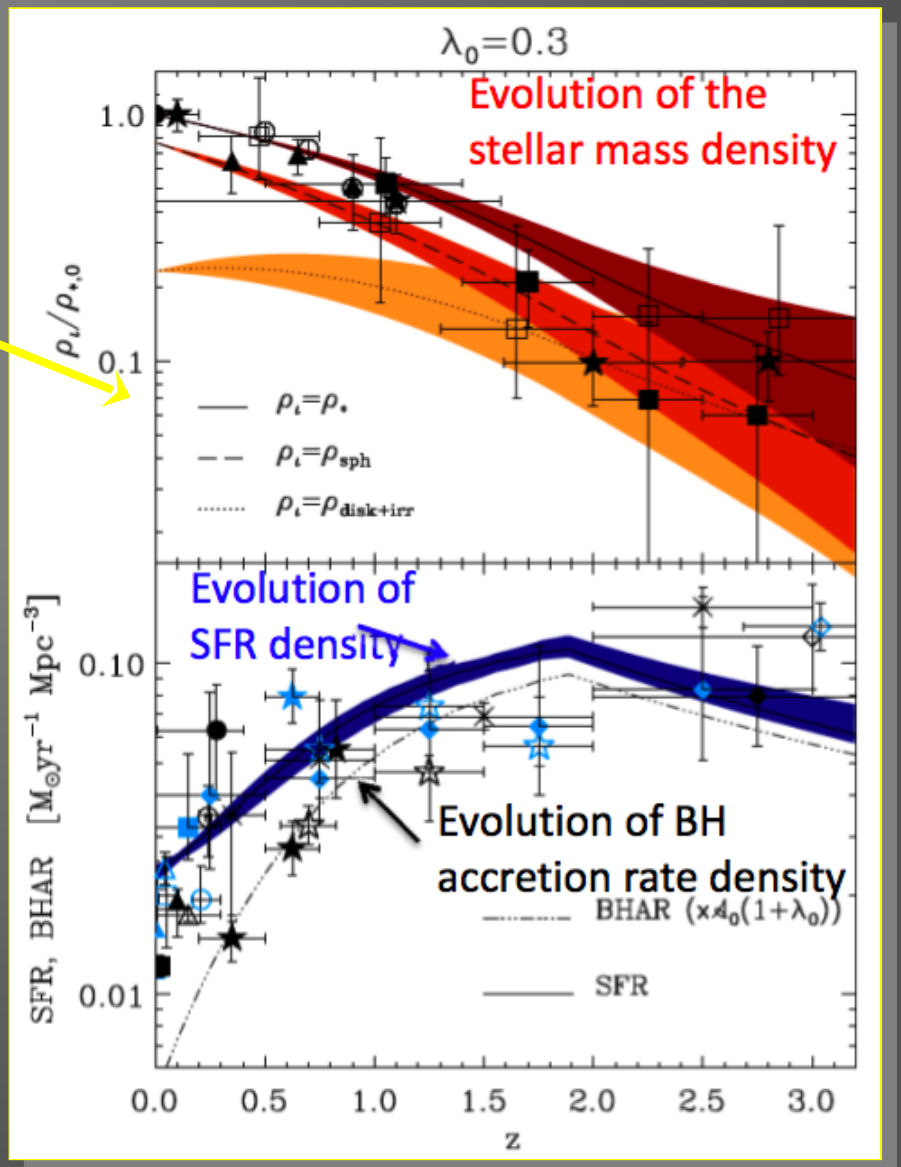

… we can find more AGN (not only Compton thick)

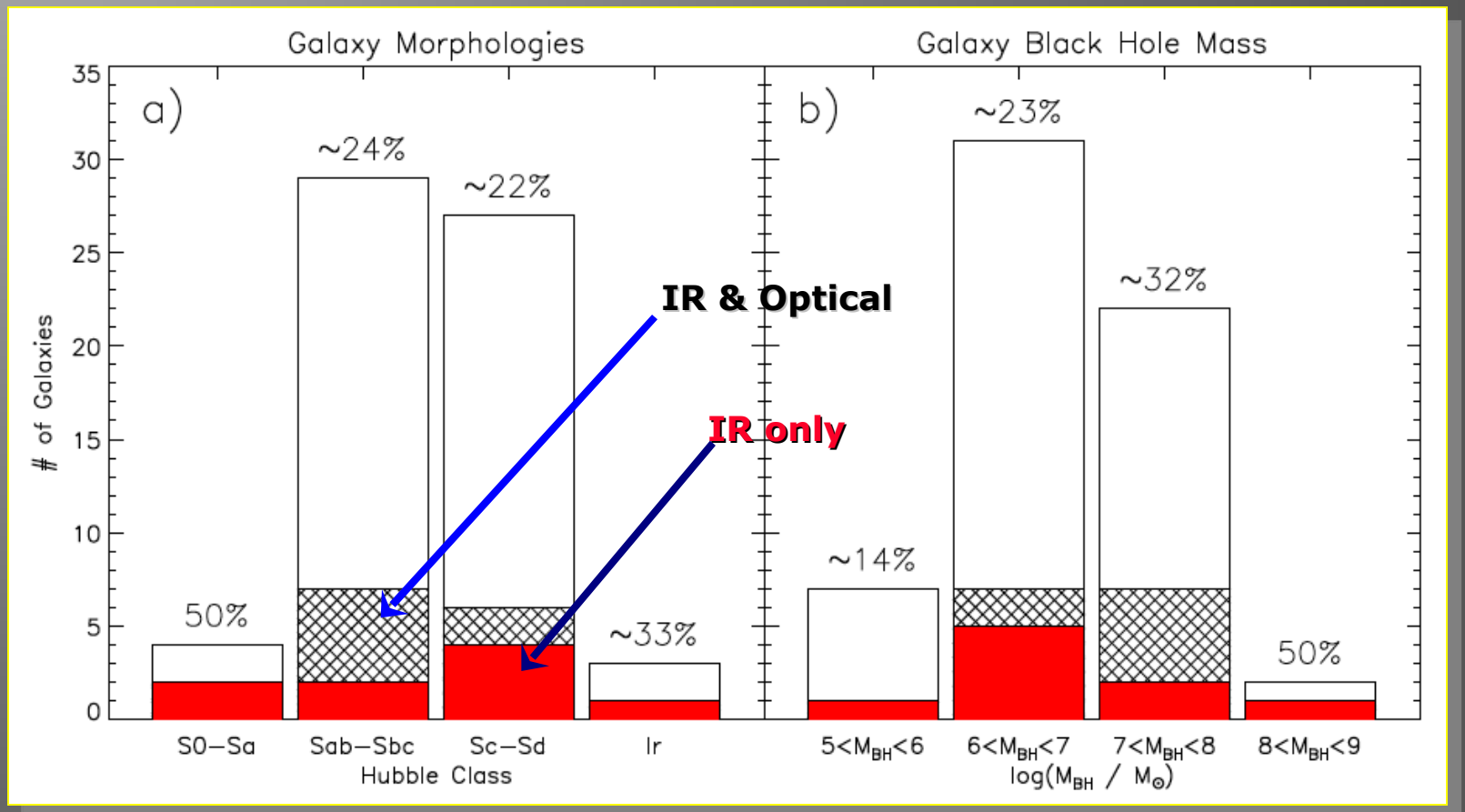

- For 66 IR bright (L_{IR} >3x10^9 L_{sun}) at distances less than 15 Mpc
- There are 27% IR identified AGN - contrary to 11% in the optical (Goulding & Alexander 2009)

Extragalactic IR from 1971 until today

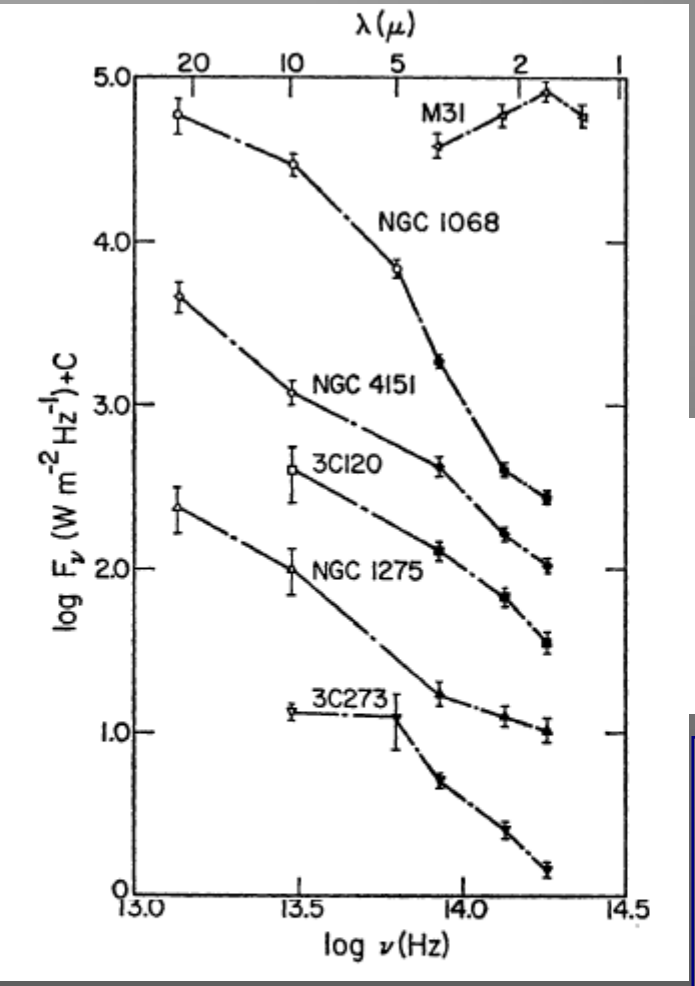

INFRARED SOURCES OF RADIATION[1]

GERRY NEUGEBAUER AND ERIC BECKLIN
Hale Observatories, California Institute of Technology
Carnegie Institution of Washington

A. R. HYLAND
Mount Stromlo & Siding Spring Observatories
Research School of Physical Sciences, The Australian National Observatory

At infrared wavelengths beyond 20 μ we know nothing about the emission from any star but the Sun. In some H II regions, in the galactic nucleus, and in NGC 1068, we see tantalizing evidence of luminosities comparable to or greater than that emitted in the rest of the observed spectral regions. Of the three decades of the electromagnetic spectrum covered by the infrared, only one decade has been explored; the exploration of the other two is certain to give us new and different challenges.

Number of extragalactic sources detected at 10μm :
1971 → 13 (Neugebauer et al. ARA&A)
1978 → ~100 (Rieke & Lebofsky ARA&A)
1988 → IRAS PSC ~250,000 entries (~75,000 CGQ)
1995: ISO is launched first mid-IR spectroscopy
2005: Spitzer is launched! New era of IR begins
2009: Herschel is launched! New Far-IR possibilities

The Advantages of Space...

The Advantages of Space:

100% Transmission and a One-Million Fold Decrease in Sky Brightness.

The outer Space is cold!

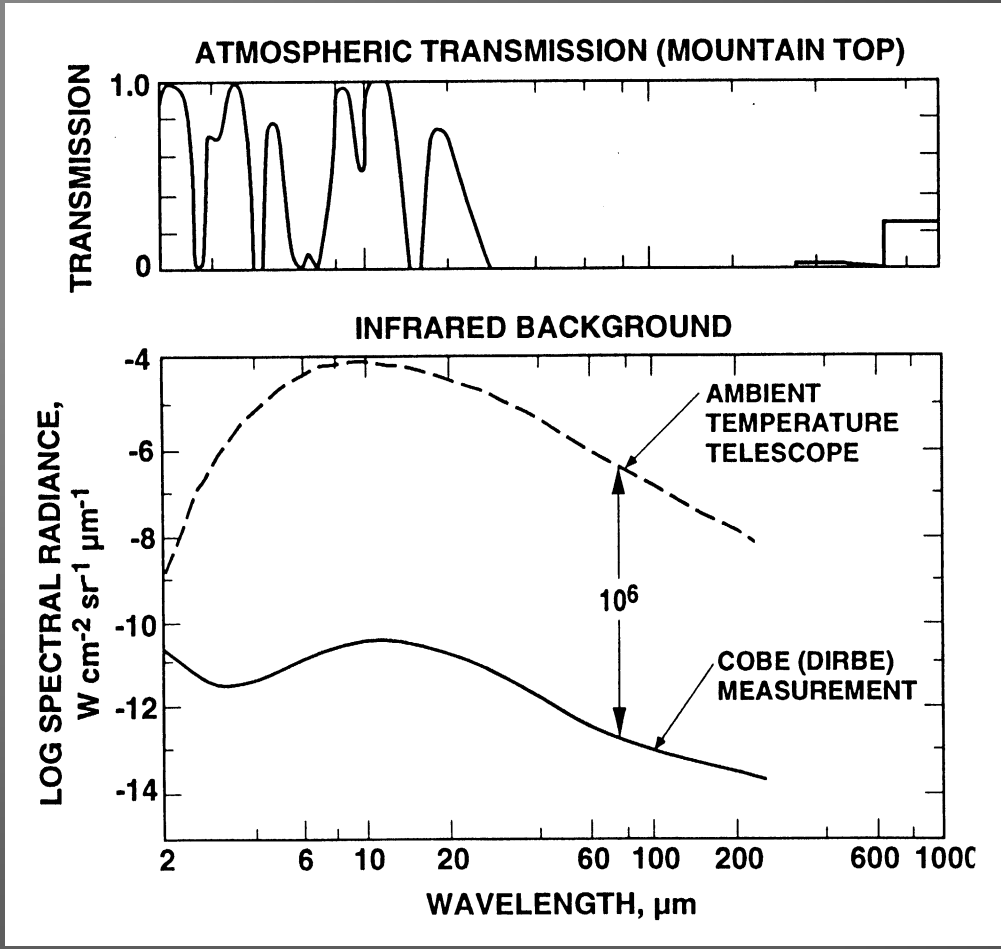

Spitzer Cape Canaveral Launch Aug. 25, 2003

Spitzer Instruments – BALL Oct. 2000

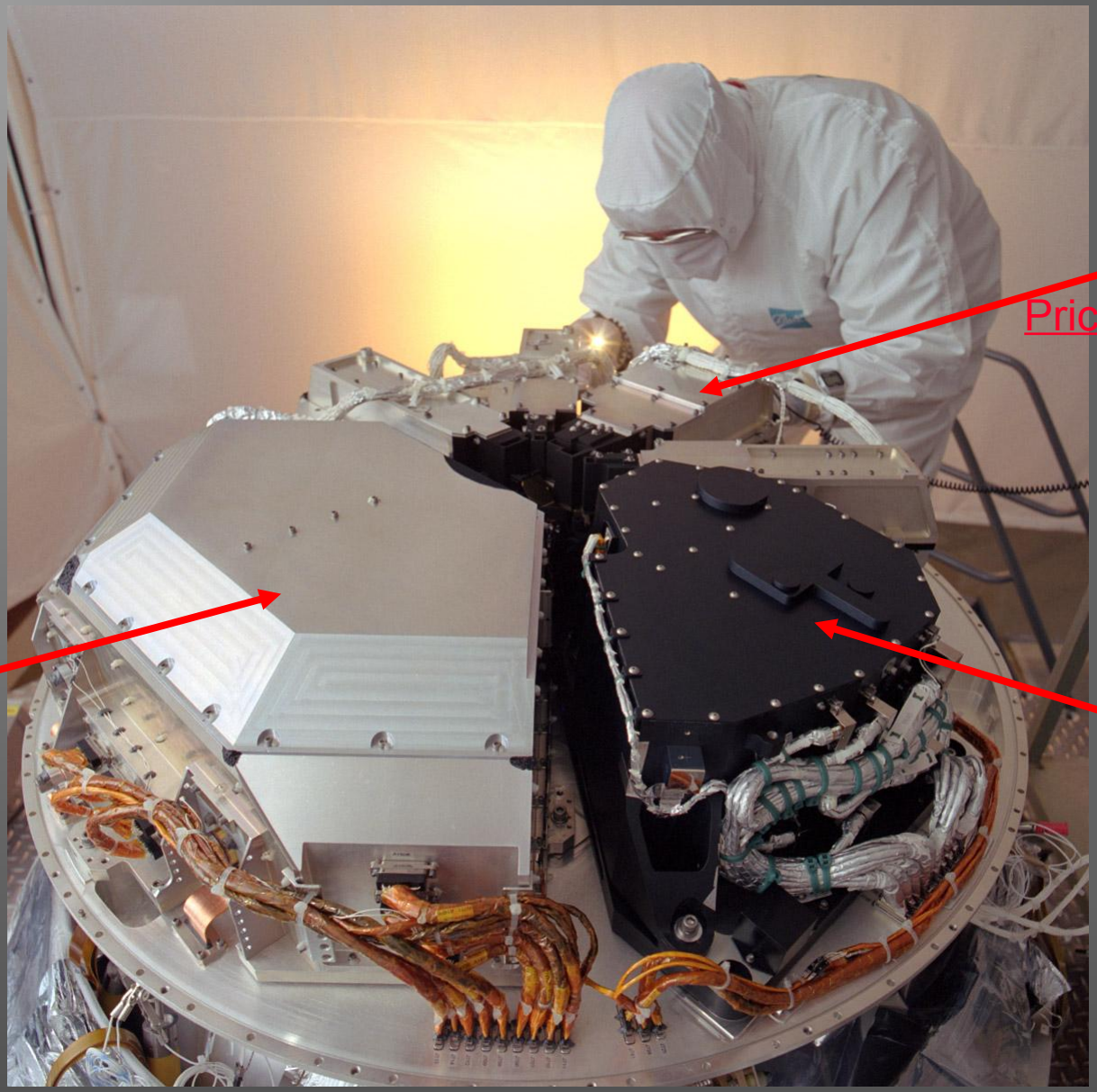

10/00

The Herschel Space Telescope

- **ESA cornerstone observatory**
  - instruments 'nationally' funded, int'l - NASA, CSA, Poland – collaboration
  - ~1/3 guaranteed time, ~2/3 open time
- **FIR (57 - 670 μm) space facility**
  - large (3.5 m), low emissivity (< 4%), passively cooled (< 90 K) telescope
  - 3 focal plane science instruments
  - 3 years routine operational lifetime
  - full spectral access
  - low and stable background
- **Unique and complementary**
  - for λ < 200 μm larger aperture than cryogenically cooled telescopes (IRAS, ISO, Spitzer, Astro-F,…)
  - more observing time than balloon- and/or air-borne instruments (~1000 SOFIA flights per year)
  - larger field of view than interferometers
- **Launch in May 2009**

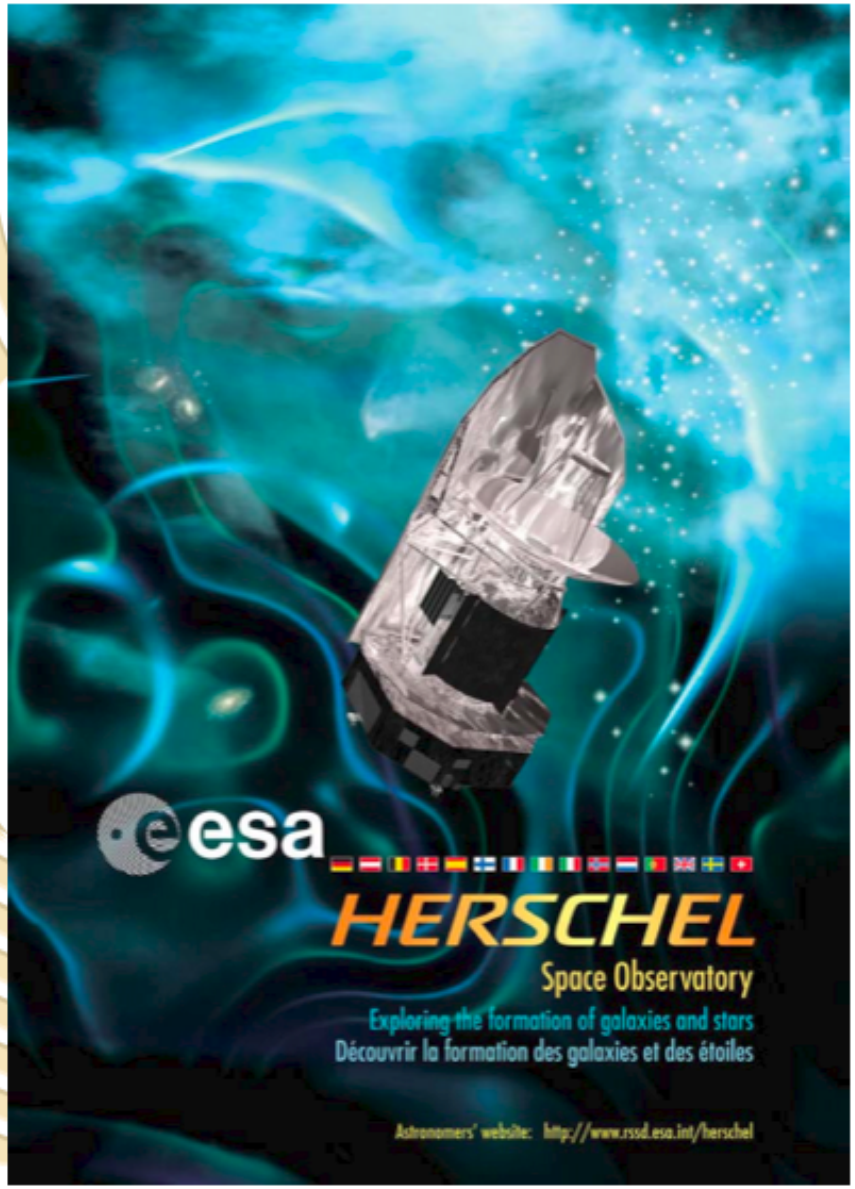

Dust and Star Formation

- Dust grains act as catalyst for the formation of molecular gas
- Wavelength dependent extinction

  Galactic center: $A_V \sim$ 30 mag $\rightarrow$ 1 photon in 10^{12} penetrates

  $A_{2.2\,\mu m} \sim$ 2.5 mag $\rightarrow$ 1 photon in 10 penetrates

- Dust grains are responsible for the heating of the gas
  - *A far-UV photon hits a dust grain and ejects an electron*
  - *The ejected photoelectron heats the gas (very inefficiently ~0.1 - 1 %)*
    - 50% of gas heating is due to grains of sizes < 15 Å
  - *Subsequently the gas cools via far-IR emission lines ([OI] 63 μm , [CII] 158 μm)*
- Emission from Polycyclic Aromatic Hydrocarbons (PAHs), dominate the mid-IR (5-20 um) flux in normal galaxies and quiescent star forming regions
- PAHs can be destroyed by strong UV fields (massive starbursts - AGN)
- One can use mid- / far-IR prescriptions to estimate star formation rates (Far-IR: Kennicutt 1998, Mid-IR/ISO: Rousell et al. 2002, Forster-Schreiber et al 2004, Mid-IR/Spitzer: Calzetti et al. 2005; 2007, Wu et al. 2005)

PAH Normal Modes

- **10-20% of the total IR luminosity of a galaxy**
- Tens - hundreds of C atoms
- Bending, stretching modes ⇒ 3.3,6.2,7.7,8.6,11.2,12.7 μ m
- PAH ratios ⇒ ionized or neutral, sizes, radiation field, etc.

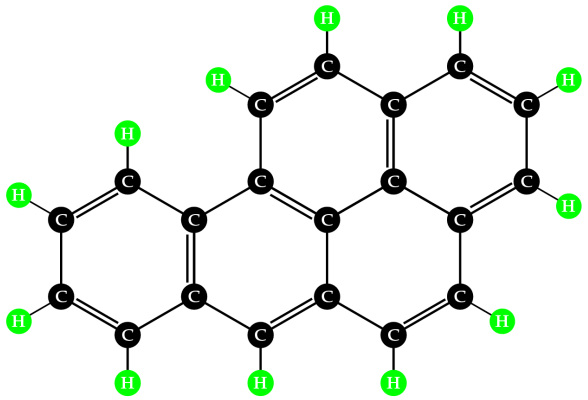

PAH molecule

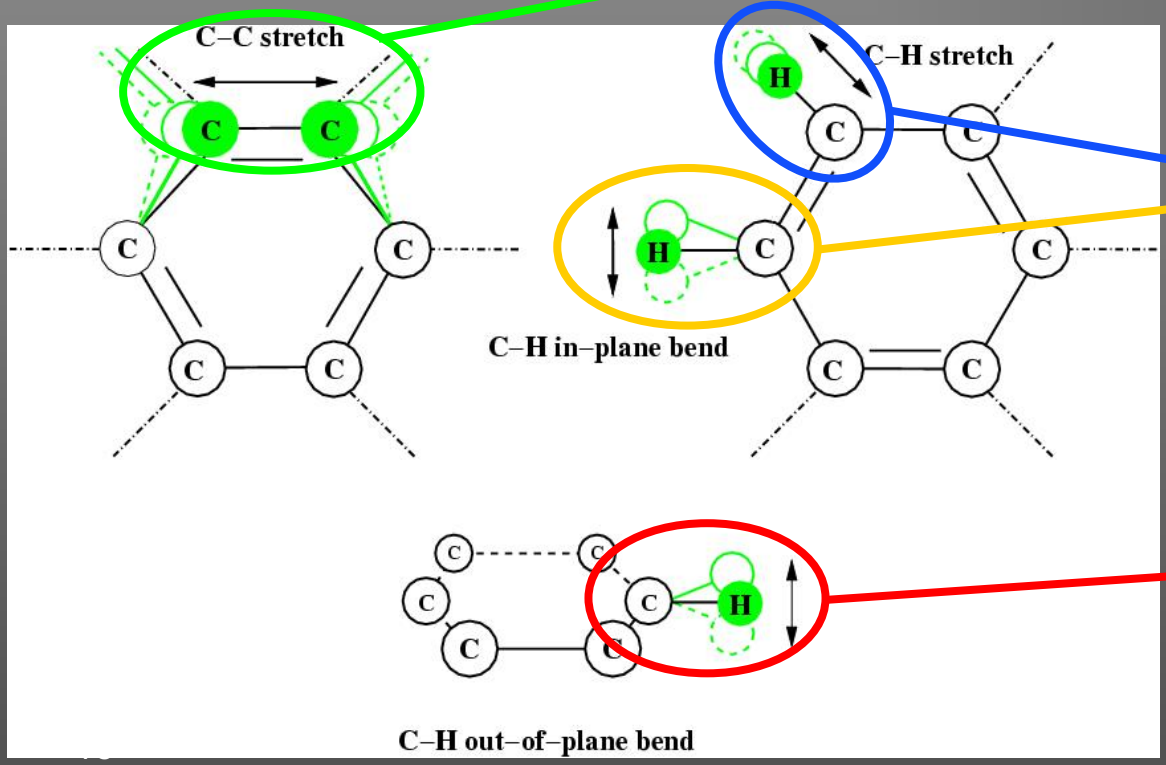

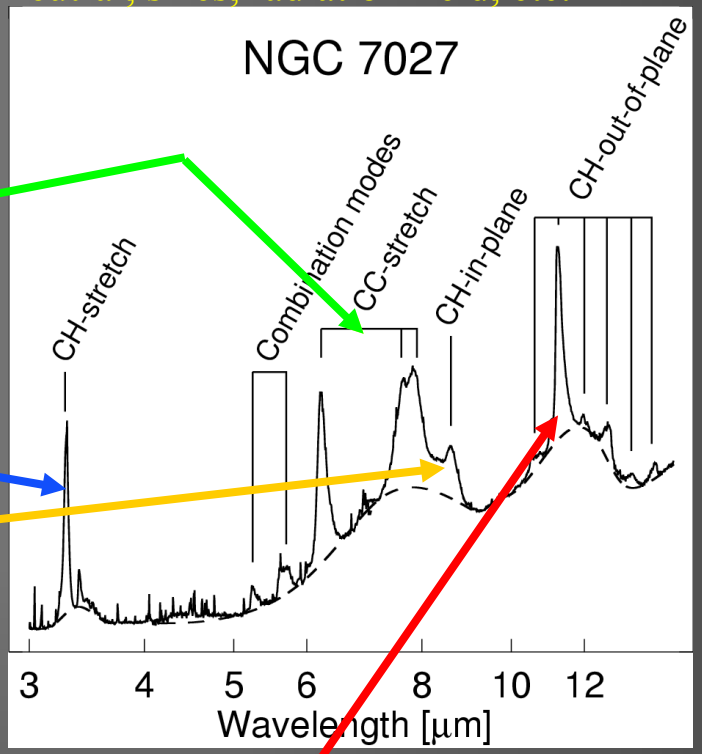

Leger & Puget (1984)
Sellgren (1984)
Desert, et al. (1990)
Draine & Li, (2001)
Peeters, et al. (2004)

Experimental Data for PAHs

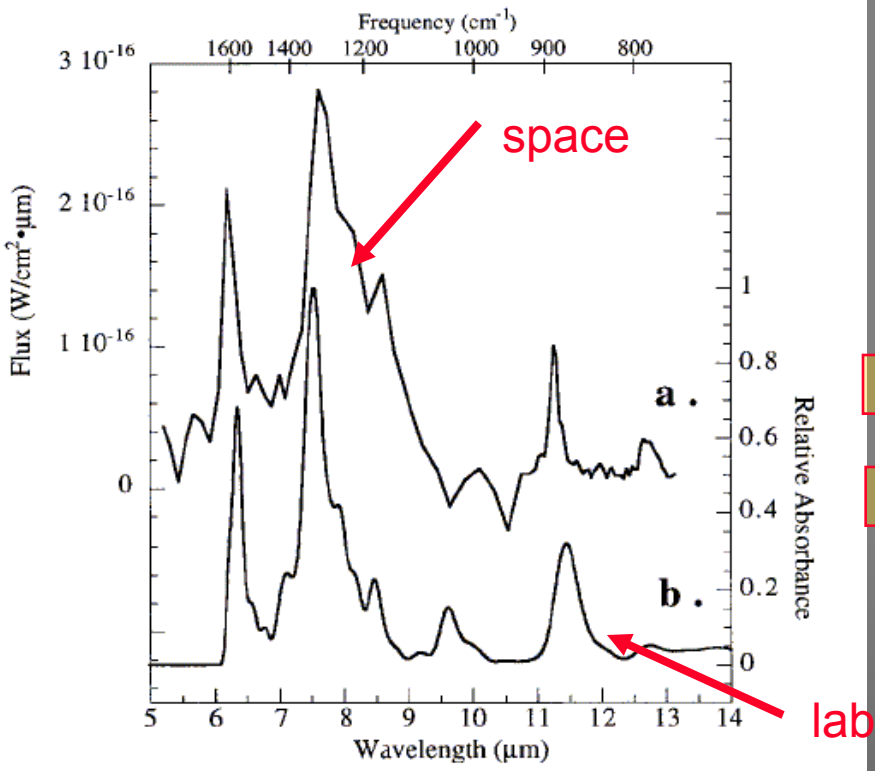

FIG. 1.—Comparison of (*a*) the infrared emission spectrum of the Orion bar with (*b*) a composite absorption spectrum generated by co-adding the individual spectra of 11 PAH cations. The individual spectra were calculated using experimentally measured frequencies and intensities and assigning a 30 cm^{-1} FWHH Gaussian band profile, consistent with that expected from the interstellar emitters (Allamandola et al. 1989). The PAH cation mixture consists of 20% benzo[k]fluoranthene$^+$ ($C_{20}H_{12}^+$) and dicoronylene$^+$ ($C_{48}H_{20}^+$); 10% coronene$^+$ ($C_{24}H_{12}^+$), benzo[b]fluoranthene$^+$ ($C_{20}H_{12}^+$), 9, 10-dihydrobenzo(e)pyrene$^+$ ($C_{20}H_{14}^+$), and phenanthrene$^+$ ($C_{14}H_{10}^+$); 5% benzo[ghi]perylene$^+$ ($C_{22}H_{12}^+$), tetracene$^+$, and benz[a]anthracene$^+$ (both $C_{18}H_{12}^+$); and 2% chrysene$^+$ ($C_{18}H_{12}^+$) and fluoranthene ($C_{16}H_{10}^+$). The Orion spectrum is reproduced from Bregman et al. (1989).

PAH / UIB infrared features

C-H stretch (3.3 μ m)
C-C stretch (6.2, 7.7 μ m)
C-H in plane bend (8.6 μ m)
C-H out of plane bend (11.3, 11.9, 12.7 μ m)
C-C bending (16.4, 18.3, 21.2, 23.1 μ m)

(Hudgins & Allamandola 1999)
(Papoular 2002)

Decompositions of PAHs

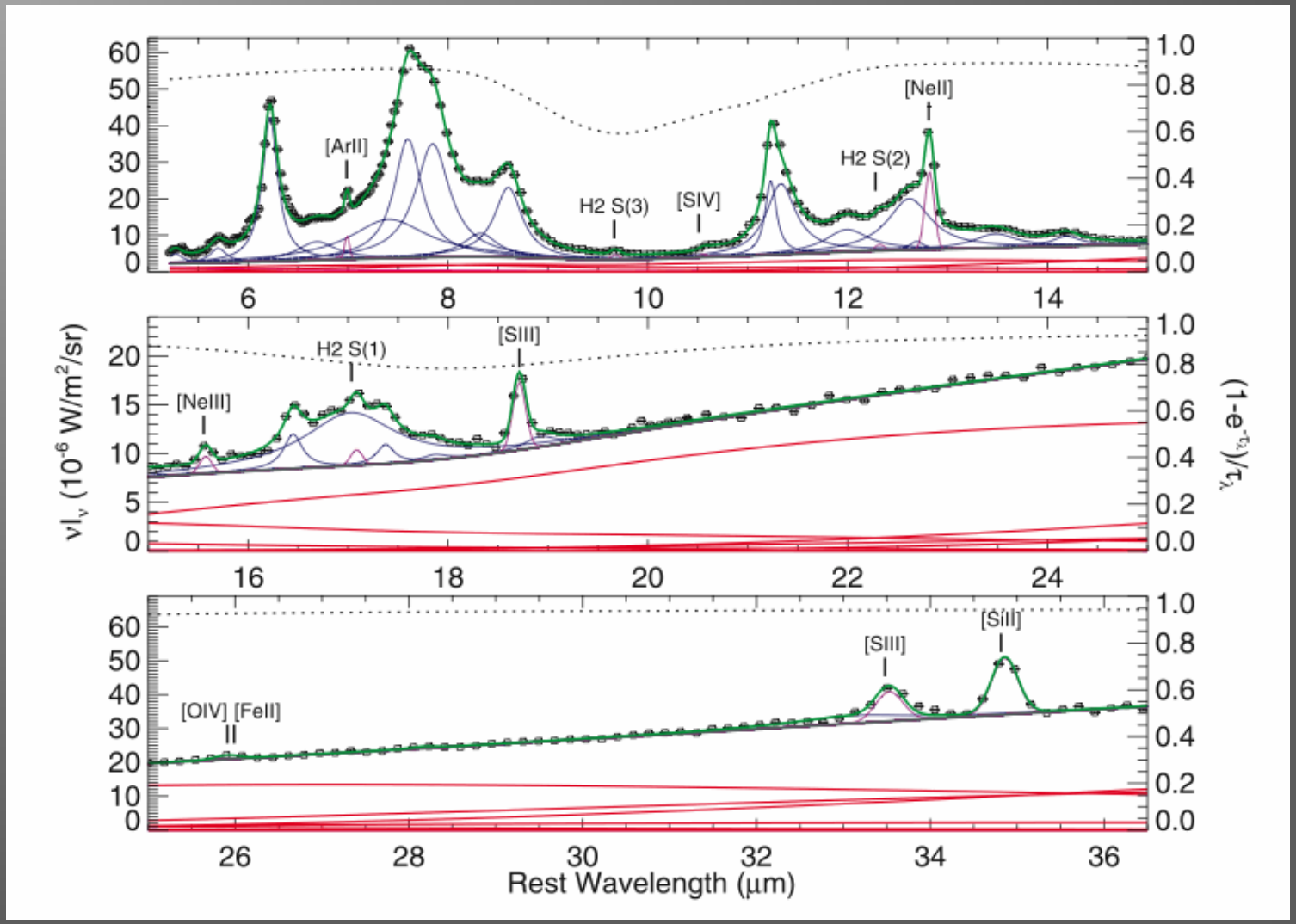

(SINGS - Smith et al. 2007)

Fractional PAH power

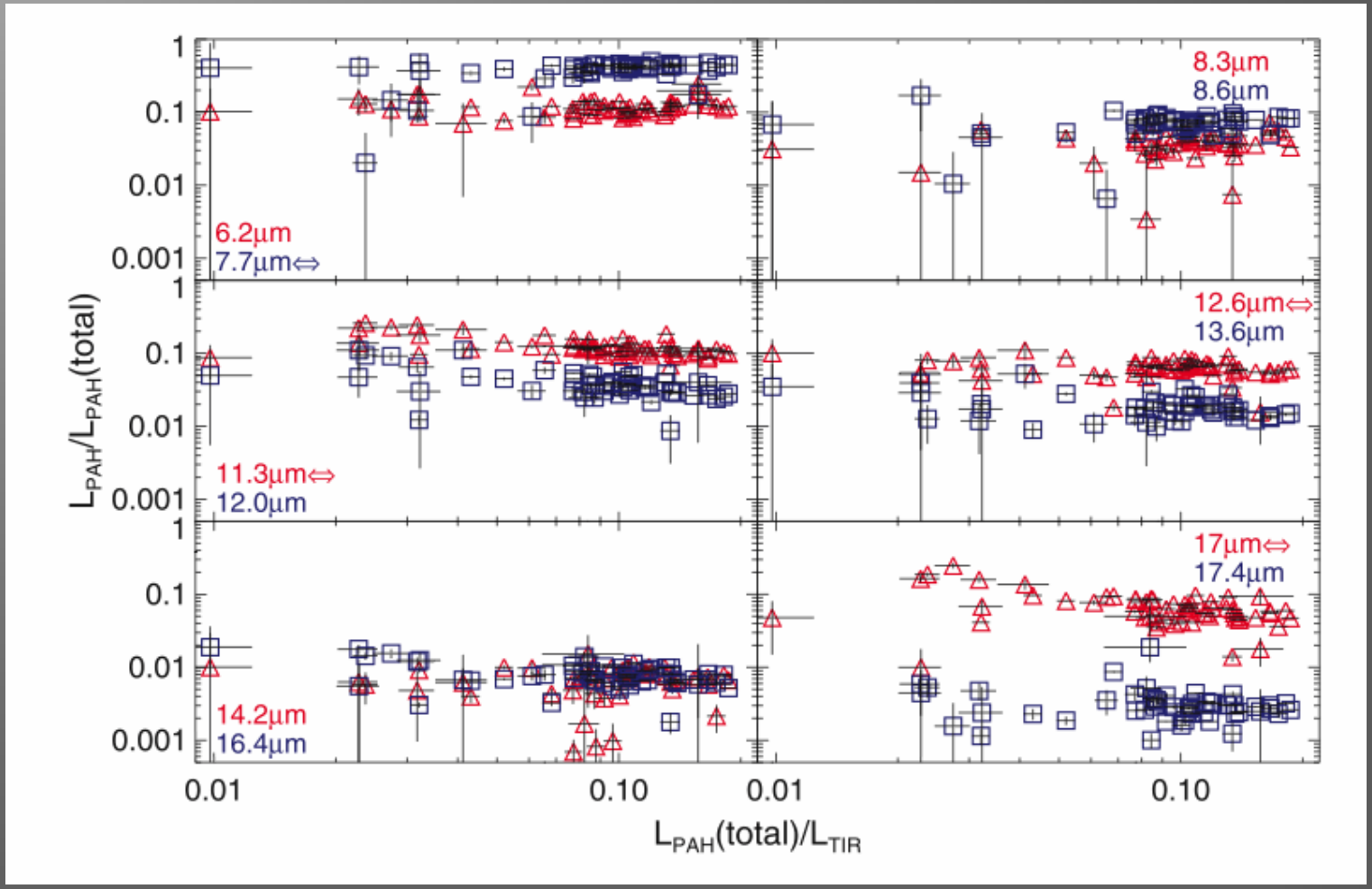

6.2μm, 12.6μm => ~10%
7.7μm => ~30%
11.2μm, 17μm => ~15%

(SINGS - Smith et al. 2007)

PAHs & Galaxy Energy Balance

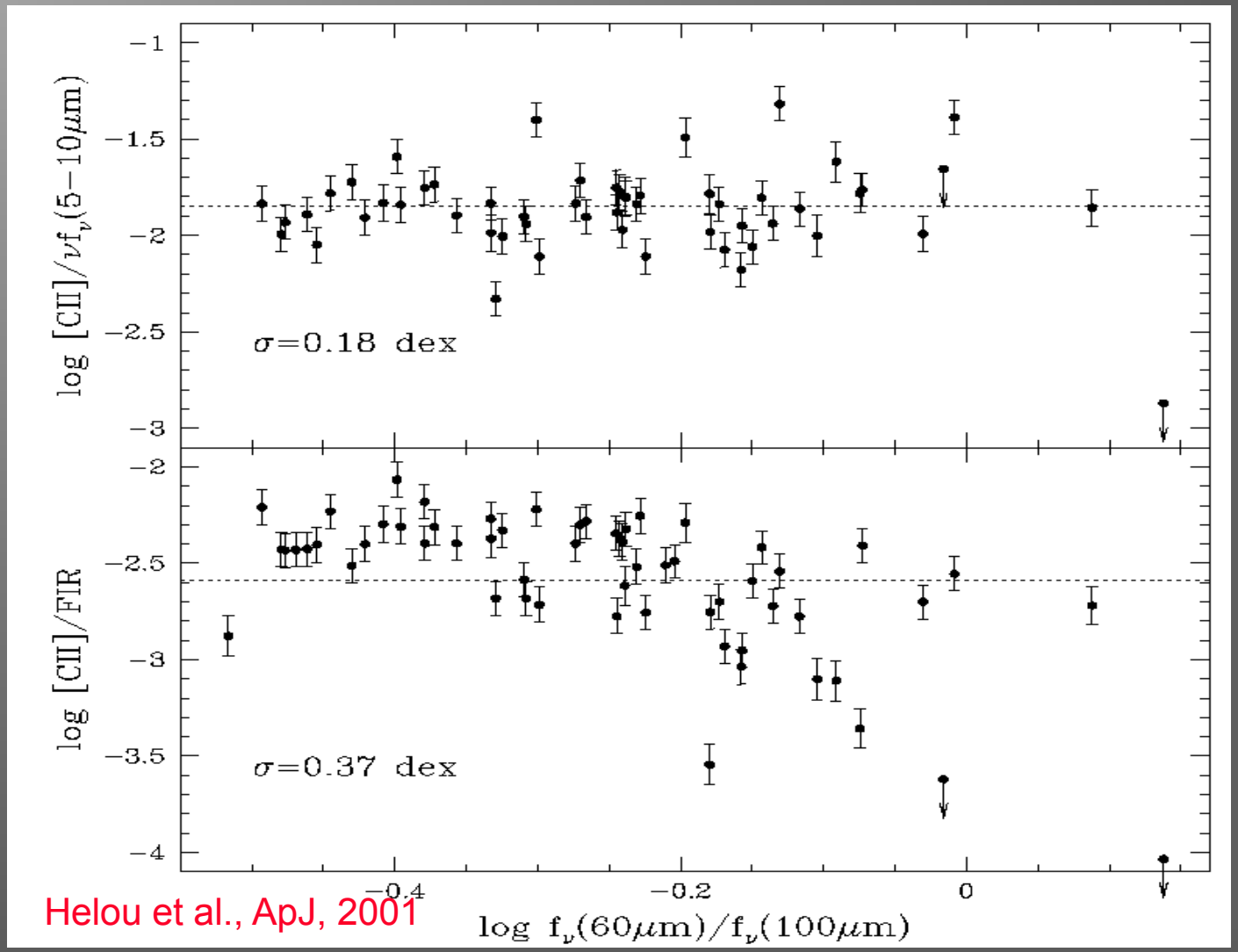

Helou et al., ApJ, 2001

Mid-IR Emission as star formation tracer

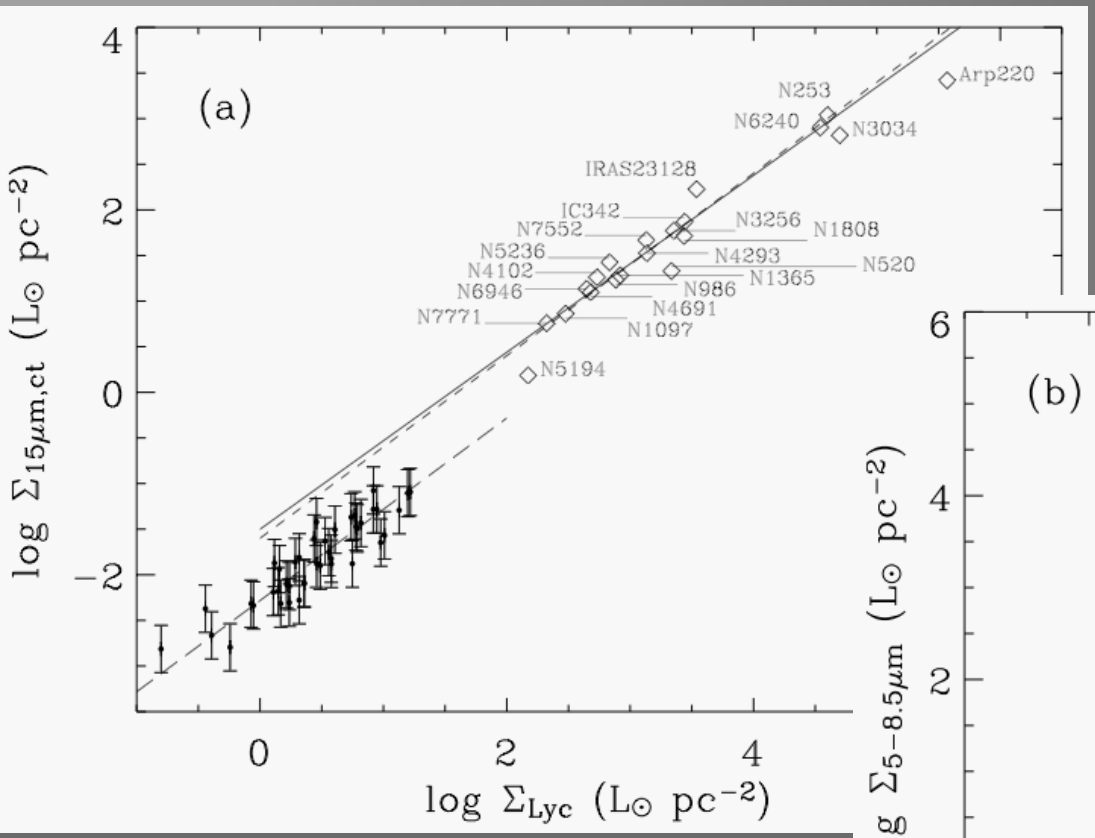

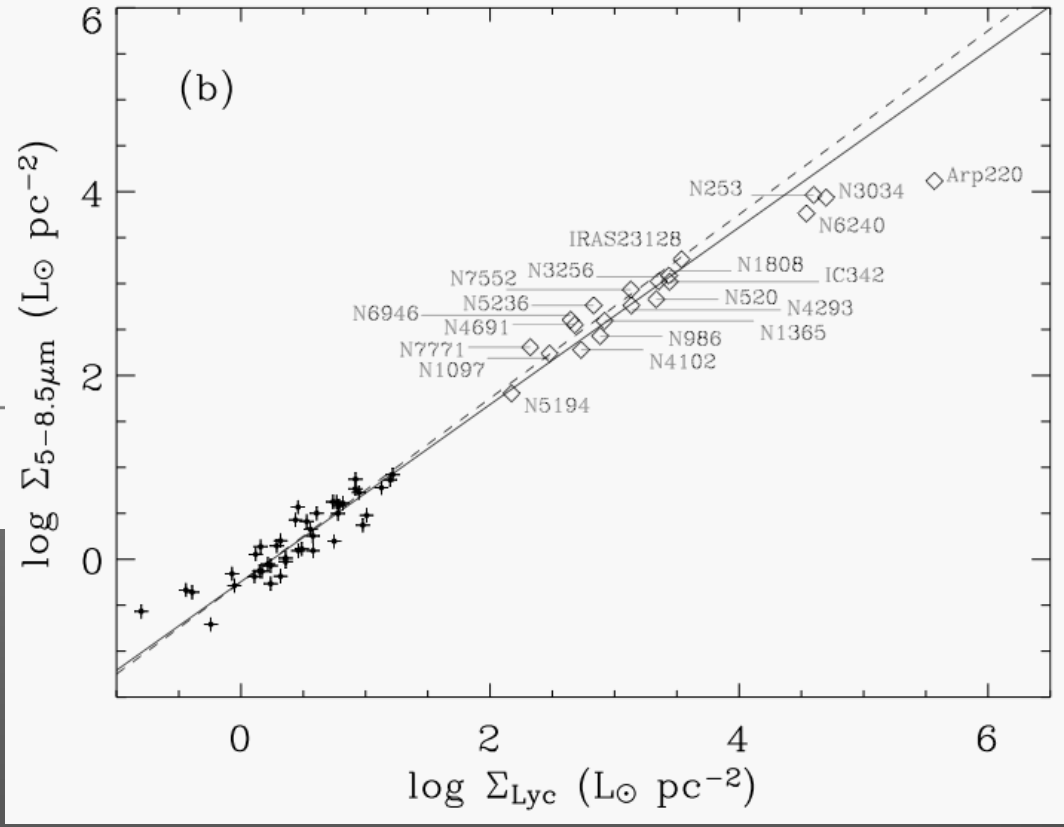

Forster-Schreiber et al., A&A, 2004

Mid-IR Emission as star formation tracer (Spitzer)

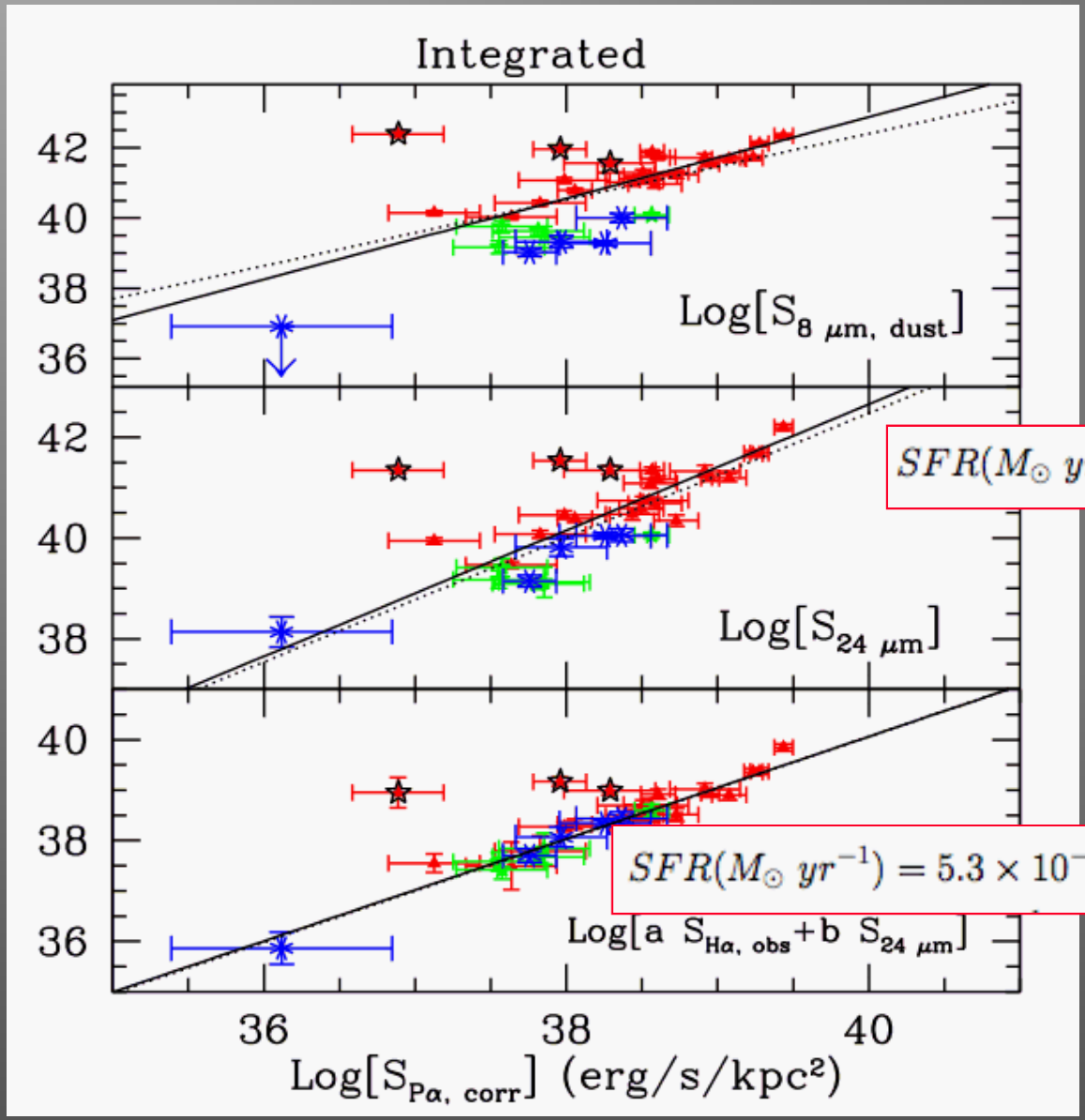

$$SFR(M_\odot\ yr^{-1}) = 1.27 \times 10^{-38}[L_{24\ \mu m}\ (erg\ s^{-1})]^{0.8850}$$

$$SFR(M_\odot\ yr^{-1}) = 5.3 \times 10^{-42}[L(H\alpha)_{obs} + (0.031 \pm 0.006)L(24\ \mu m)],$$

Calzetti et al., ApJ, 2007

Probing the dominant energy source of galaxies

Many methods developed to quantify the fraction of star formation or emission from an accretion disk (AGN) in galaxies.

(Mushotzsky @astro-ph/0405144)

The presence of an AGN can be detected most ambiguously via:

- Hard X-rays (>10keV)
- Multi frequency radio observations (thermal/synchrotron fraction)

Difficulties:

- Very few hard X-ray photons
- Problems of self absorption in the interpretation of radio

For practical reasons most work has been performed via:

- Optical spectroscopy (i.e. Kim et al. 1998)
- Near-IR spectroscopy (i.e. Veilleux et al. 1999)

Advantages of IR:

- Most galaxies emit a larger fraction of their energy in the IR.
- Less affected by extinction than optical/near-IR

IR diagnostics of AGN

Most work on identifying AGN in the IR started from IRAS using the differences in IRAS colors - warm/cold sources (i.e. de Grijp 1985)
Difficulty: Broadband colors only.

The availability of sensitive mid-IR spectrographs on board ISO enabled us to make considerable progress:

- Detect High Ionization lines (Genzel et al 1998, Sturm et al. 2002)
  - [NeV] at 14.3μm / 23.2μm (Ep~97eV)
  - [OIV] at 25.9μm (Ep~55eV)

  Difficulty: the lines are faint

- Detect changes in continuum / broad features
  - Presence of 7.7μm PAH (Lutz et al. 1999)
  - Relative strength of 7.7μm PAH with respect to the 5.5μm and 15μm continuum (Laurent et al. 2000)

  Difficulties:
  - The 7.7PAH is affected by the 9.7μm silicate feature
  - The mid-IR continuum was not well defined with ISO PHOT-S (~11.8μm) & ISOCAM/CVF (~16μm)

Spitzer IR Spectroscopy of (U)LIRGs

ULIRG Basics

Properties

- $L_{IR} \geq 10^{12} L_{\odot}$; $L_{bol} \sim L_{IR}$; $L_{opt} < 0.1 L_{IR}$
- 90 – 95% are interacting, or in merging systems
- very strong OIR emission lines (H+, [OI,] [OIII], [NII], [SII], [FeII], etc.)
- NIR CO absorption bands from young stars
- large, compact reservoirs of cold molecular gas ($> 10^{9}$ - 10^{10} $M_{\odot}$) in their nuclei ($R \leq$ 1 Kpc).
- drive “superwinds” of hot, enriched gas into the IGM
- relatively rare in the local Universe - only ~3% of galaxies in IRAS BGS are ULIRGs, but much more important at high-z

Questions

- What are the dominant power sources (50-500 $M_{\odot} yr^{-1}$ SB or AGN ?)
- Do we see any mid-IR spectral “evolution” indicative of a change in SF properties with redshift or luminosity (e.g. PAH strength, H_2 fraction, etc.) ?

Most (U)/LIRGs are Interacting Systems

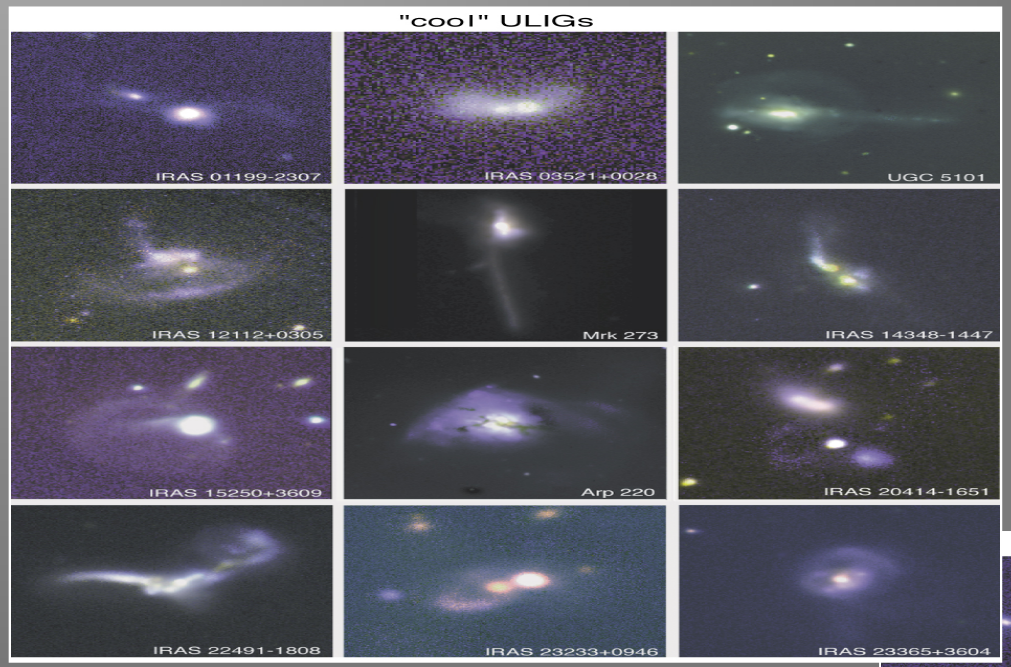

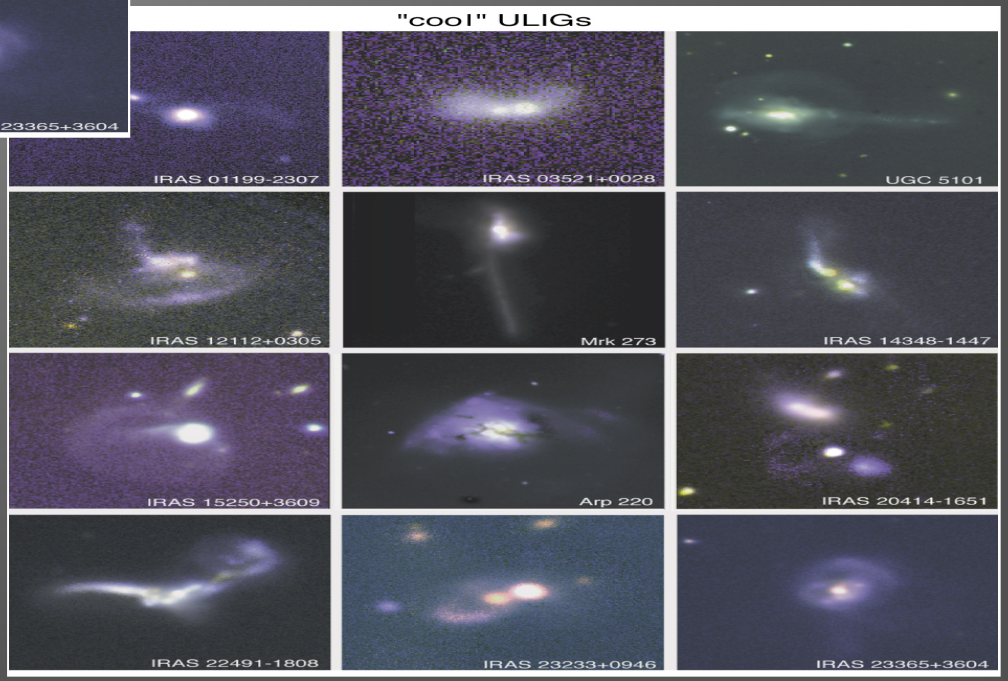

Sanders et al. 1988
Surace & Sanders 2001

The (U)LIRG program - details

Of the 110 sources

- Flux limited: 32 have S25 ≥ 0.3 Jy and log L_{FIR} ≥ 11.85 $L_{\odot}$.
  We are observing all 32 in low and high-res modes.
- High redshift: 27 have z ≥ 0.3.
  12/27 are being observed in low and high-res.
- High luminosity: 11 sources have log L_{FIR} ≥ 12.5 $L_{\odot}$.
  10/11 are being observed in low and high-res..
- Mix of Far-IR colors: 68 are "cold" ($S_{25}/S_{60} < 0.2$) and 21 are "warm".
  This is a higher fraction of warm sources than in a flux-limited survey (typically ≤ 10%).

- Additional GO Programs: Veilleux et al., Lutz et al., Imanishi et al., Verma et al. Sturtm et al. (~80 objects)

- GOALS: dditional Legacy data on LIRGs of ~220 objects

The IRS ULIRG Program

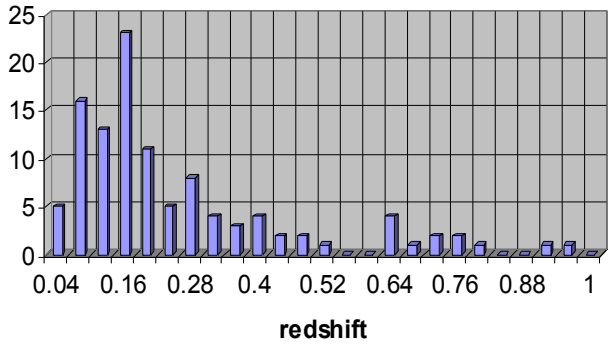

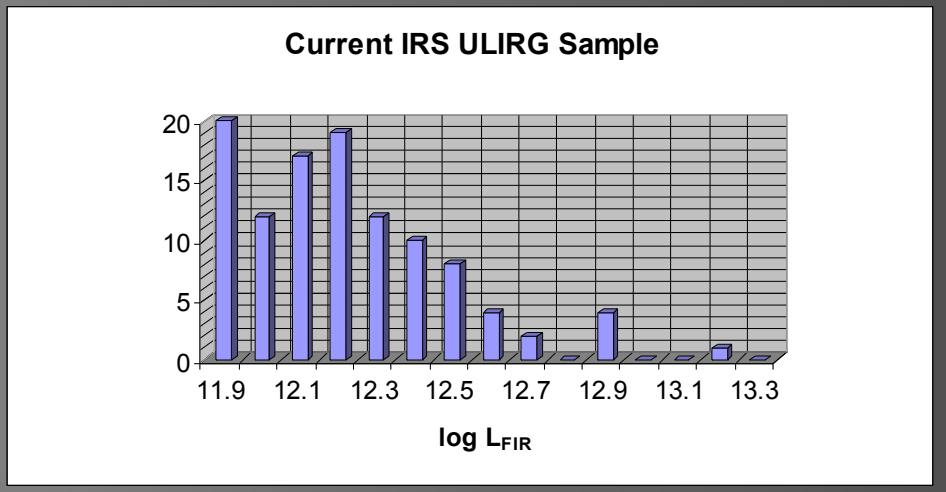

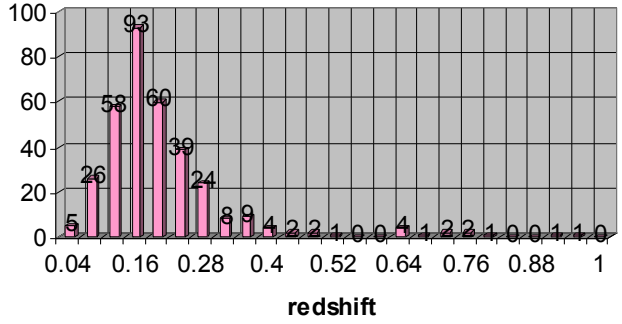

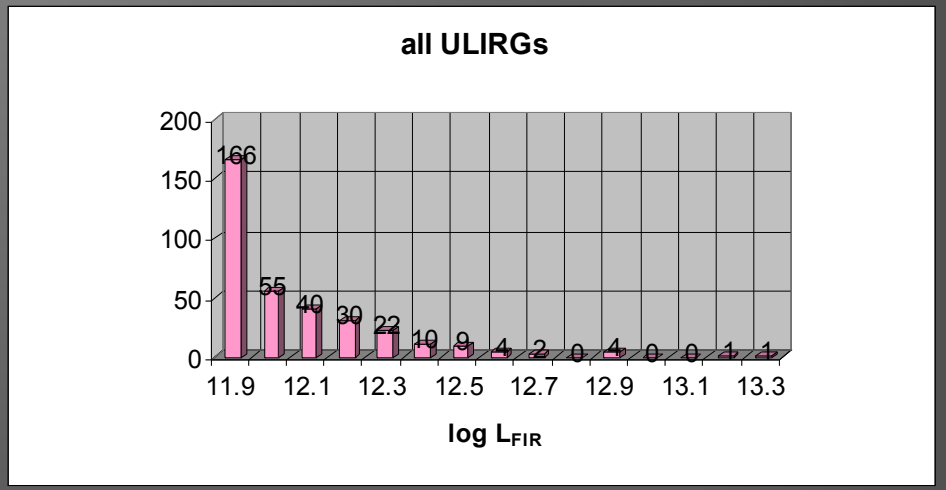

PAHs and Extragalactic Templates

- Sources of PAH templates used to date:
  - *Theoretical/Lab PAH band models.*
  - *Few bright ISO galaxies (e.g. Arp220)*
  - *Average ISO Key Project "normal" galaxy spectrum.*

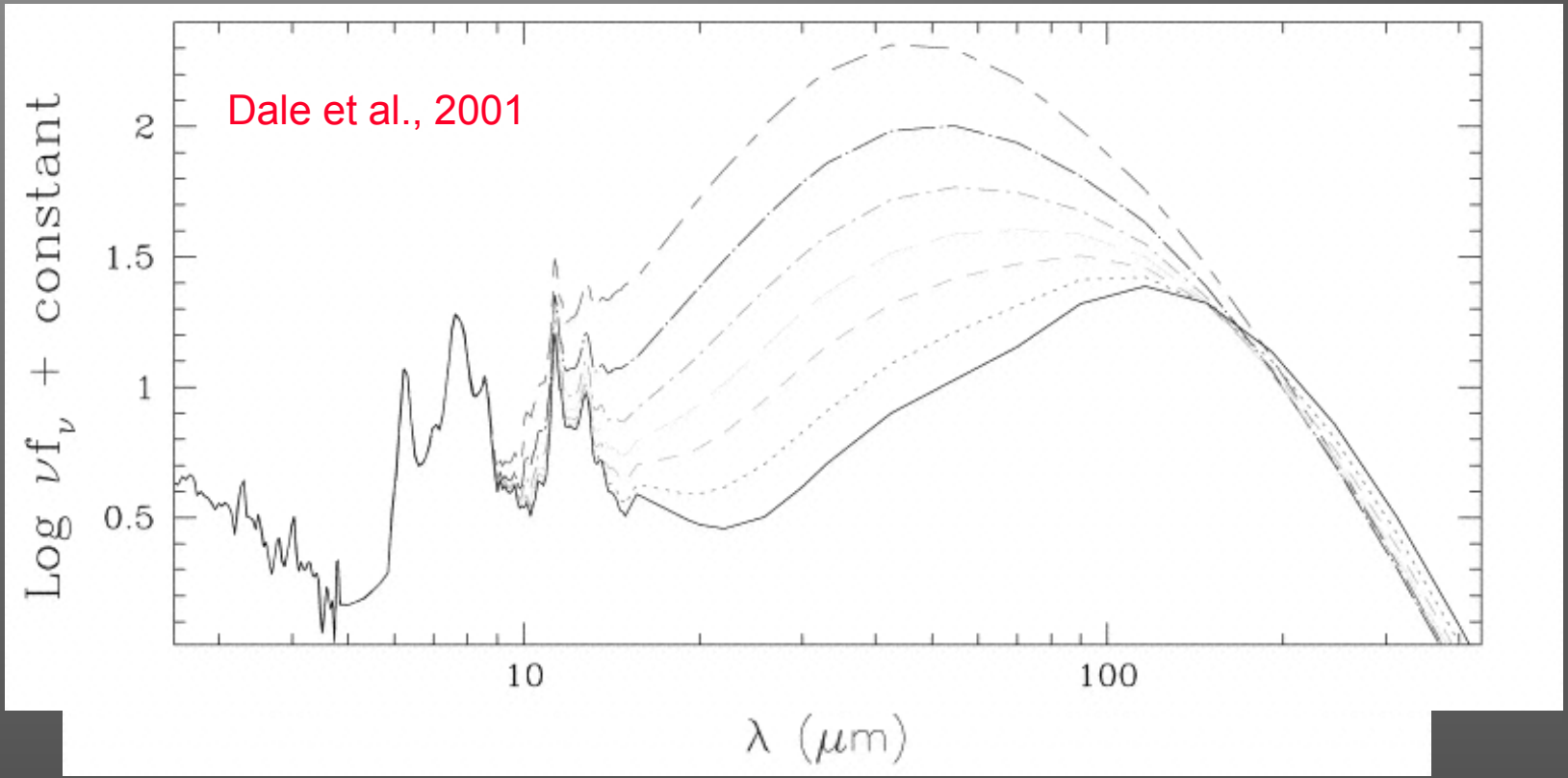

Fitting the Number Counts

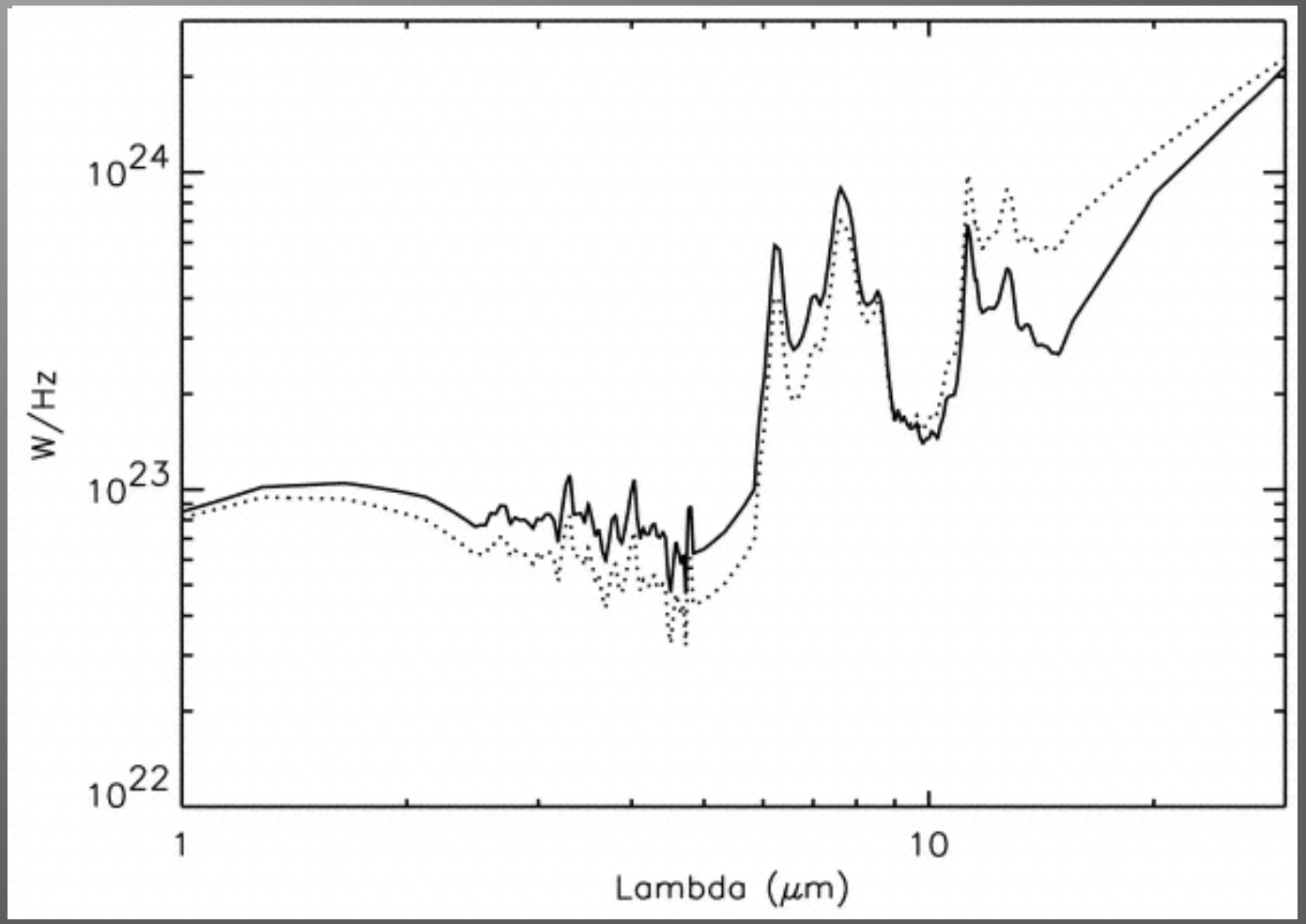

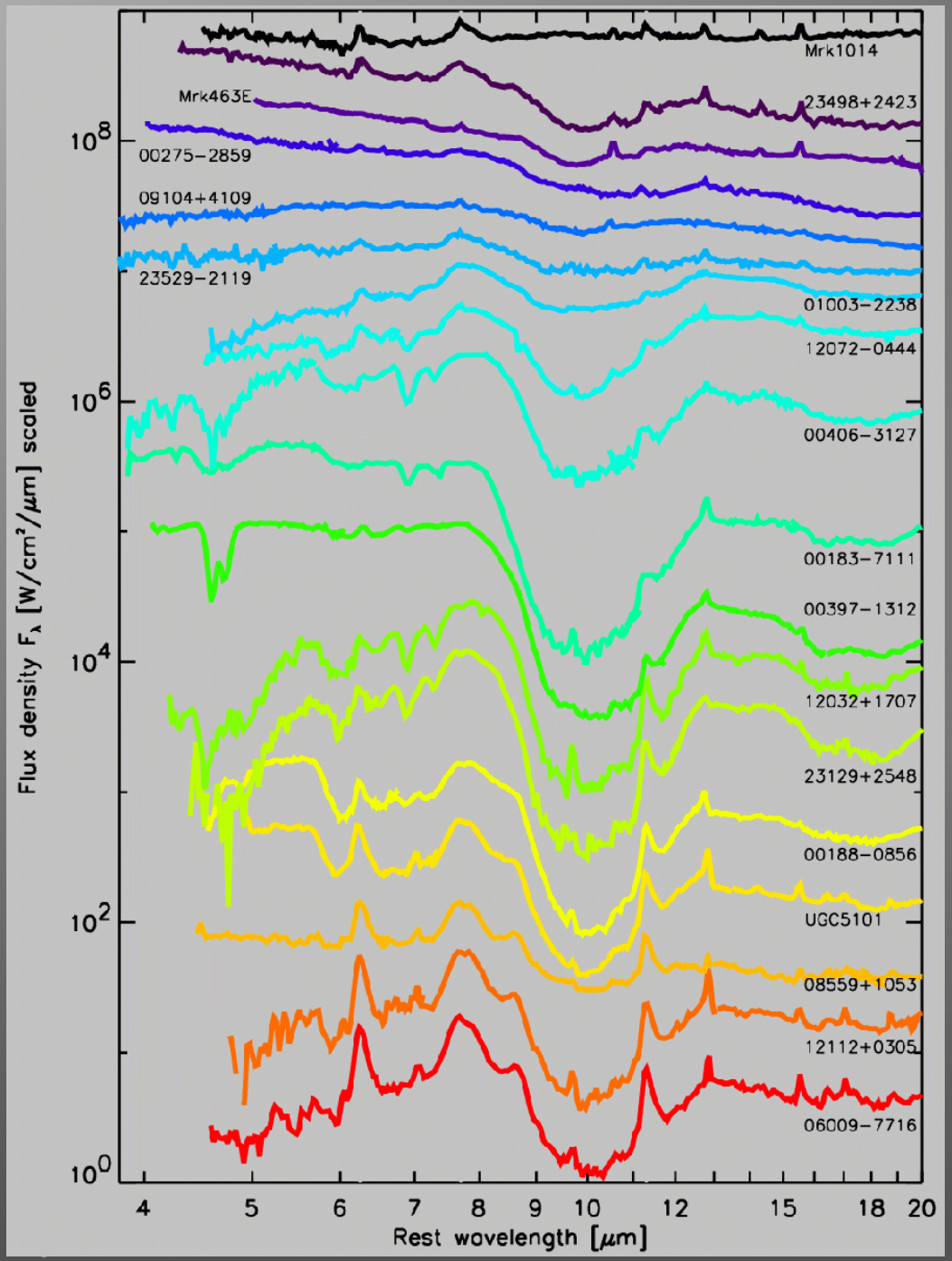

The first 18
low-resolution
IRS spectra
of ULIRGs

Diversity!
is the name of the game…

IRS Spectra of BGS Sources

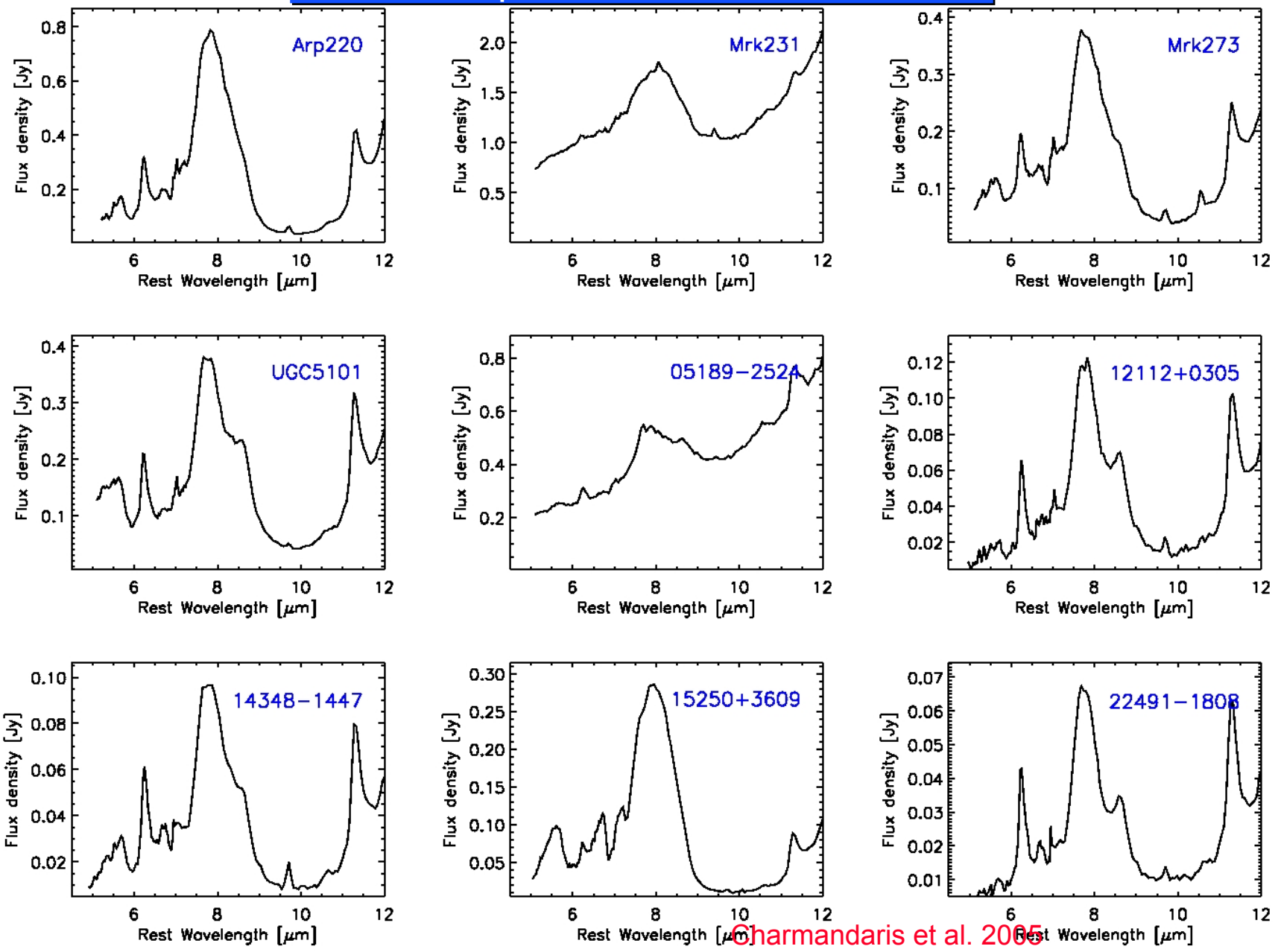

Charmandaris et al. 2005

IRS SL and LL Spectra

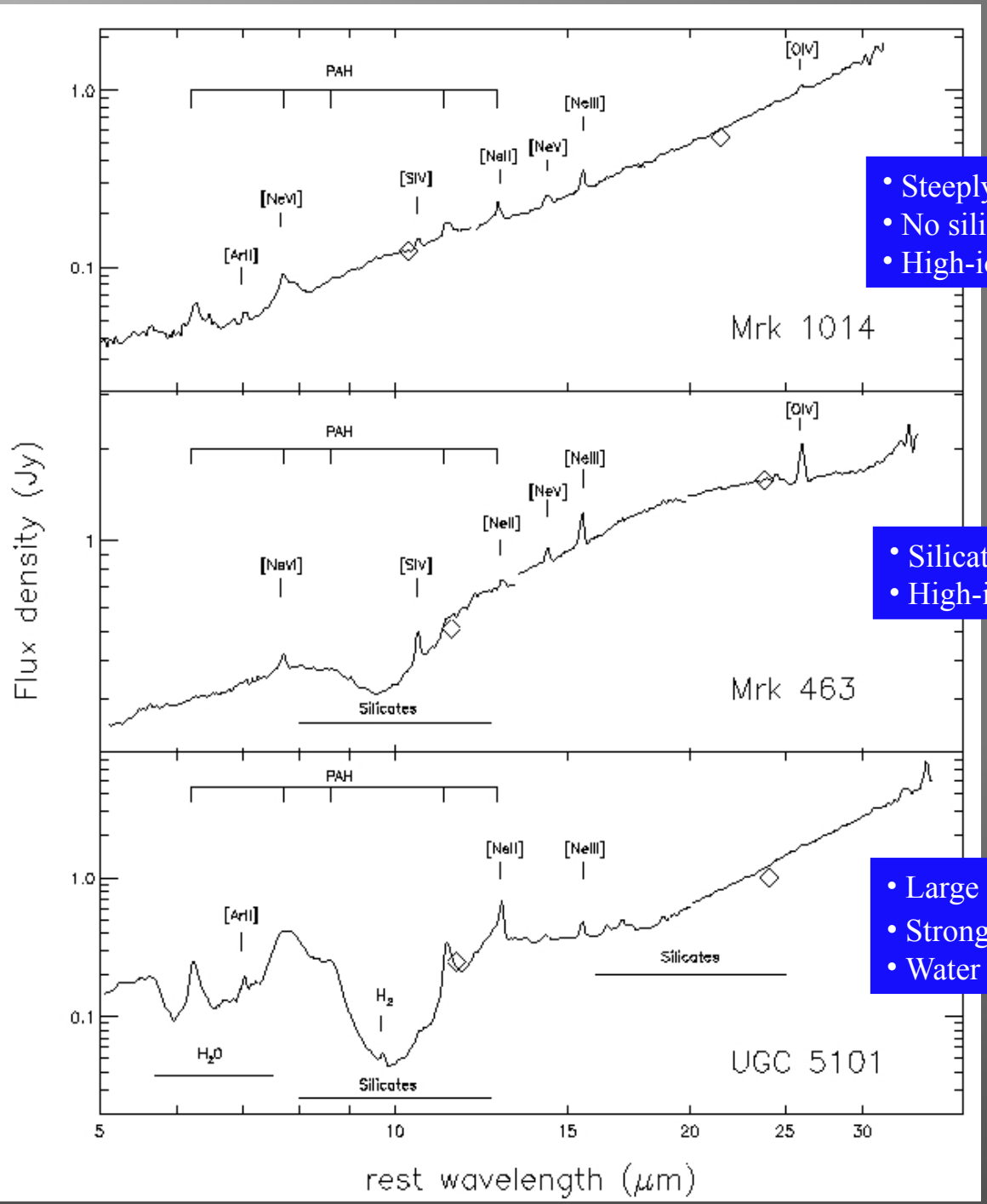

- Steeply rising continuum
- No silicate absorption
- High-ionization lines and PAH

L_{IR} ~ 4.2x10^{12} $L_\odot$)

…oad-line, dusty QSO with twin tidal tails.

Mrk 463 (z=0.051; L_{IR} ~ 6.4x10^{11} $L_\odot$)

Merging, twin Seyfert 2 nuclei.
Mrk 463e dominates in IR.

- Silicate absorption
- High-ionization lines but no PAH

$_R$ ~ 9.5x10^{11} $L_\odot$)

…ER nucleus with a circum-nuclear starburst.

XMM and Chandra data suggest a buried AGN behind N_H ~10^{24} cm^{-2}.

- Large silicate absorption (A_V > 30 mag)
- Strong PAH emission
- Water ice and hydrocarbon absorption (5-7.5 μ m)

Armus, et al. 2004

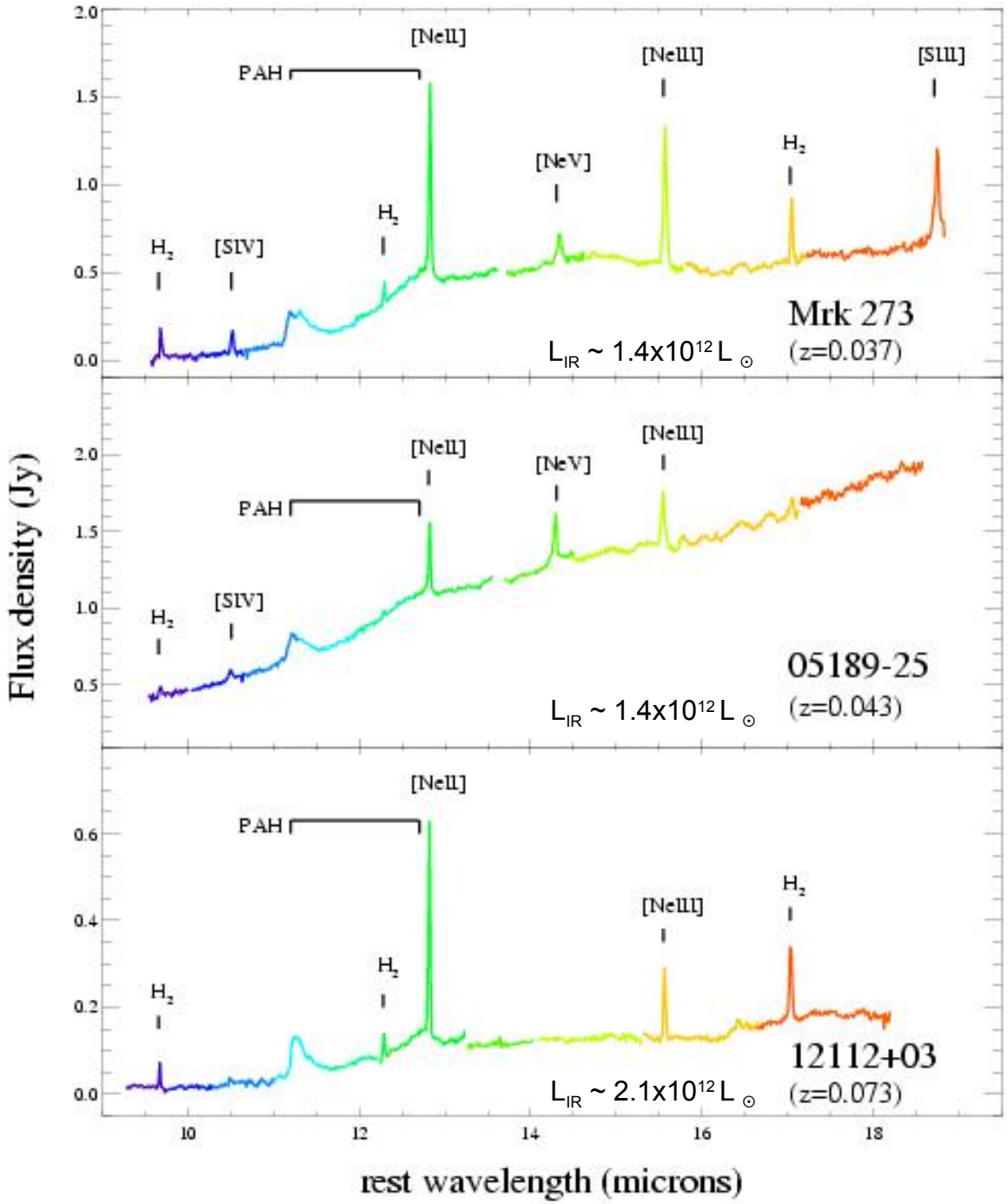

IRS SH Spectra

- Both Seyfert 2's show strong [NeV]. In 05189 [NeV]/[NeII] ~ 1
- The limit on [NeV]/[NeII] in 12112 is the lowest in the sample. The large PAH flux suggests a pure SB.
- Both Mrk 273 and 12112 have strong H_2 emission.

Arp220

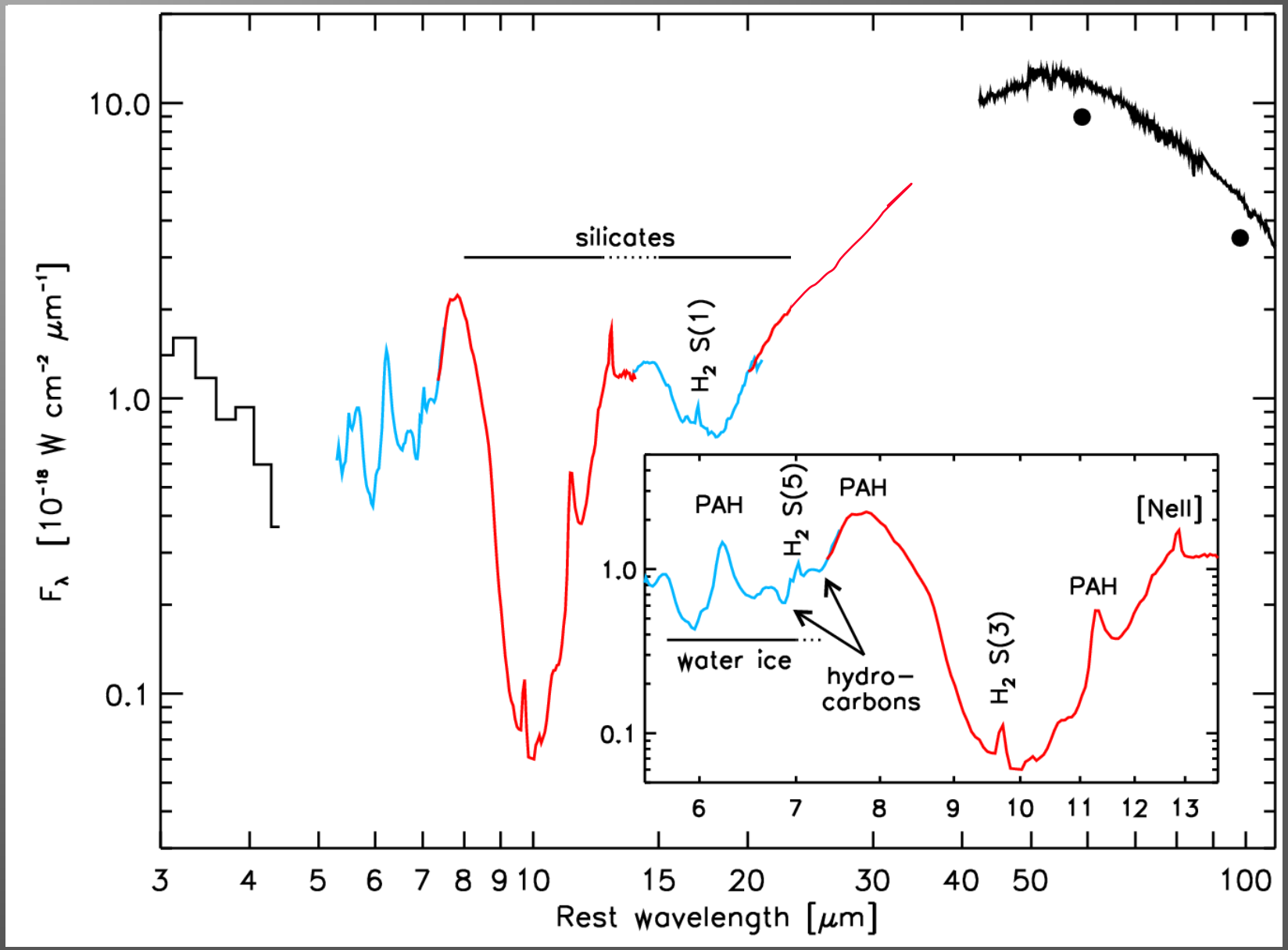
10.0
1.0
0.1
F_λ [10^{-18} W cm^{-2} μm^{-1}]
silicates
H_2 S(1)
PAH
H_2 S(5)
PAH
[NeII]
water ice
hydro–
carbons
H_2 S(3)
PAH
3
4
5
6
7
8
9
10
15
20
30
40
50
100
Rest wavelength [μm]

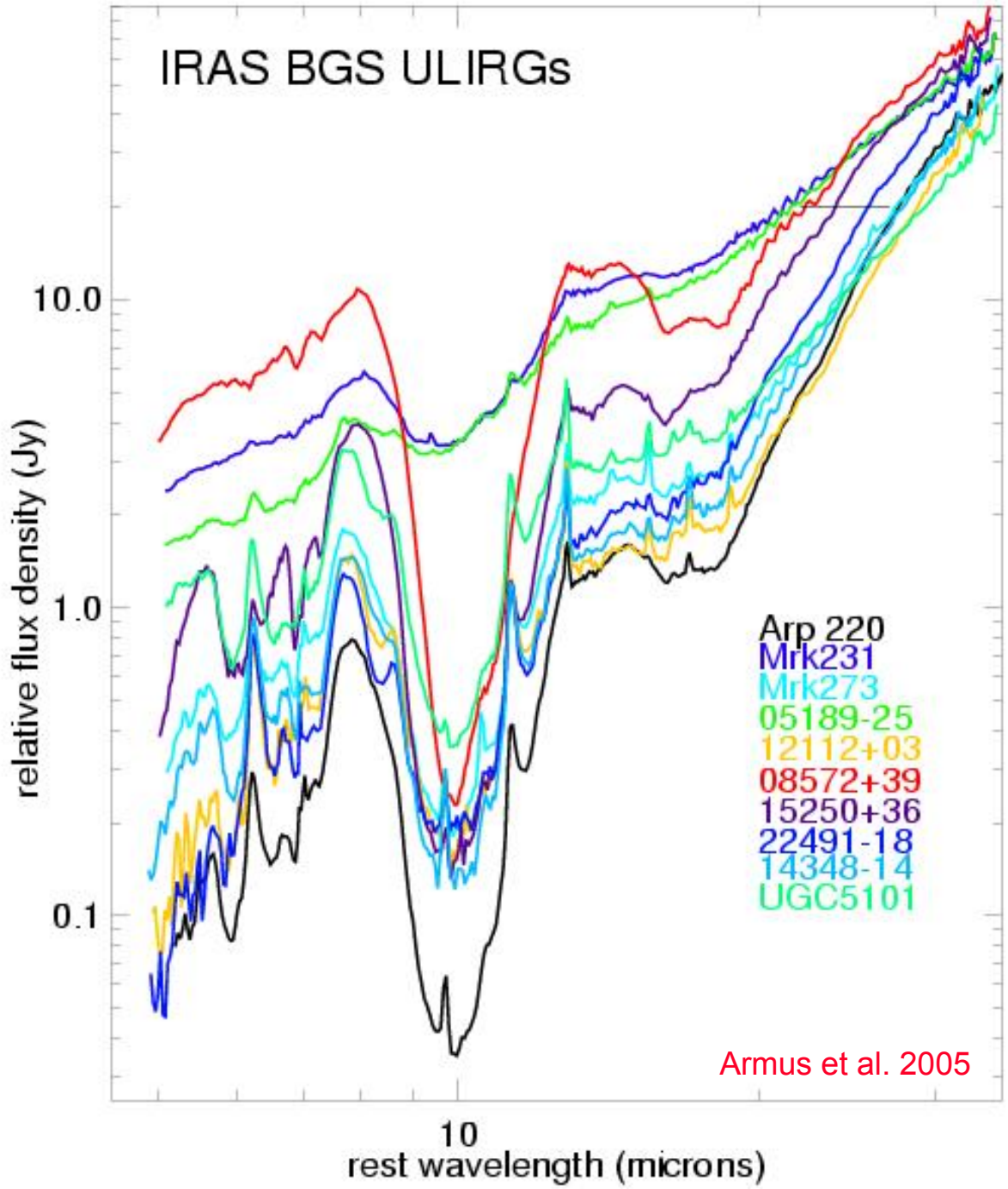
IRAS BGS ULIRGs
10.0
1.0
0.1
relative flux density (Jy)
10
rest wavelength (microns)
Arp 220
Mrk231
Mrk273
05189-25
12112+03
08572+39
15250+36
22491-18
14348-14
UGC5101
Armus et al. 2005

ULIRG IRS line ratios

	z	[NeV] / [NeII]	[NeV] 14.3 flux (1E-21 W cm^{-2})	Optical/N IR class	6.2 EQW	L_{HX}/L_{IR} (10^{-4})
UGC 5101	0.040	0.13	6.1	L/H	0.147	(15)
Arp 220	0.018	< 0.02	< 1.5	L	0.249	0.2
Mrk 231	0.042	< 0.18	< 4.3	S1	0.006	(35)
Mrk 273	0.037	0.28	15.0	S2	0.138	4.7
05189-25	0.043	0.98	21.8	S2 /S1	0.034	27
08572+39	0.058	< 0.11	< 1.0	H	< 0.01	
12112+03	0.073	< 0.02	< 0.3	L/H	0.694	0.2
14348-14	0.083	< 0.04	< 0.5	L/H	0.303	0.3
15250+36	0.055	< 0.06	< 0.7	H	0.039	0.4
22491-18	0.077	< 0.07	< 0.4	H	0.568	0.1
Mrk 1014	0.16 3	0.9	6.8	S1	0.061	
Mrk 463	0.050	1.6	18.3	S2	< 0.03	
NGC 6240	0.024	0.04	12.9	L	0.376	13

IRS [NeV] limits are 5-20x lower than SWS limits *(Genzel, et al. 1998)*

Hard X-ray data: Ptak et al. 2003; Franceschini et al. 2003; Braito et al. 2004; Imanishi et al. 2003; Iwasawa et al. 2004

Low Ionization Narrow Lines

	I	II	III	IV	V	VI	VII
$_{1}H$	13.6						
$_{2}He$	24.6	54.4					
$_{6}C$	11.3	24.4	47.9	64.6	392.1		
$_{7}N$	14.5	29.5	47.4	77.7	97.9	552.1	
$_{8}O$	13.6	35.1	54.9	77.4	113.9	138.1	739.3
$_{10}Ne$	21.6	41.0	83.5	97.1	126.2	157.9	207.3
$_{12}Mg$	7.6	15.0					
$_{14}Si$	8.2	16.3	33.5	45.1			
$_{16}S$	10.4						

High Ionization Narrow Lines

	I	II	III	IV	V	VI	VII
$_{1}H$	13.6						
$_{2}He$	24.6	54.4					
$_{6}C$	11.3	24.4	47.9	64.6	392.1		
$_{7}N$	14.5	29.5	47.4	77.7	97.9	552.1	
$_{8}O$	13.6	35.1	54.9	77.4	113.9	138.1	739.3
$_{10}Ne$	21.6	41.0	83.5	97.1	126.2	157.9	207.3
$_{12}Mg$	7.6	15.0					
$_{14}Si$	8.2	16.3	33.5	45.1			
$_{16}S$	10.4						

Broad Permitted Lines

	I	II	III	IV	V	VI	VII
$_{1}$H	13.6						
$_{2}$He	24.6	54.4					
$_{6}$C	11.3	24.4	47.9	64.6	392.1		
$_{7}$N	14.5	29.5	47.4	77.7	97.9	552.1	
$_{8}$O	13.6	35.1	54.9	77.4	113.9	138.1	739.3
$_{10}$Ne	21.6	41.0	83.5	97.1	126.2	157.9	207.3
$_{12}$Mg	7.6	15.0					
$_{14}$Si	8.2	16.3	33.5	45.1			
$_{16}$S	10.4						

Critical Densities of (semi)critical lines

Narrow Forbidden Lines	
[Ne V] λλ3343,3426,	1.7×10^{7} cm^{-3}
[O II] λ3727	1.4×10^{4}
[Ne III] λλ3869,3967	8.3×10^{6}
[O III] λ4363	4.0×10^{7}
[O III] λλ4959,5007	7.2×10^{5}
[O I] λλ6300,6363	1.8×10^{6}
[N II] λλ6548,6584	8.3×10^{4}
[S II] λ6716	2.0×10^{3}
[S II] λ6731	1.1×10^{4}

Broad Semi-Forbidden Lines	
O IV] λ1400	1.0×10^{11} cm^{-3}
O III] λ1663	6.6×10^{9}
N III] λ1748	1.3×10^{10}
Si III] λ1892	1.3×10^{11}
C III] λ1909	3.8×10^{9}

Spitzer Mid-IR Diagnostic Diagram

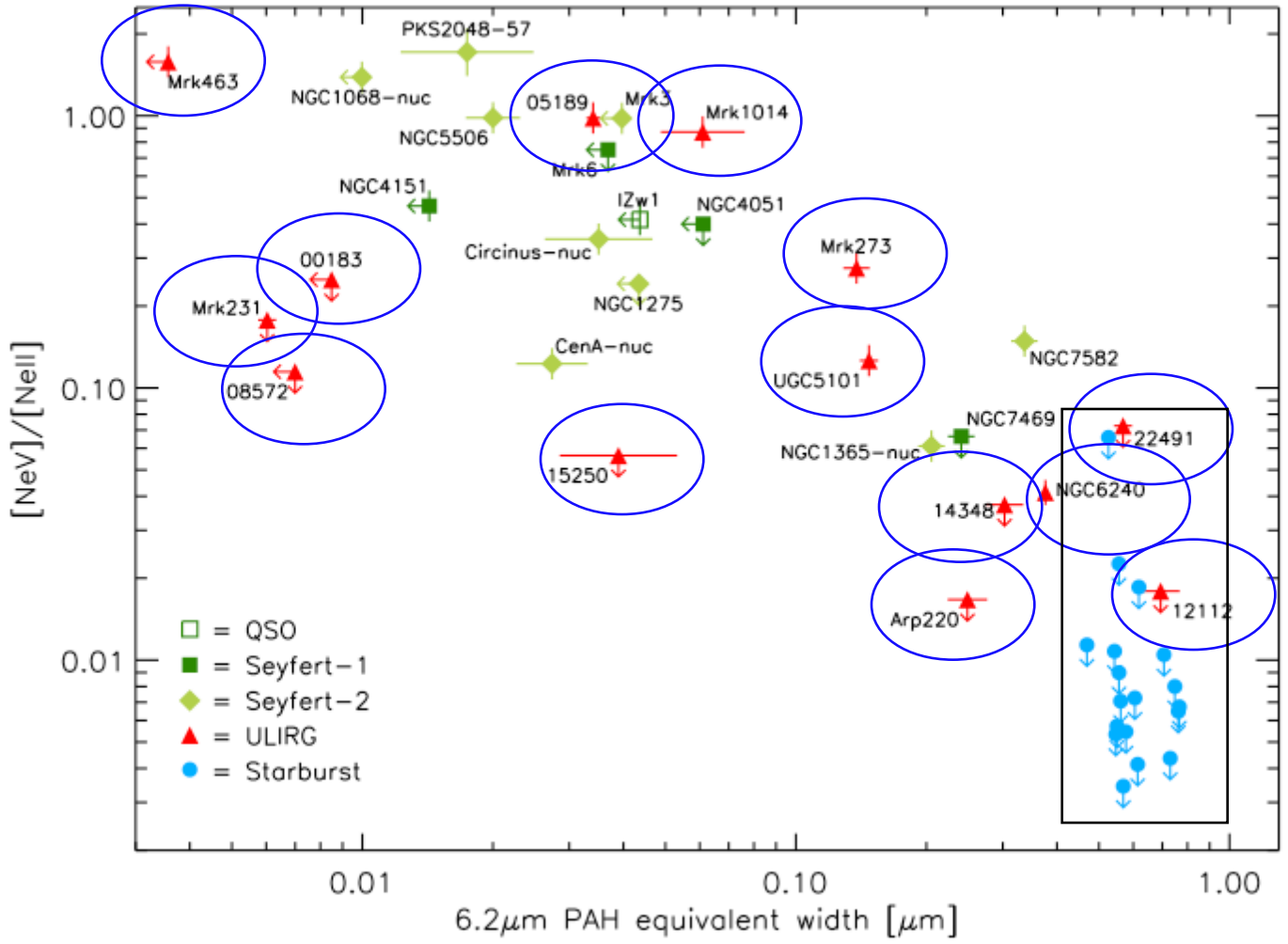

ISO Diagnostic Diagram

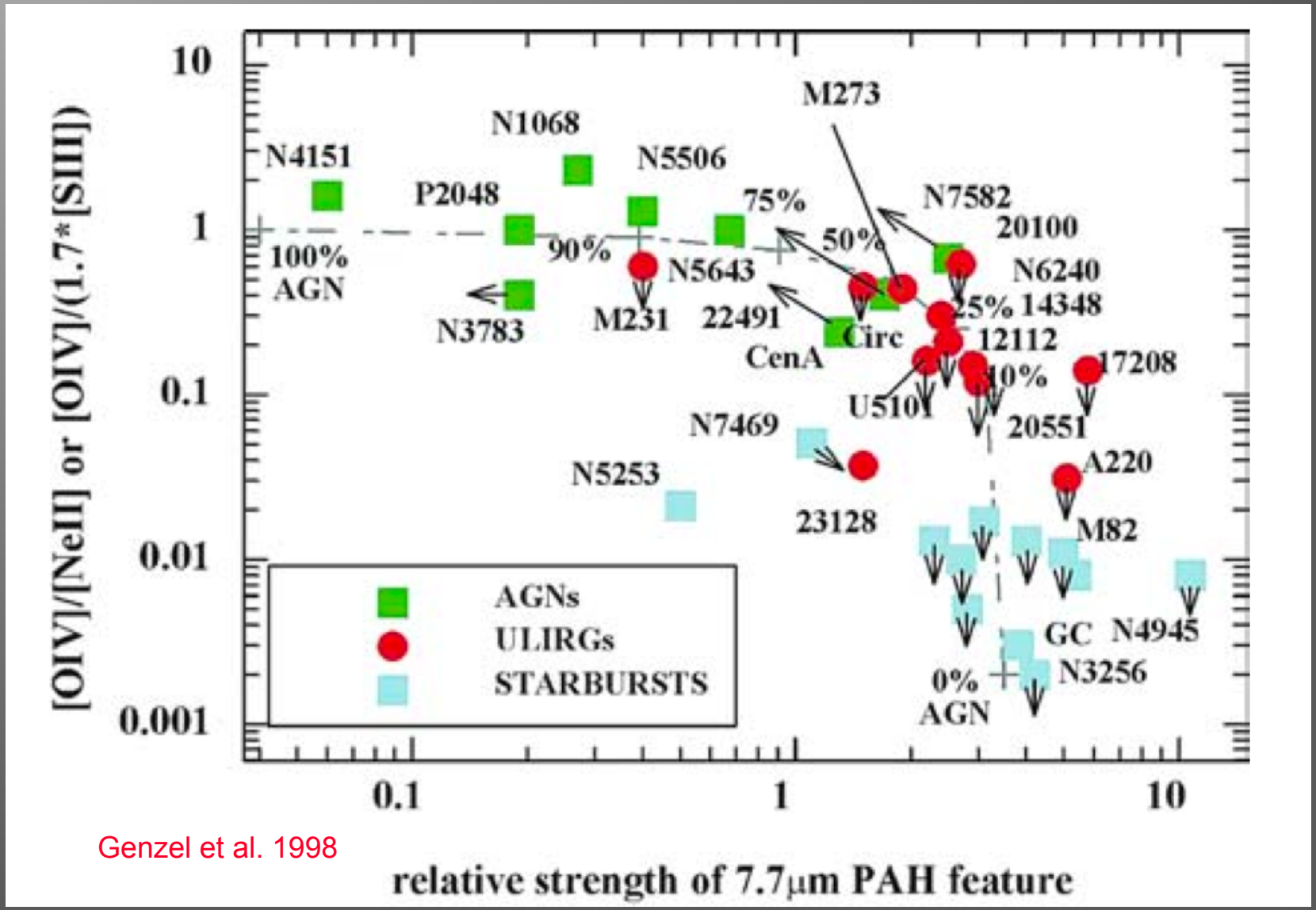

Genzel et al. 1998

AGN thermal emission in mid-IR continuum

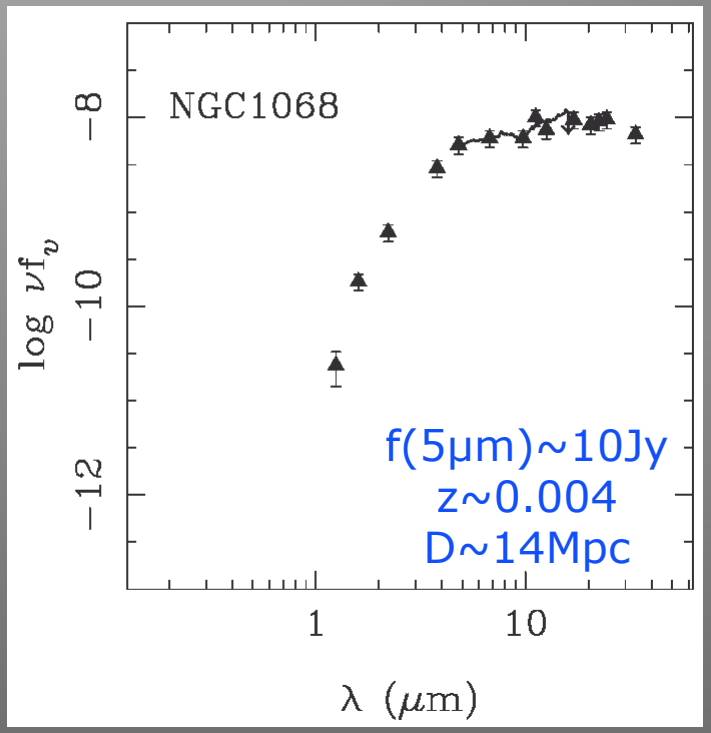

Alonso-Herrero et al. 2003

- Rising slope of thermal emission from the AGN torus from 2-5μm due to grains radiating in near-equilibrium
- Excess over starlight at ~4-5μm

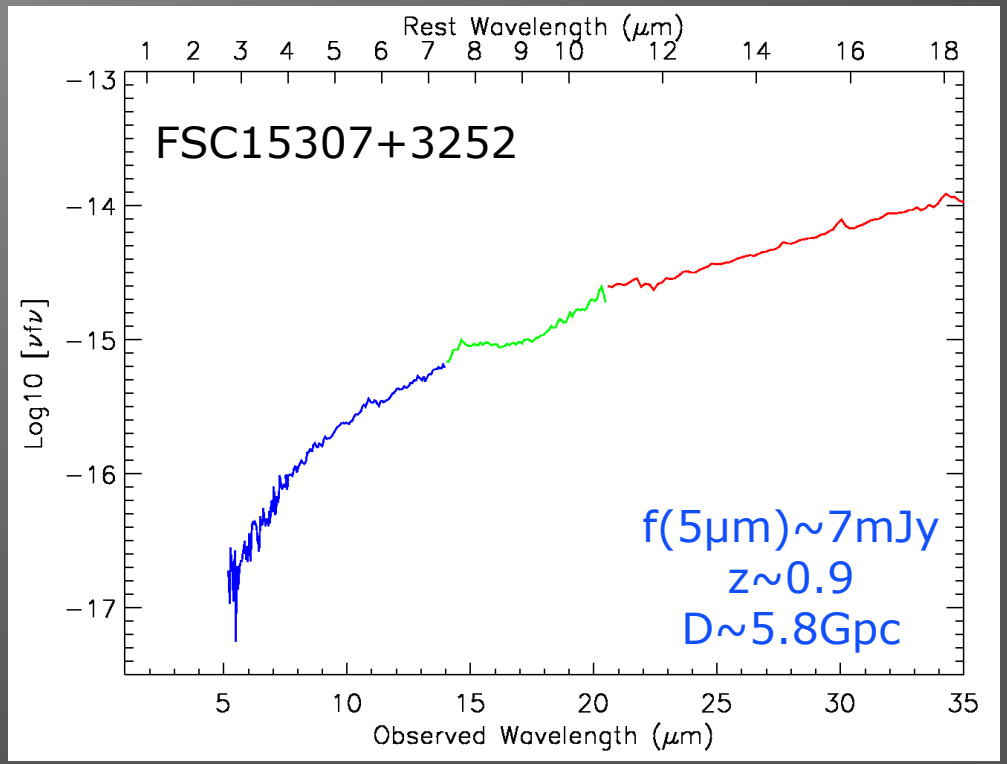

Variation in IRS low resolution spectra

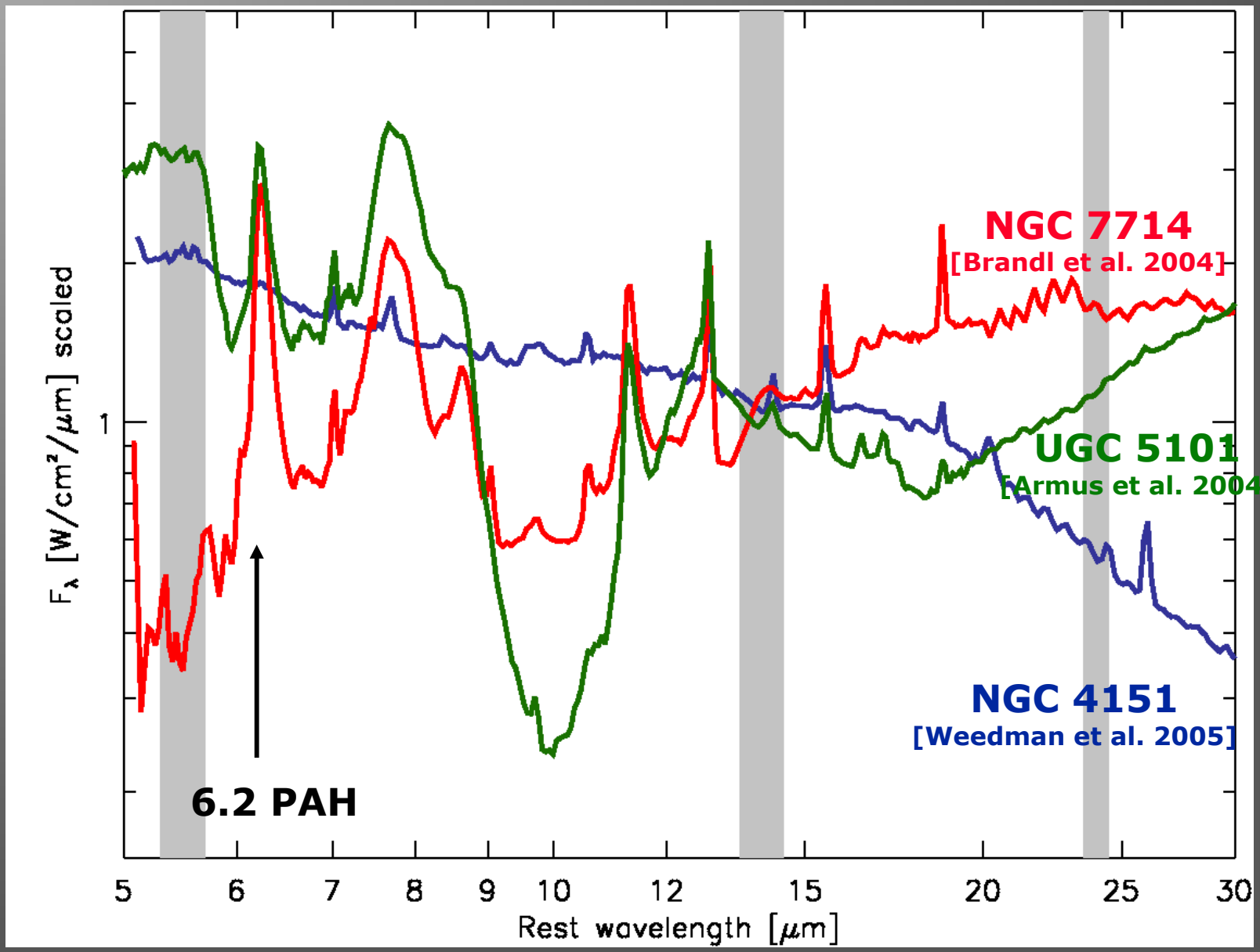

Selection of the three extreme spectra

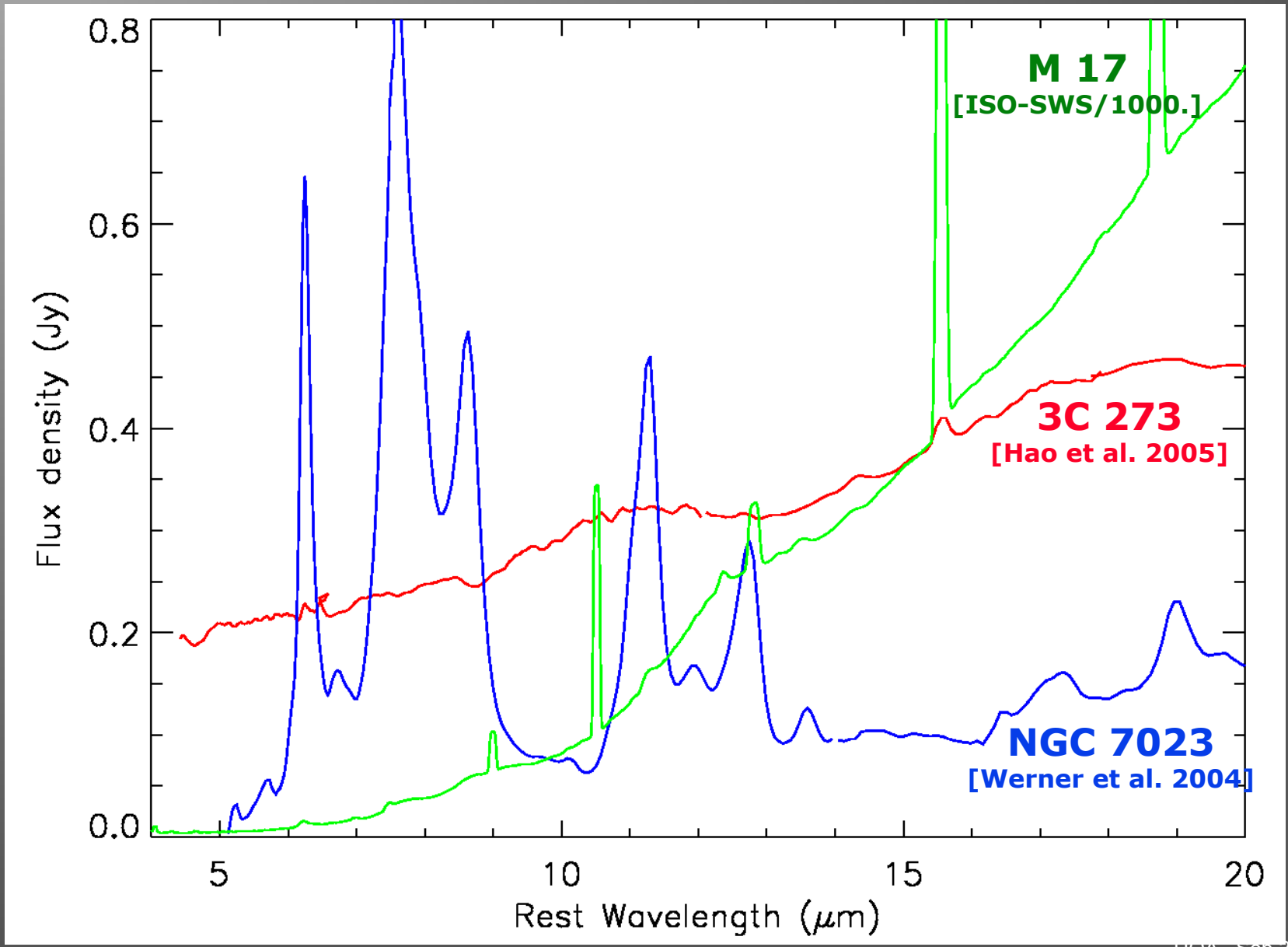

The mid-IR [AGN/SB/PDR] parameter space

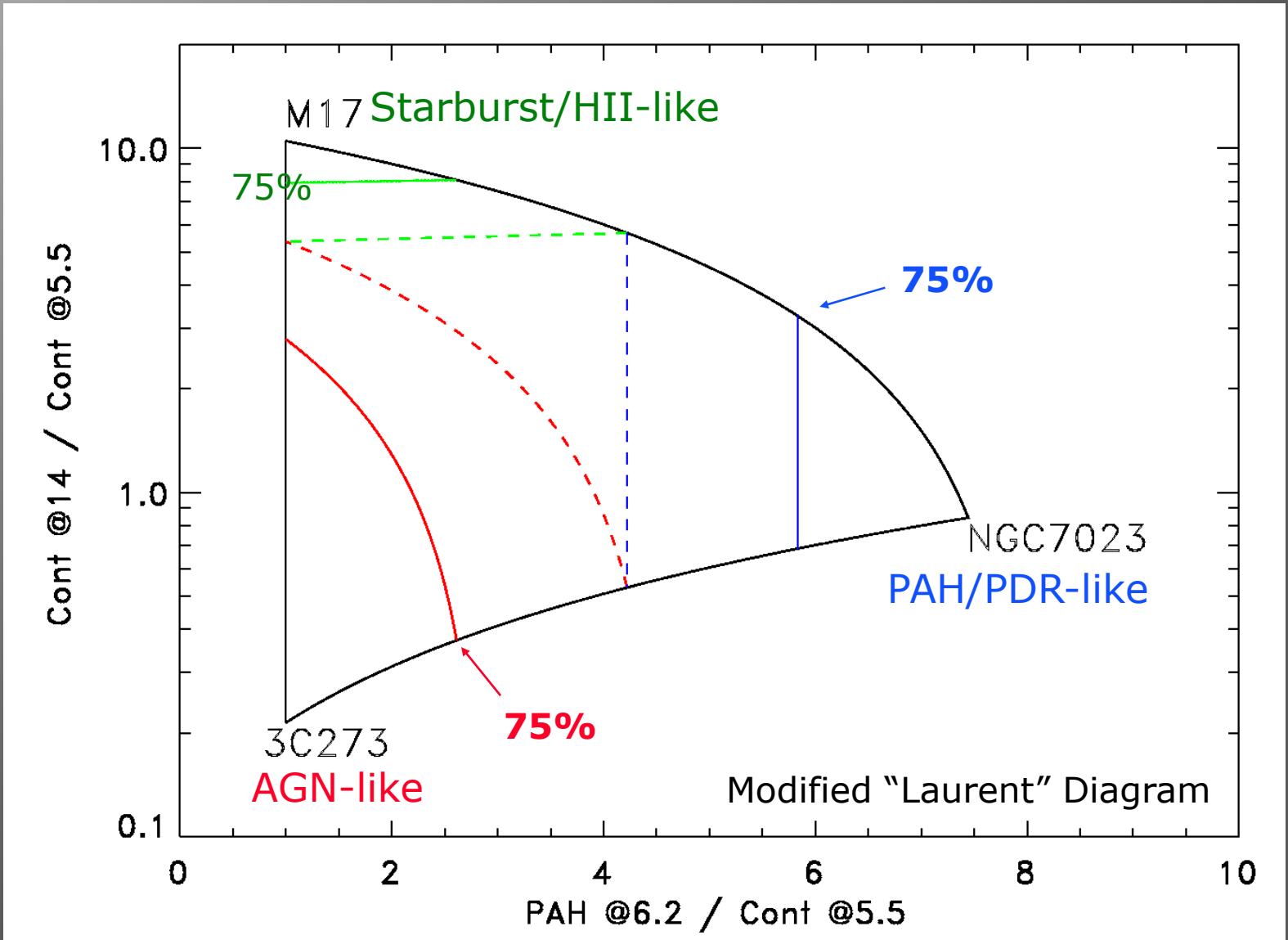

Populating the [AGN/SB/PDR] diagram

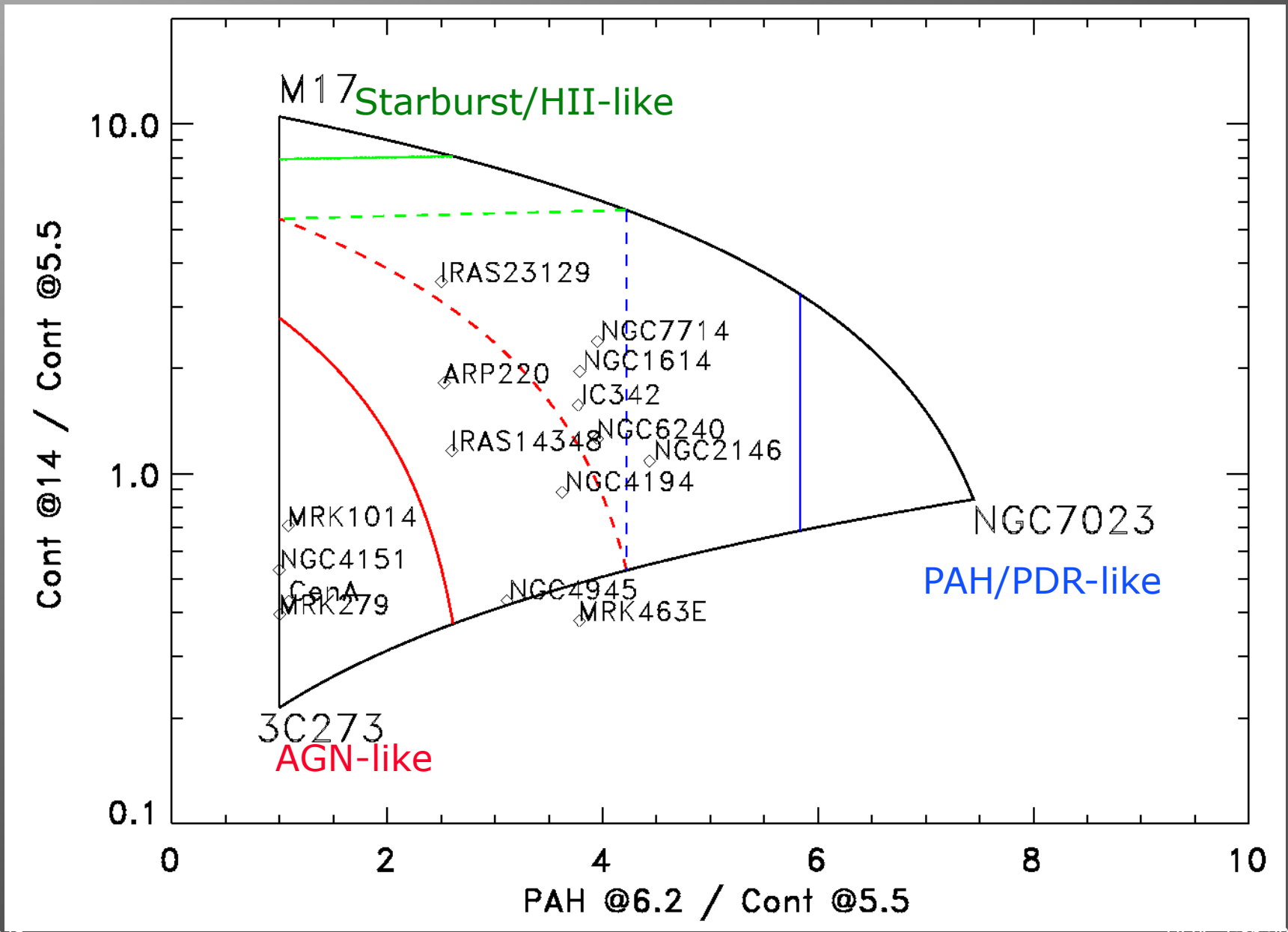

Infrared Continuum Fitting

- Another approach to quantitatively access the contribution of the various components in the observed IR emission from a source is to fit the IR spectrum using theoretical models.

- Full radiative transfer modeling of the source (ie. Siebenmorgen & Grugel 1992,1993; Nenkova & Elitzur 2001,2002; Dopita et al. 2005) is challenging since in addition to dust it requires major assumptions on the geometry of the source. Typically applicable to detailed studies of individual sources.

- For studies of larger samples, semi-empirical methods using linear composition of known IR templates with different extinctions have proven very useful (ie. Tran et al. 2001)

- Recently a new fitting approach relying on the Spitzer/IRS 5-38μm spectra, using constrains from near-/far-IR observations has been developed (Marshall et al. 2005)…

Decomposition of the Infrared Spectrum

Core of the method

- Assume absorption cross sections from Li & Draine (2001) and an MRN grain-size distribution
- Calculate the opacities of PAH, graphitic and smoothed astronomical silicate grains.

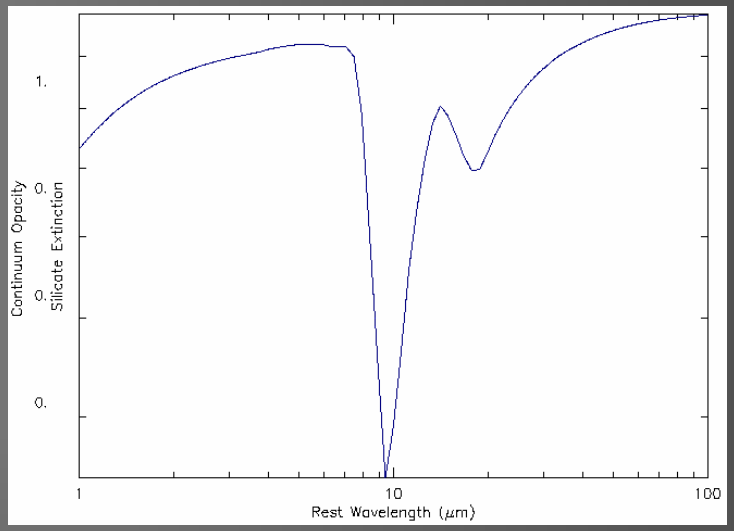

- Each dust component has a quasi-fixed temperature i.e.. the fitting process is really an expansion into several temperature basis components.
- The number of dust components is fixed for the sample so that all galaxies are fit in a uniform manner.
- In addition to a ~3500 K stellar blackbody and PAH component, we find that we need ~3 additional continuum dust components with T~400, ~150, and ~30 K to accurately fit the entire sample.
- An AGN manifests its presence with the requirement of an additional hot dust component T~800K (Laurent et al. 2000)

The case of NGC7714: a starburst

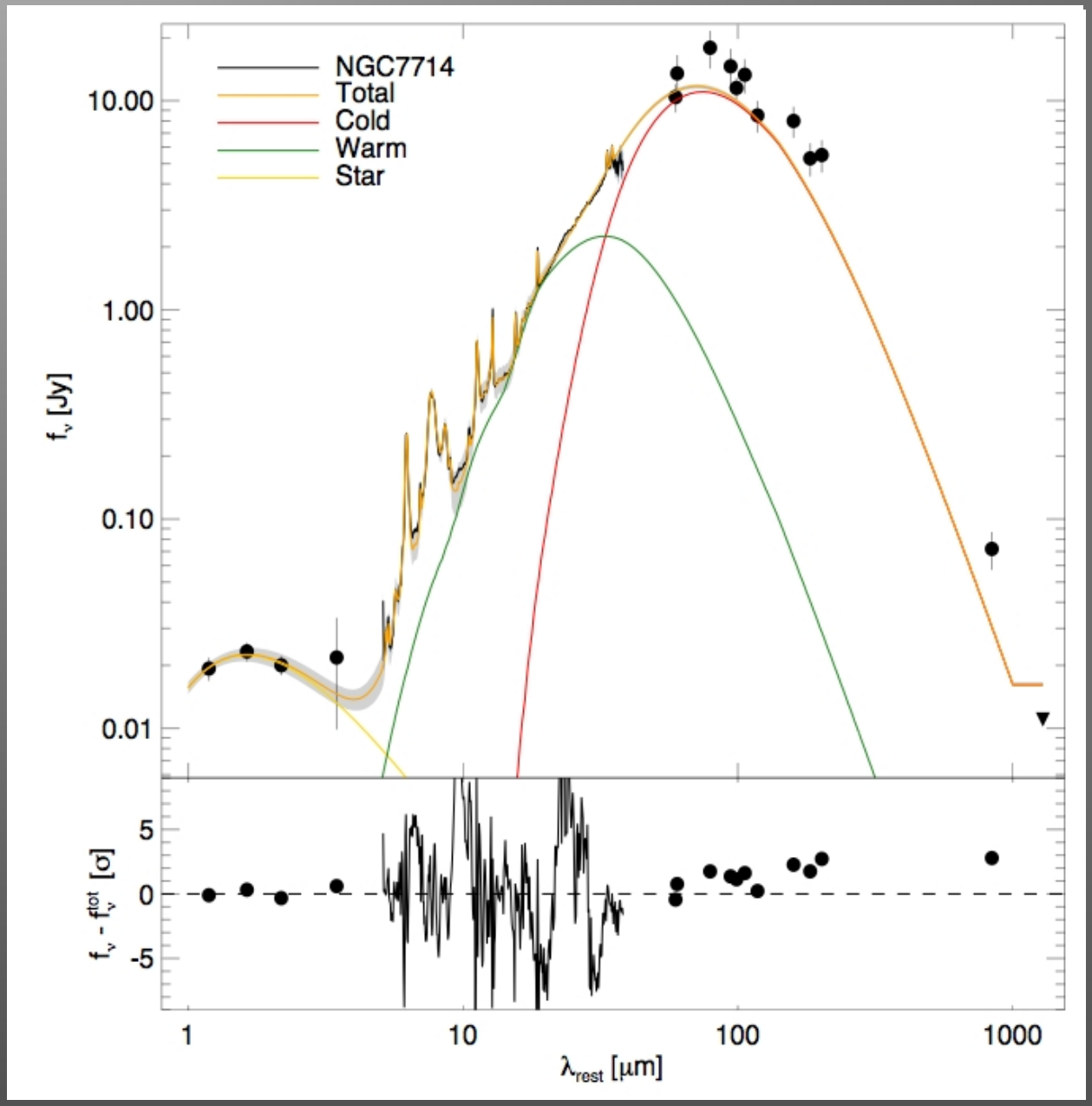

$T_* \sim 3100$ K

$T_{cold} \sim 30$ K

$T_{warm} \sim 85$ K

$\tau_{warm} \sim 0.6$

$L_{dust} \sim 4.5 \times 10^{10}\ L_\odot$

$L_{cold}/L_{dust} \sim 0.67$

$L_{warm}/L_{dust} \sim 0.33$

$L_{PAH}/L_{dust} \sim 0.05$

$M_{cold} \sim 5.7 \times 10^{6}\ M_\odot$

$M_{warm} \sim 8.3 \times 10^{3}\ M_\odot$

The case of PG0804-761: a QSO/AGN

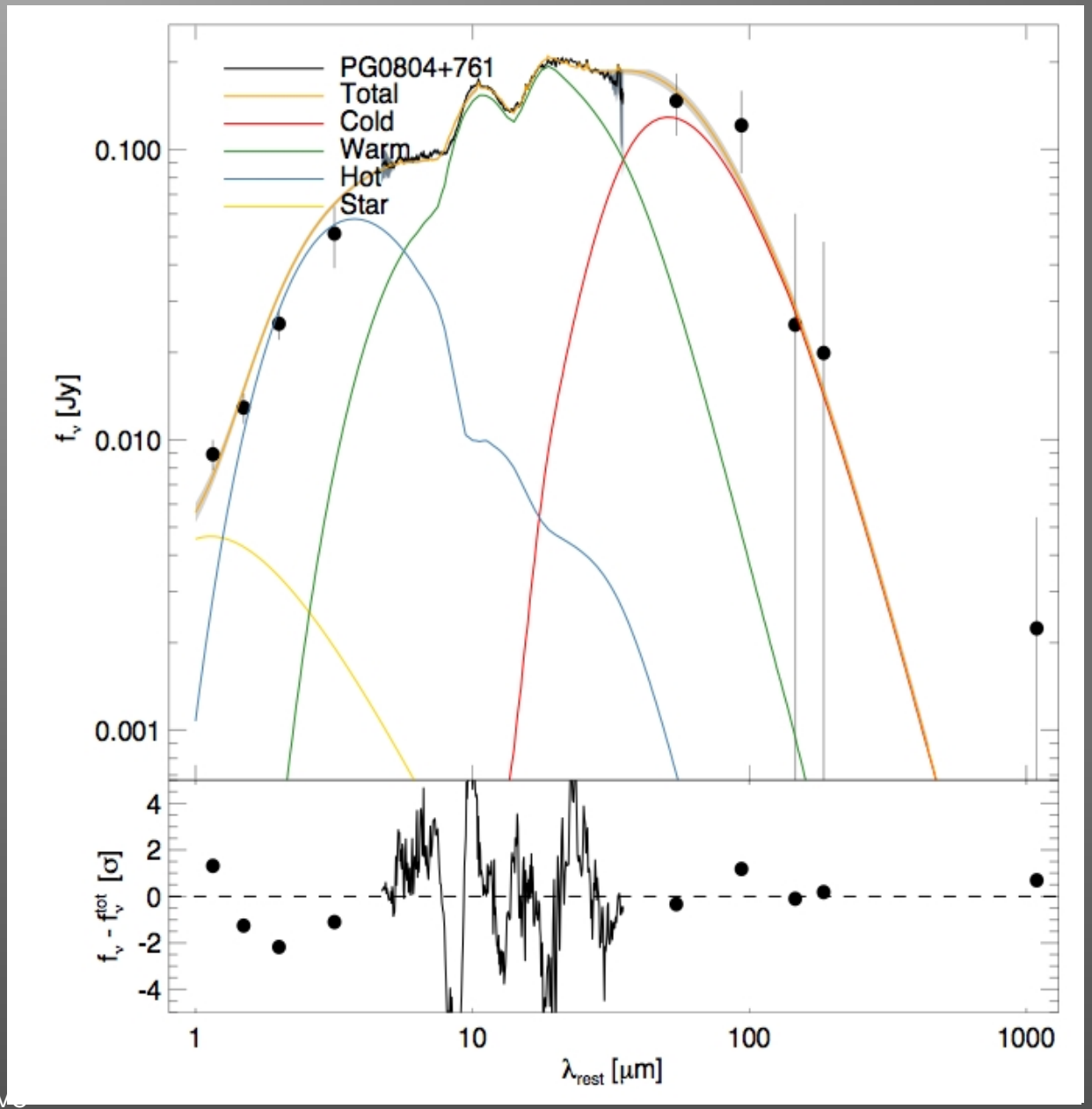

$T_* \sim 4500$ K

$T_{cold} \sim 43$ K

$T_{warm} \sim 215$ K

$T_{hot} \sim 817$ K

$\tau_{warm} \sim 0.7$

$\tau_{hot} \sim 0.7$

$L_{dust} \sim 8.4 \times 10^{11}\ L_\odot$

$L_{cold}/L_{dust} \sim 0.07$

$L_{warm}/L_{dust} \sim 0.61$

$L_{hot}/L_{dust} \sim 0.48$

$M_{cold} \sim 1.4 \times 10^{6}\ M_\odot$

$M_{warm} \sim 3.4 \times 10^{3}\ M_\odot$

$M_{hot} \sim 30\ M_\odot$

The case of Mrk1014: a ULIRG

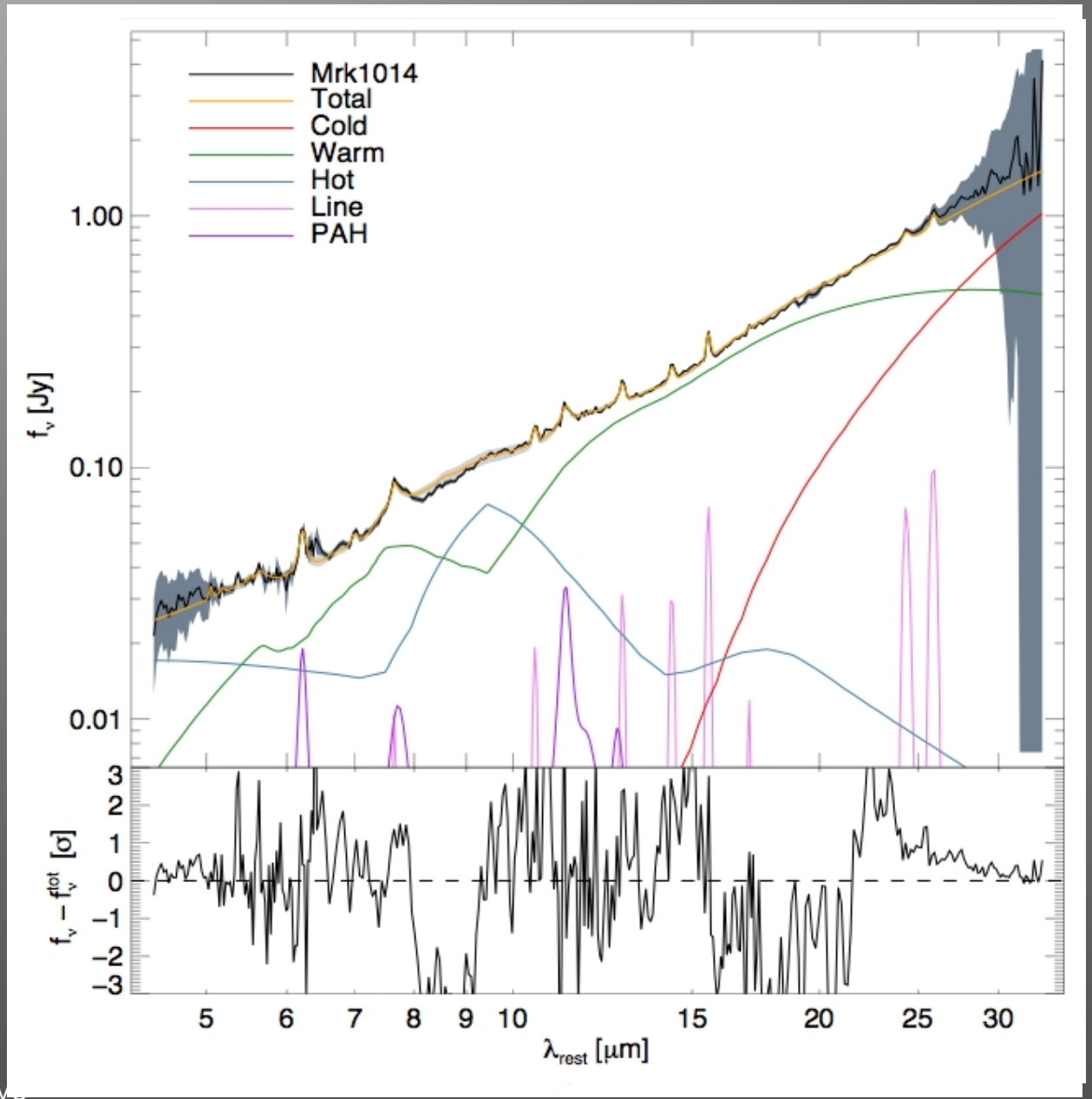

$T_* \sim 3300$ K

$T_{cold} \sim 38$ K

$T_{warm} \sim 121$ K

$T_{hot} \sim 454$ K

$\tau_{warm} \sim 1.7$

$\tau_{ice} \sim 0.3$

$L_{dust} \sim 4.2 \times 10^{12}\ L_\odot$

$L_{cold}/L_{dust} \sim 0.57$

$L_{warm}/L_{dust} \sim 0.32$

$L_{hot}/L_{dust} \sim 0.1$

$M_{cold} \sim 1.5 \times 10^{8}\ M_\odot$

$M_{warm} \sim 2.6 \times 10^{5}\ M_\odot$

$M_{hot} \sim 83\ M_\odot$

PAH EQW vs. LIR

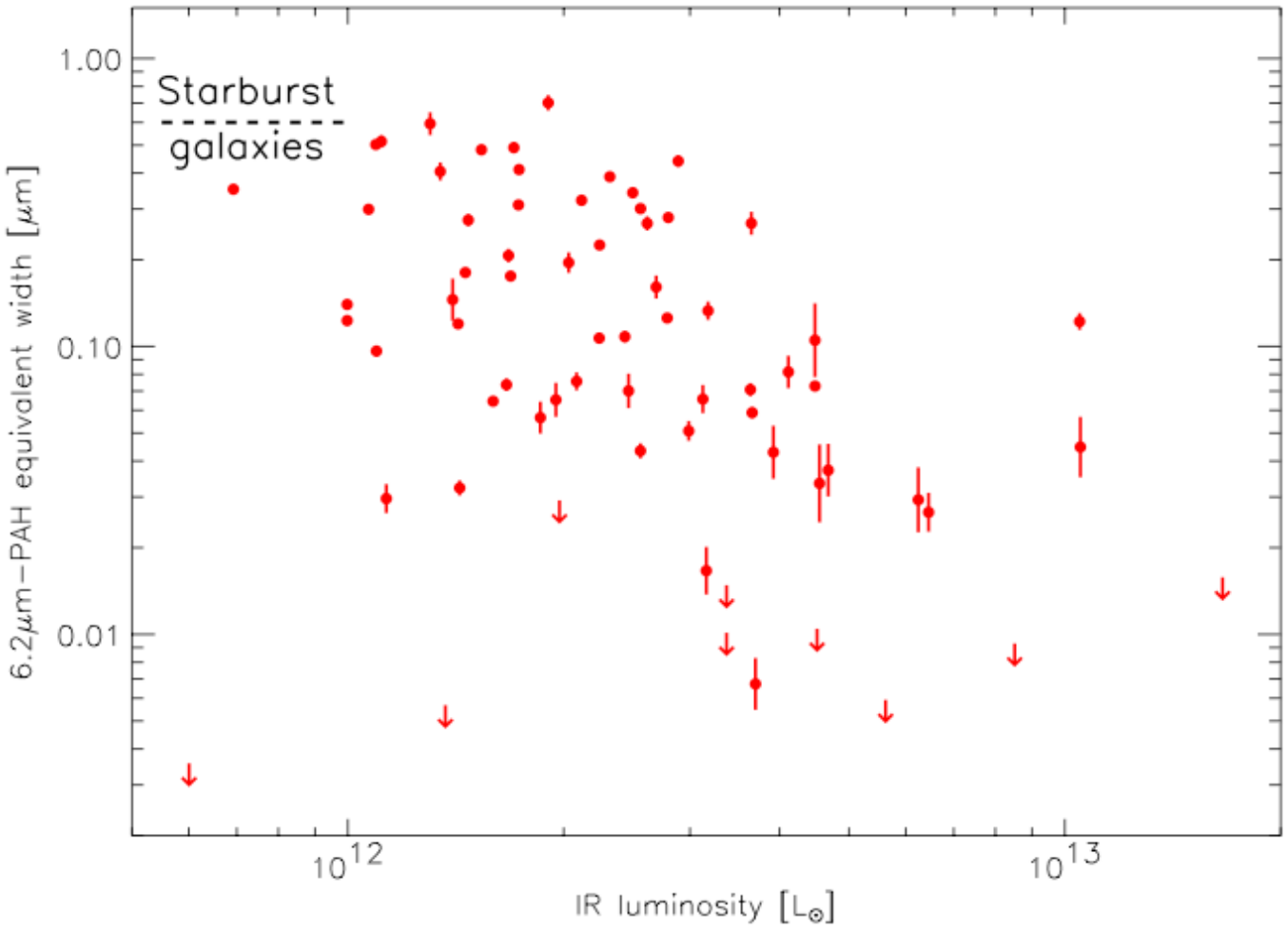

Mid-IR spectral of ULIRGs

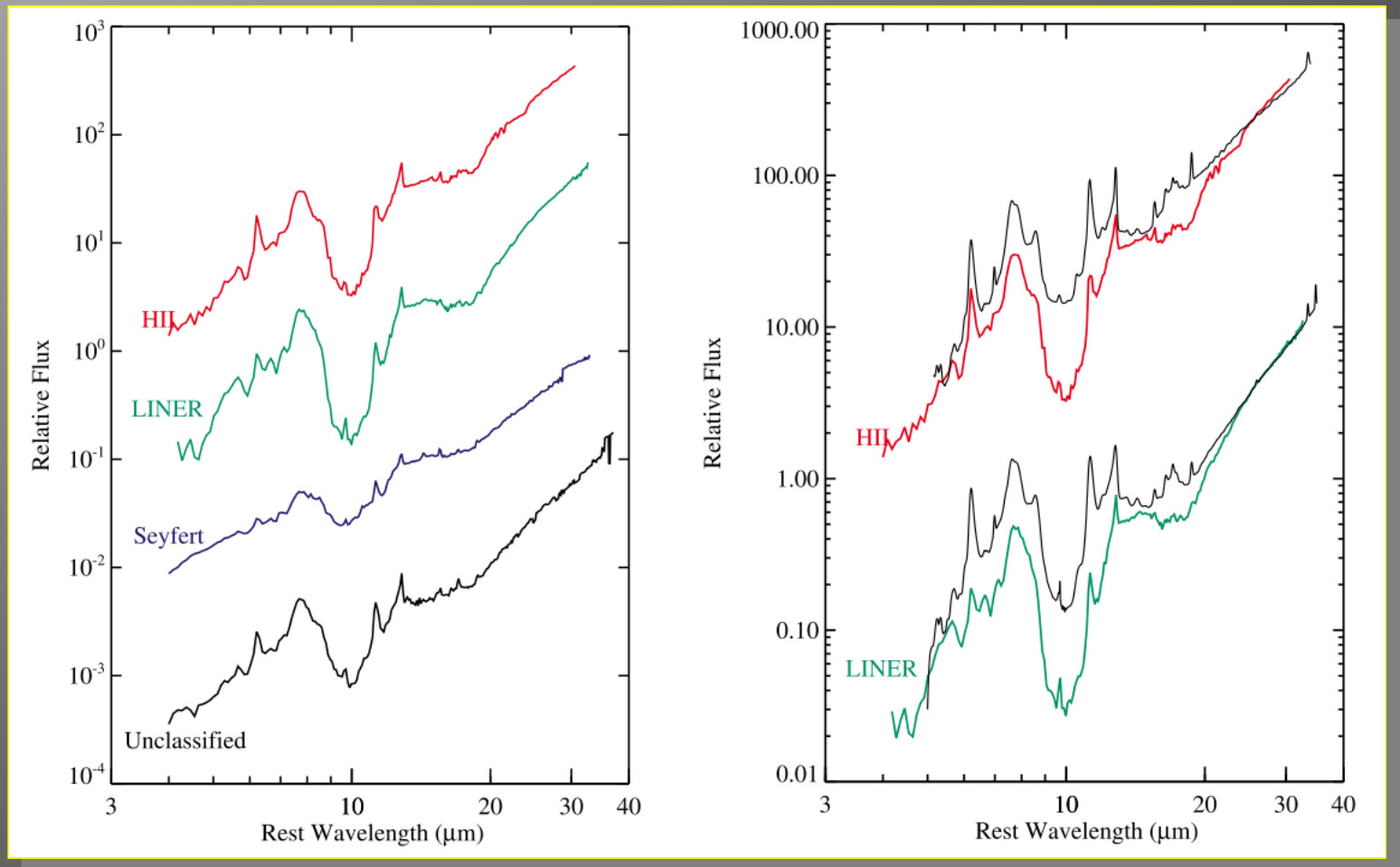

Based on 107 local ULIRGs (Armus et al. 2007, Desai et al. 2007)
The PAHs of starburst galaxies (HII) with L(IR) $>10^{12}$ Lsun do not scale

Averaged ULIRG SEDs

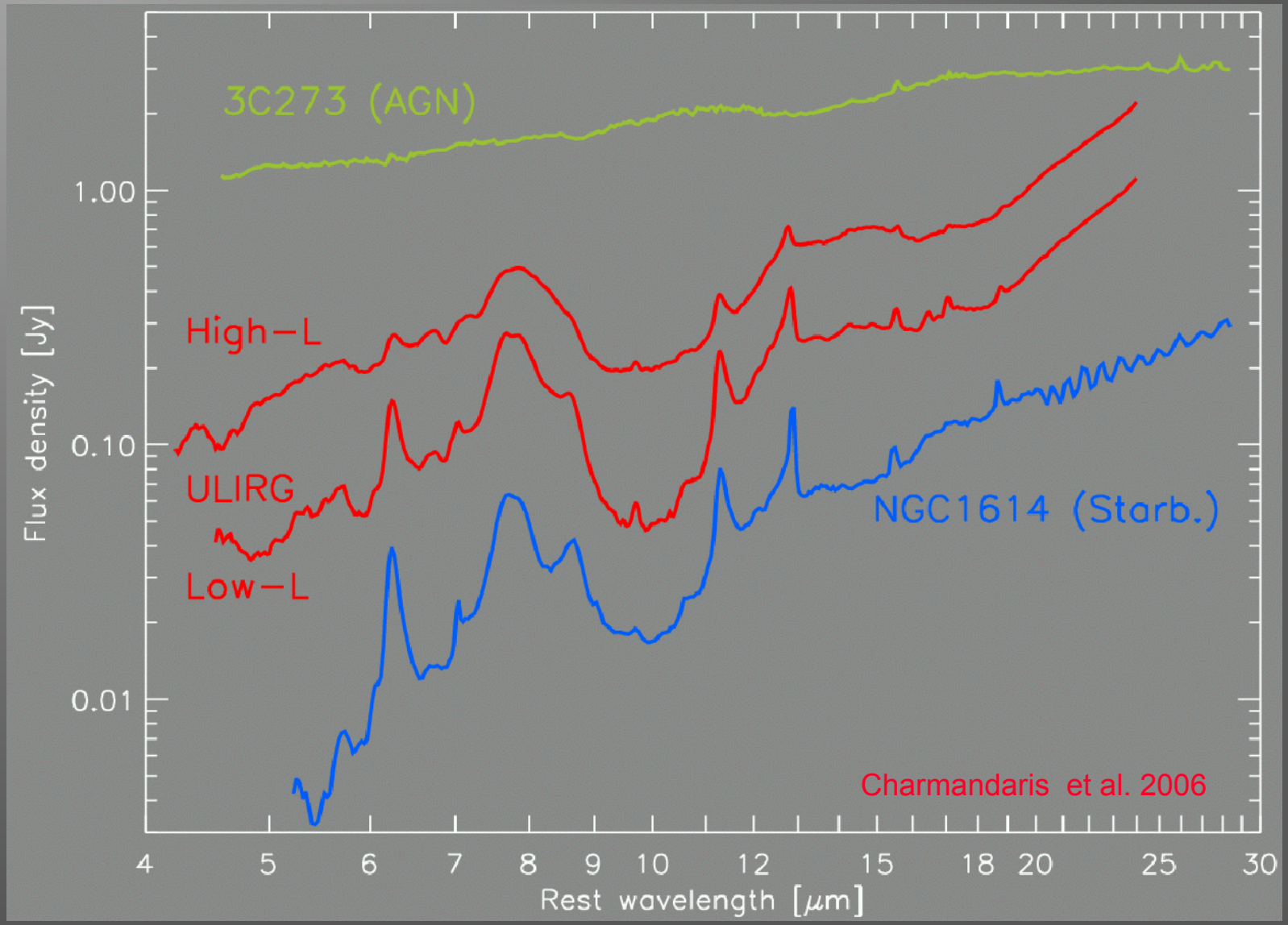

The Most Luminous local ULIRGs

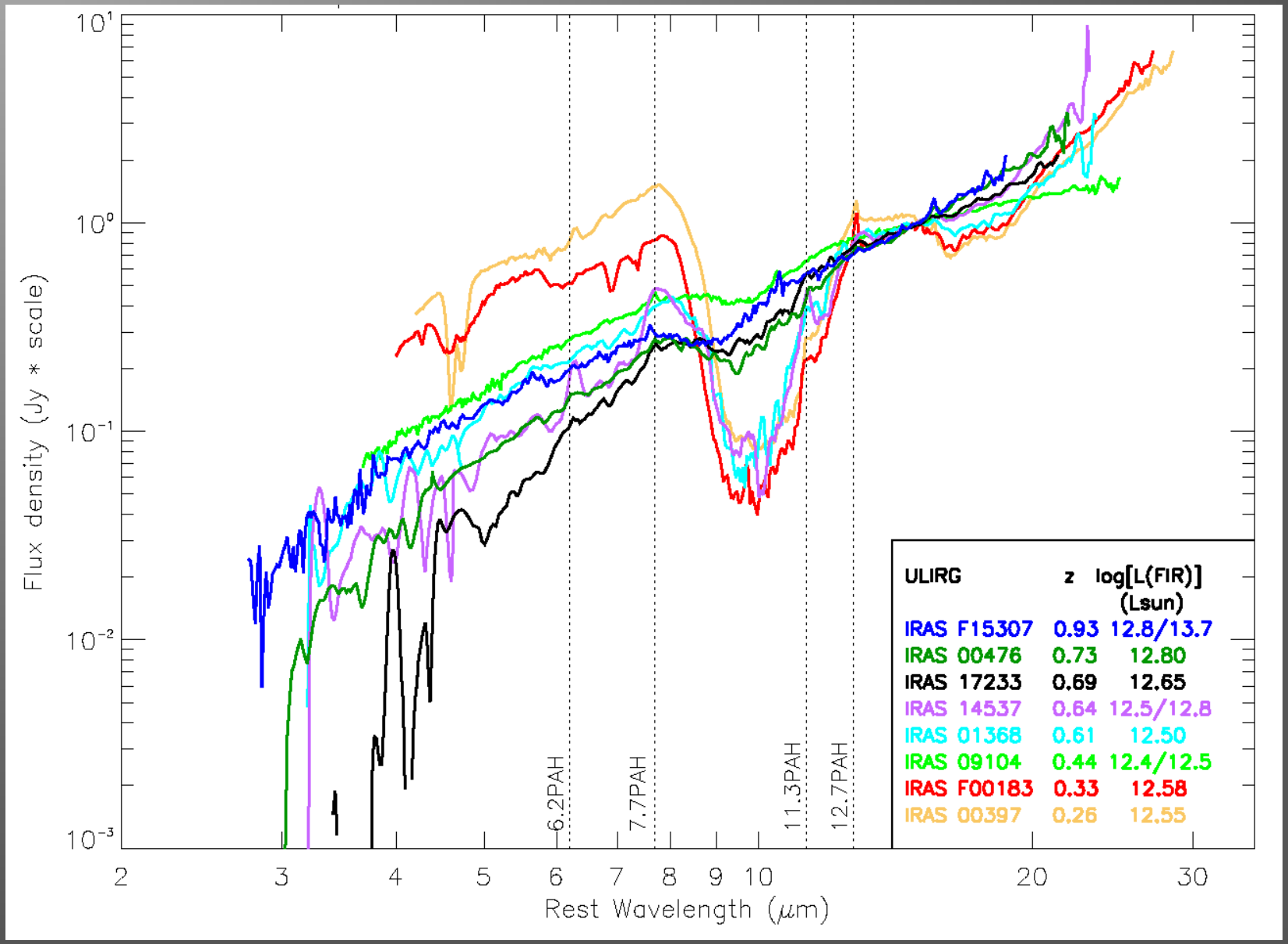

Studying the Infrared properties of the 12μm IRAS Seyfert Sample

The 12μm IRAS Sample

- IRAS 12>0.22 Jy, complete down to 0.3 Jy (893 sources - Rush et al. 1993)
- Average redshift ~0.013
- 116 Seyferts: 53 Sy 1s, 63 Sy 2s
- 103 were observed with the Spitzer/IRS (47 Sy 1s, 56 Sy 2s) at low resolution (95 in high-resolution)

- Note: Since the Seyfert classification is done via optical spectroscopy this is not strictly an IR "flux limited" sample

- Control Sample of star forming galaxies
  - 16 Starbursts "usual suspects" (Brandl et al. 2006)
  - 22 Star forming systems from SINGS (Smith et al. 2007)

The Spitzer/IRS 12μm Seyfert Sample

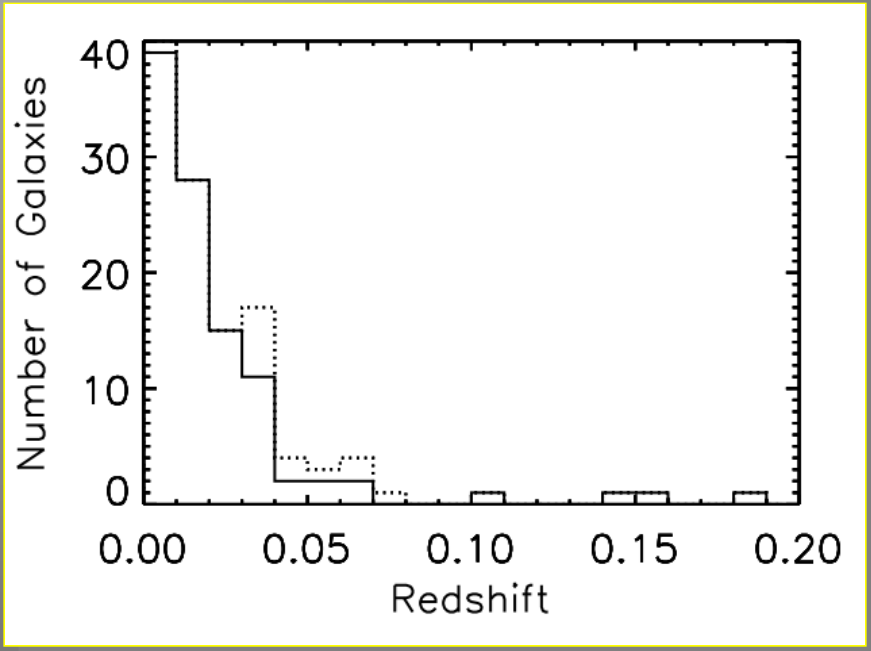

Mostly near-by ($z < 0.03$)
Mostly $L_{IR} \sim 10^{11} L_{sun}$

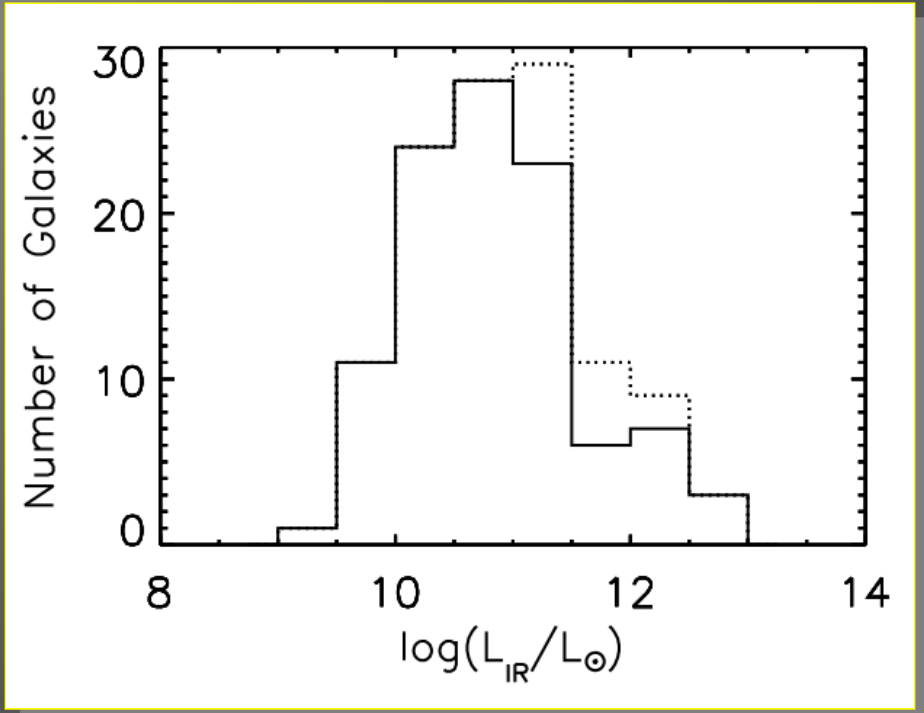

Observations

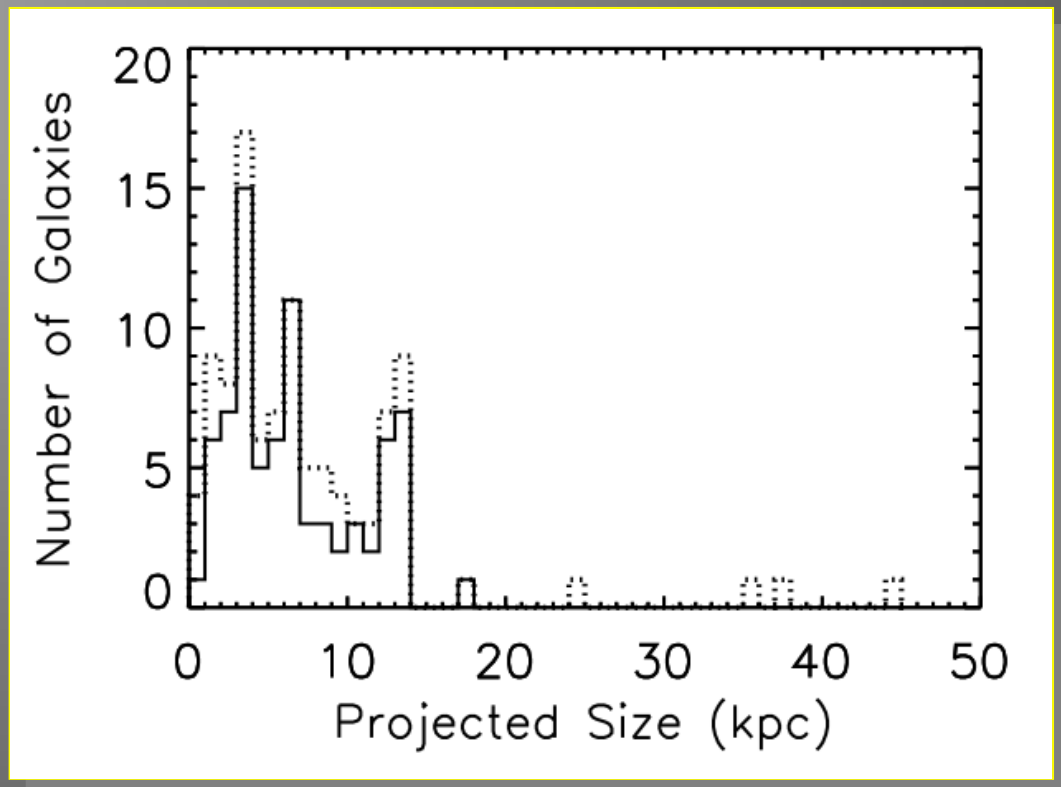

- Complete IRS low-resolution spectra 5-38μm (R~ 68-128) (Wu et al. 2009)
- Extraction over an aperture with size 20x15 arcsec to match all IRS slits
- 5-15μm properties were examined using aperture 4 times smaller

  Still we are not really talking about "nuclear spectra"
- High-resolution 10-35μm spectra also available (R~600)

  Tommasin et al . 2008 & 2009 (in preparation)

Typical mid-IR Spectra

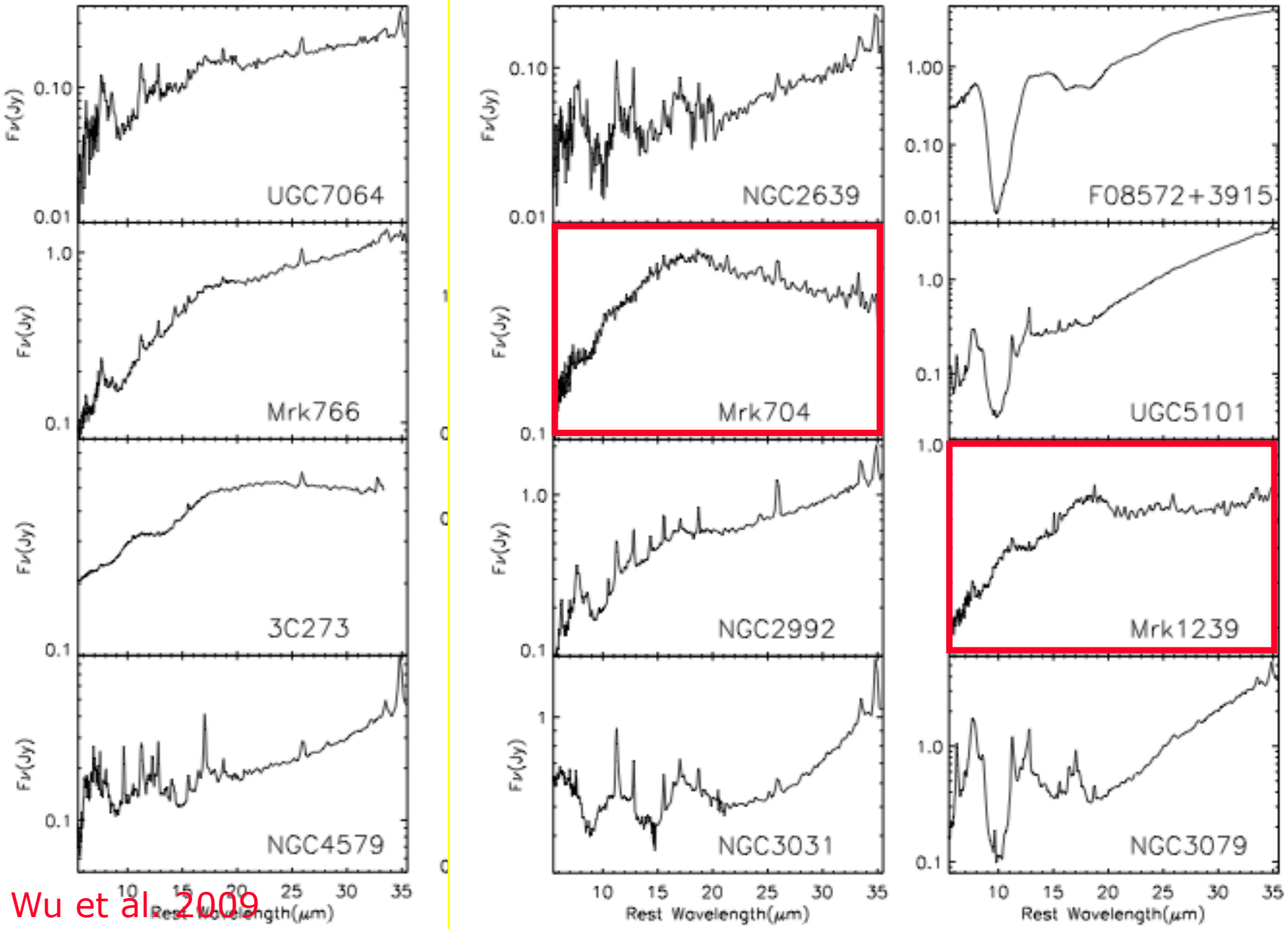

Wu et al. 2009

Average mid-IR Spectra

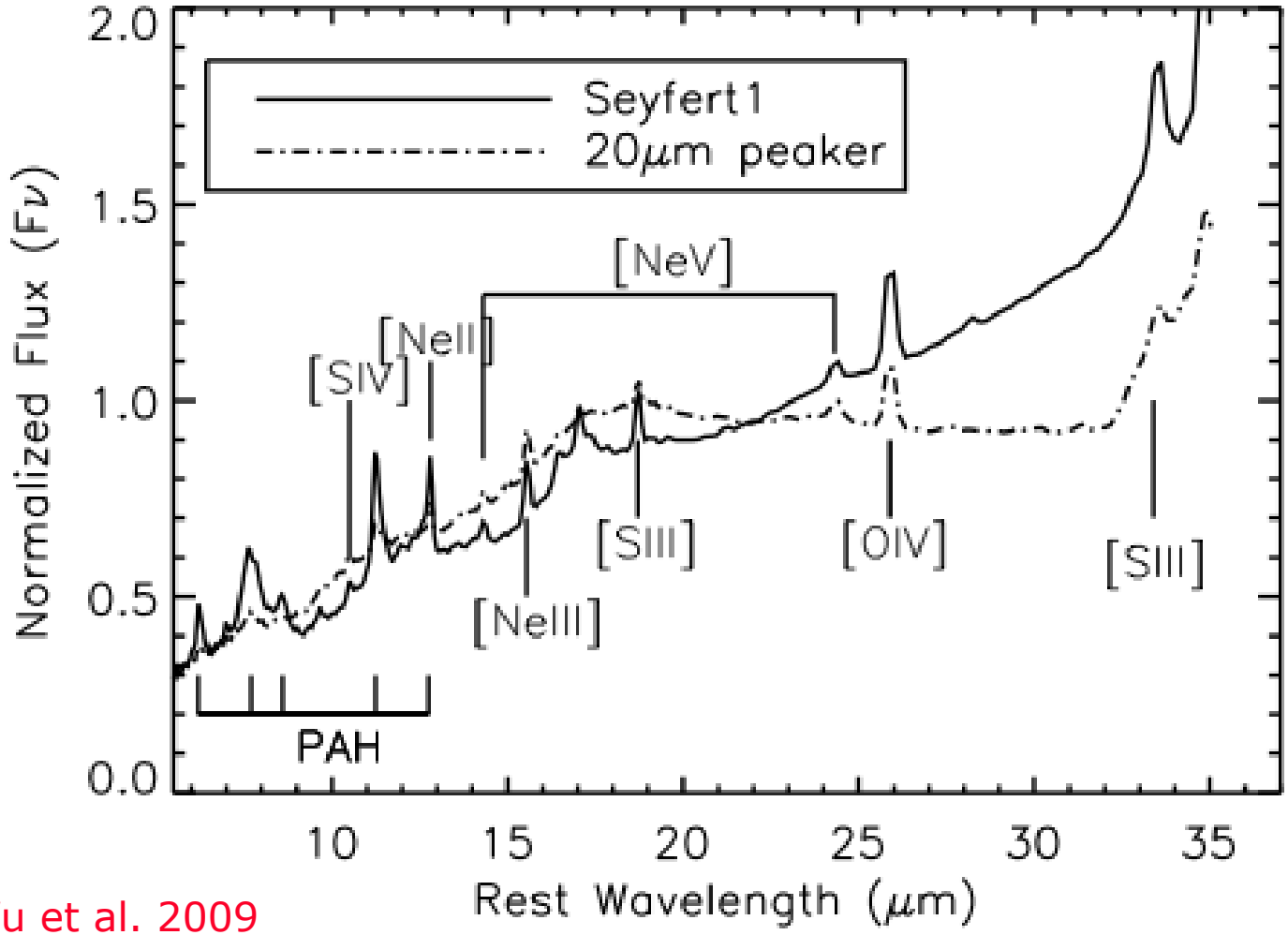

Wu et al. 2009

Average IR SEDs of all Seyferts

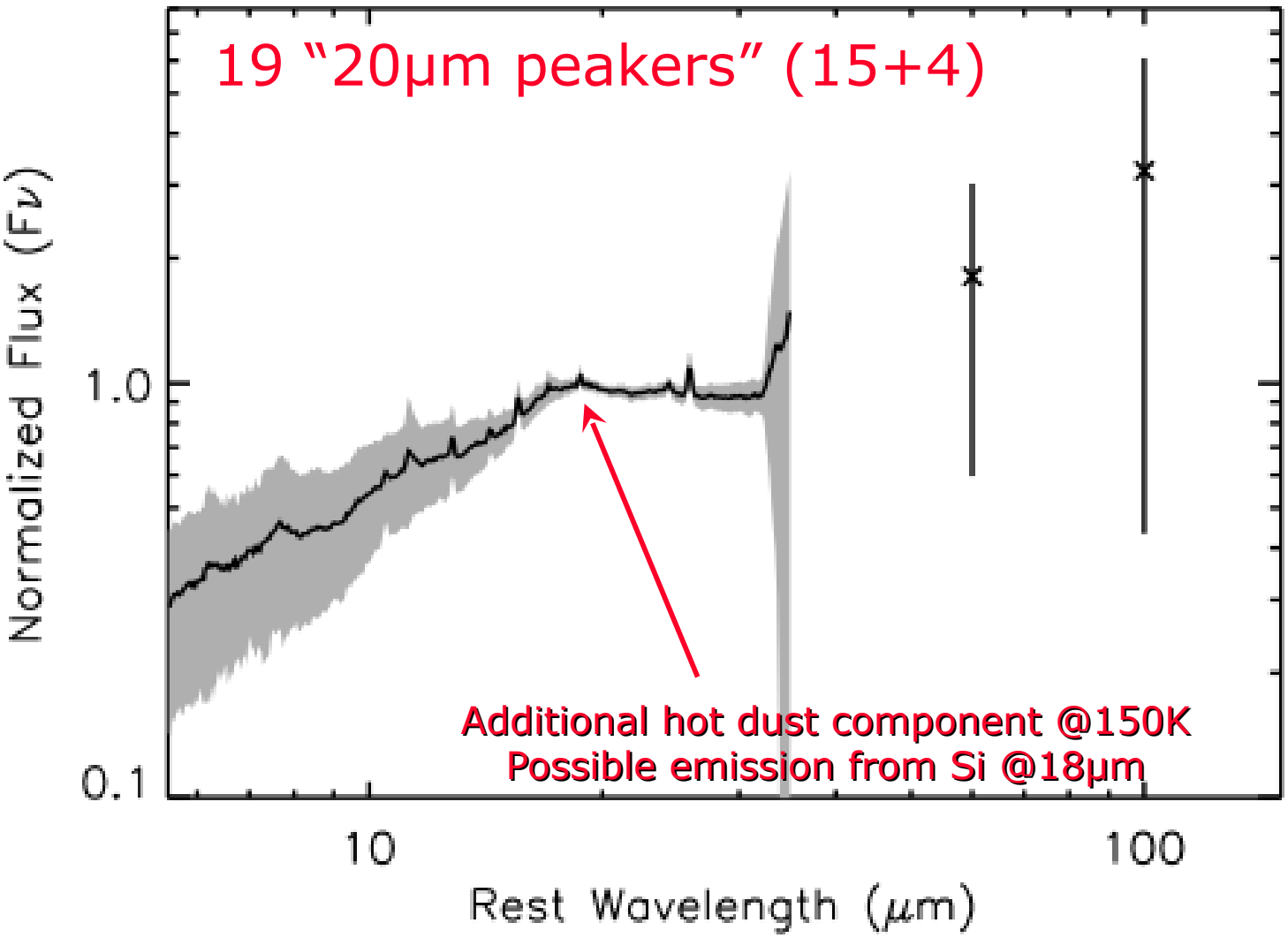

Wu et al. 2009

Average IR SEDs of all Seyferts

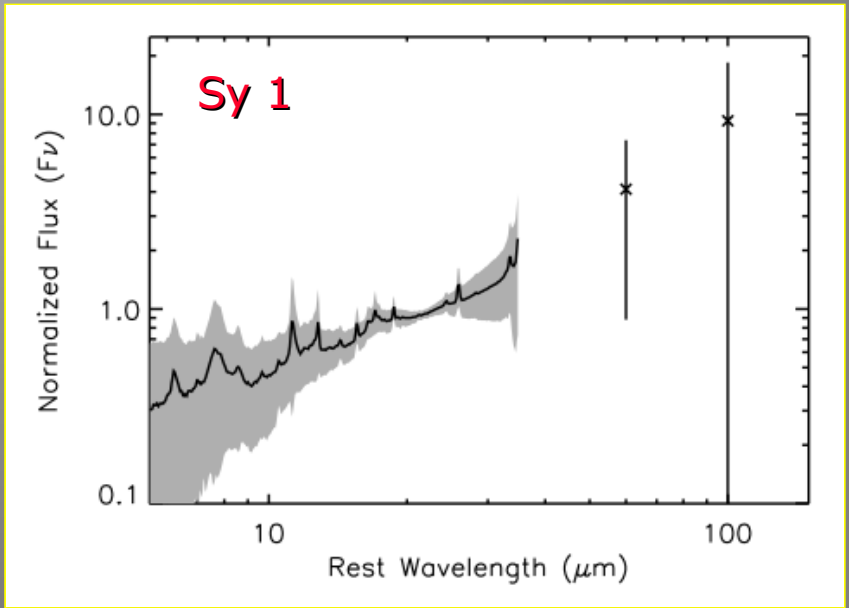

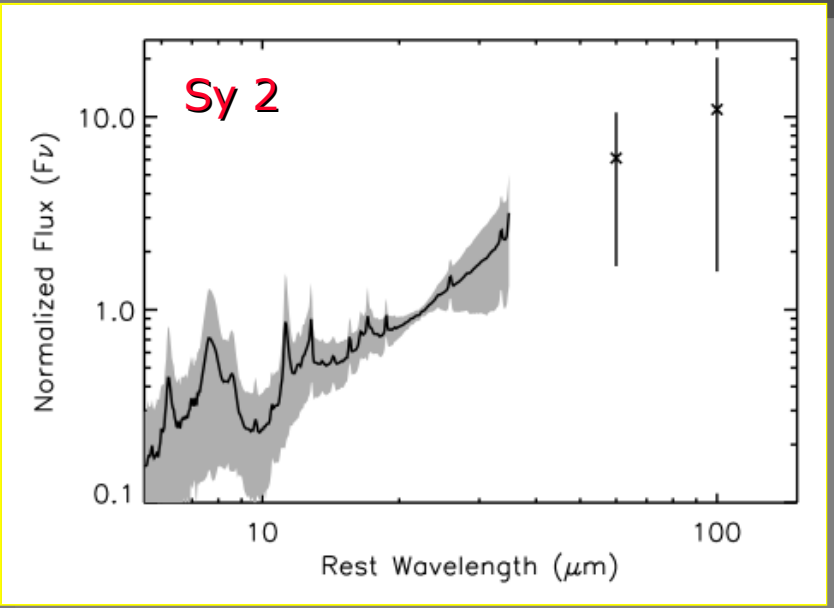

Slope α(15-30μm)

Sy 1: -0.85+/-0.61
Sy 2: -1.53+/-0.84
No real diference

F25/F60

Sy 1: 0.3
Sy 2: 0.1

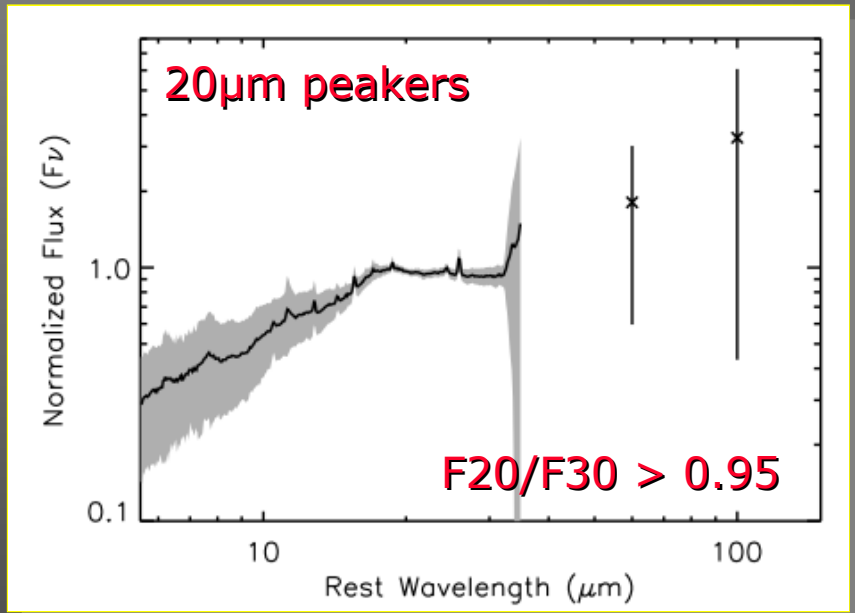

20μm peakers

32% of all Sy 1
9% of all Sy 2

F25/F60 ~ 0.75

PAHs Properties (1)

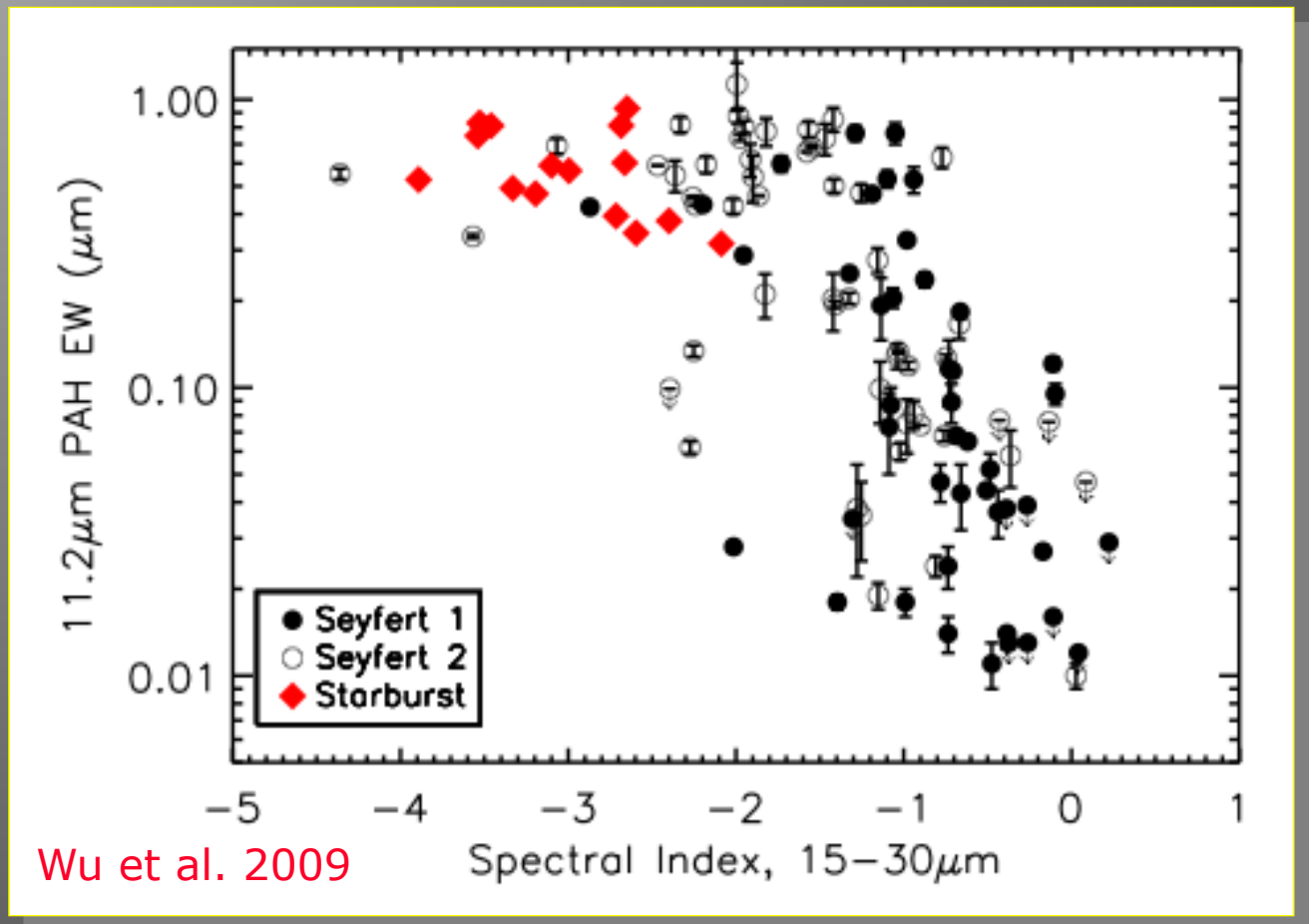

PAH 11.2μm EW decreases in both types as mid-IR f_ν slope increases

No difference is seen between Sy 1s and Sy 2s (contrary to Clavel et al 2000)

PAHs Properties (2)

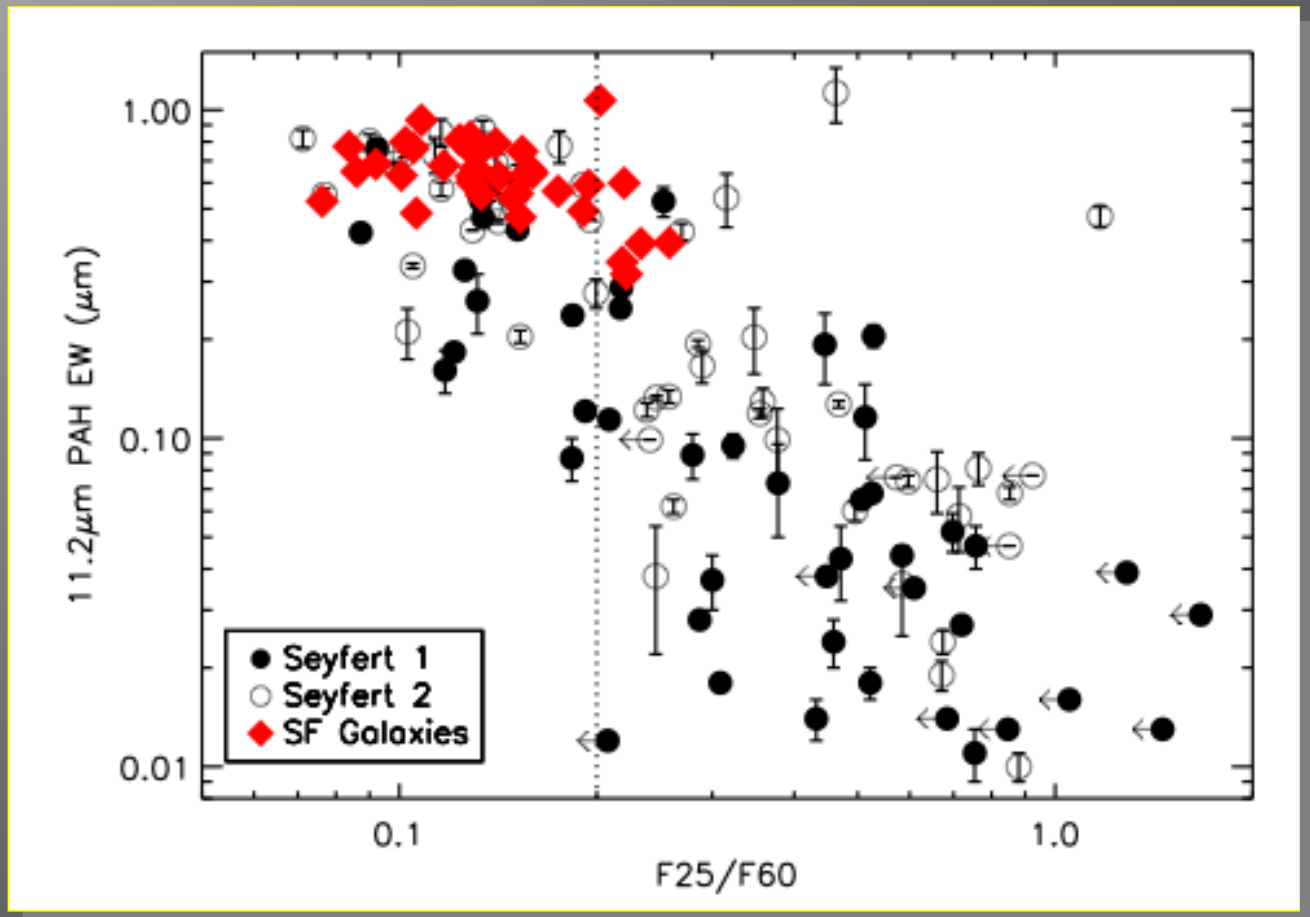

PAH 11.2μm EW decreases in warmer sources (as in ULIRGs Desai et al 2007)

No difference is seen in PAHs between Sy 1s and Sy 2s

Average EW: Sy 1s = 0.21 +/- 0.22μm , Sy 2s =0.38 +/- 0.30μm

PAHs Properties (3)

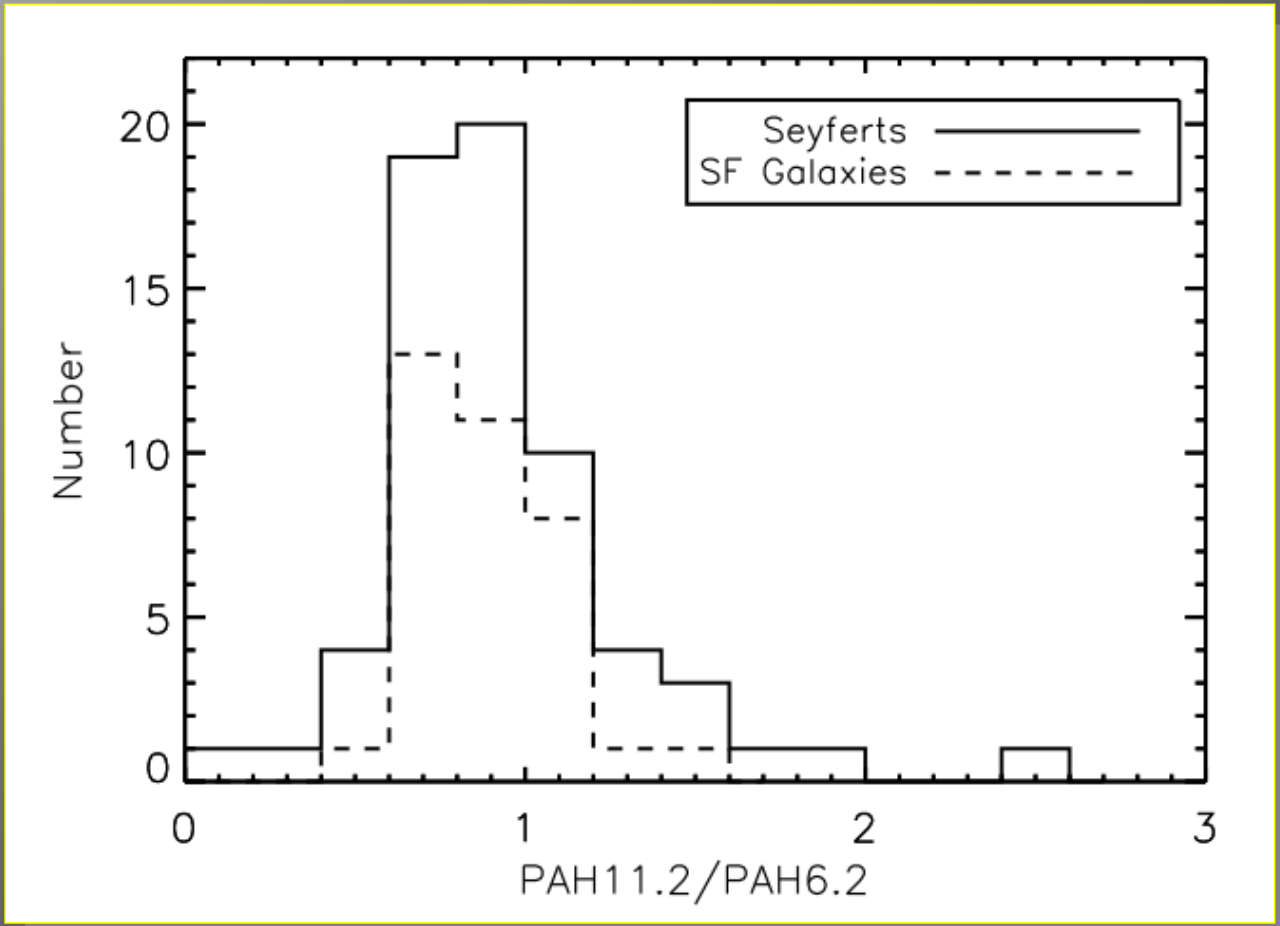

PAH @ 6.2μm C-C streching mode / PAH @ 11.2μm C-H out of plane mode
No difference in PAH flux ratios is seen between Seyferts and Starbursts
Chemistry remains the same over the volume sampled (~500pc scales)

PAHs Properties (4)

	Seyfert 1		Seyfert 2	
	EW(μm)	Sources	EW(μm)	Sources
Whole sample[a]	0.154±0.216	47	0.352±0.312	56
Whole sample[b]	0.205±0.215	37	0.384±0.299	52
$L_{IR}<10^{11}L_{\odot}$[a]	0.171±0.235	29	0.356±0.318	35
$L_{IR}\geq10^{11}L_{\odot}$[a]	0.127±0.184	18	0.345±0.310	21
$L_{IR}<10^{11}L_{\odot}$[b]	0.217±0.232	24	0.395±0.303	32
$L_{IR}\geq10^{11}L_{\odot}$[b]	0.185±0.188	13	0.367±0.300	20
F25/F60>0.2[a]	0.068±0.116	33	0.143±0.237	30
F25/F60≤0.2[a]	0.358±0.262	14	0.592±0.191	26
F25/F60>0.2[b]	0.102±0.119	24	0.177±0.237	26
F25/F60≤0.2[b]	0.397±0.227	13	0.592±0.191	26

[a]Values calculated including the upper limits on PAH EWs.

[b]Values calculated excluding the upper limits on PAH EWs.

The 11.2μm PAH EW does show marginal decrease for L(IR) >10^{11} Lsun but nothing as dramatic as in local ULIRGs (Desai et al. 2007)

Comparison with local ULIRGs

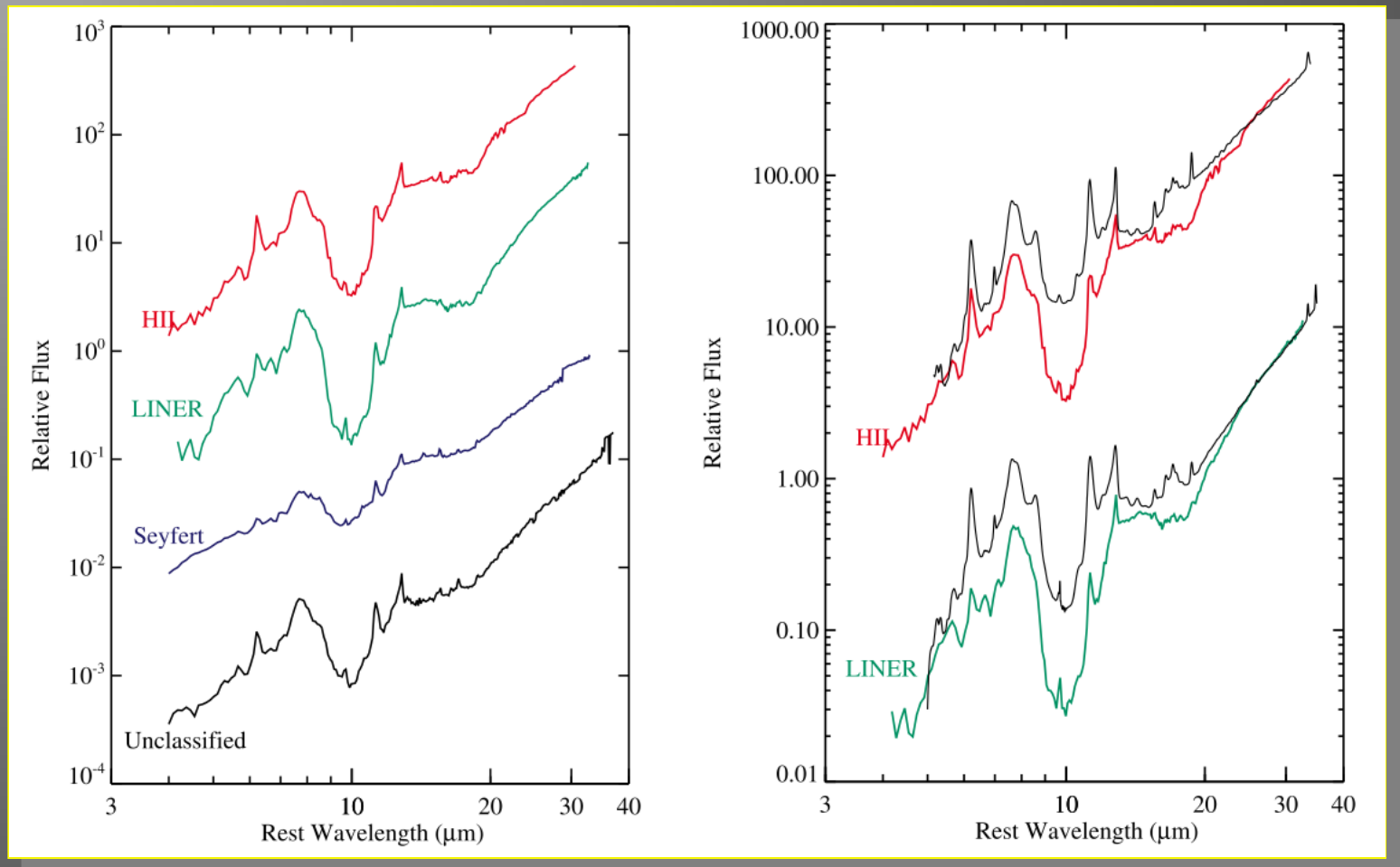

Based on 107 local ULIRGs (Armus et al. 2007, Desai et al. 2007)
The PAHs of starburst galaxies (HII) with L(IR) $>10^{12}$ Lsun do not scale

Comparison with local ULIRGs

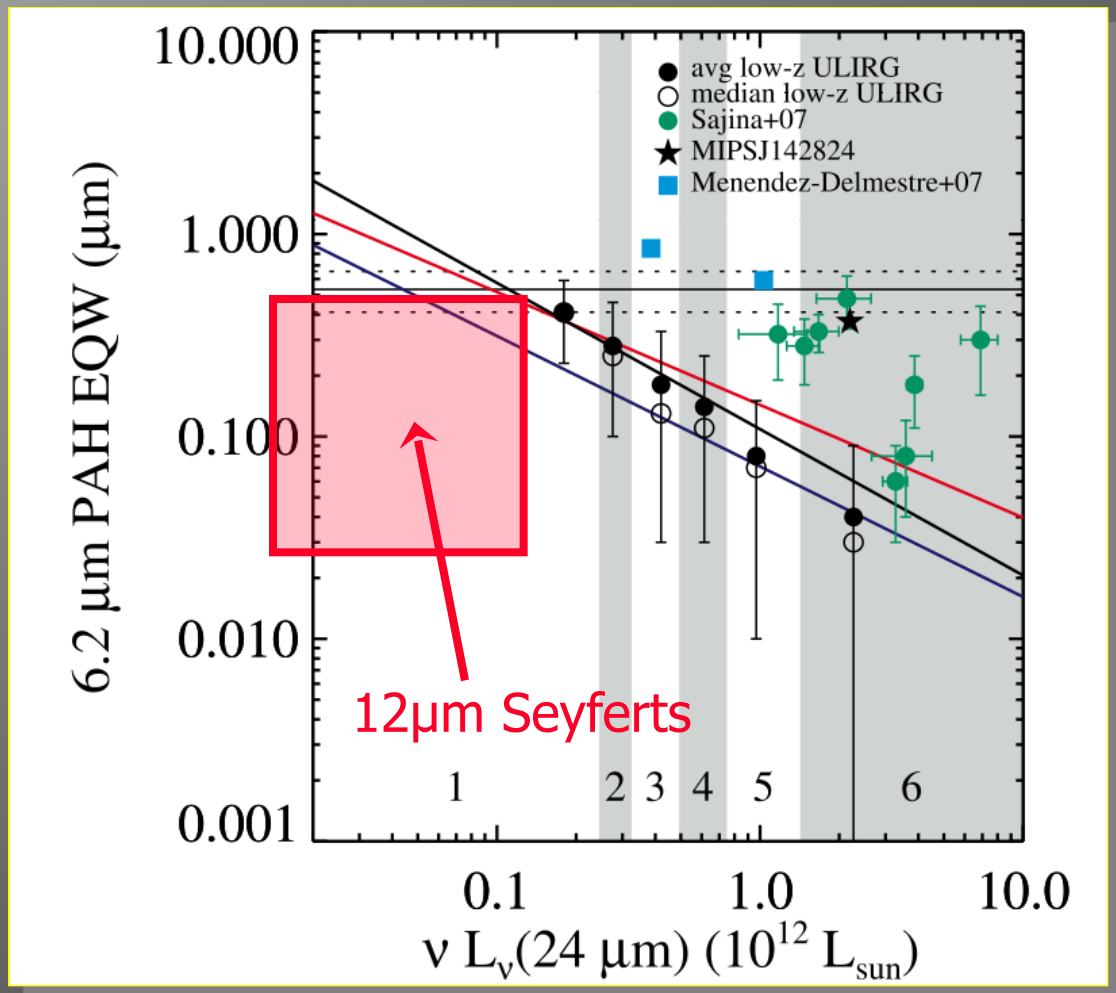

The PAH EW decreases with IR luminosity in ULIRGs (Desai et al. 2007)
The 12μm Seyferts display more scatter

What powers the 12μm Luminosity?

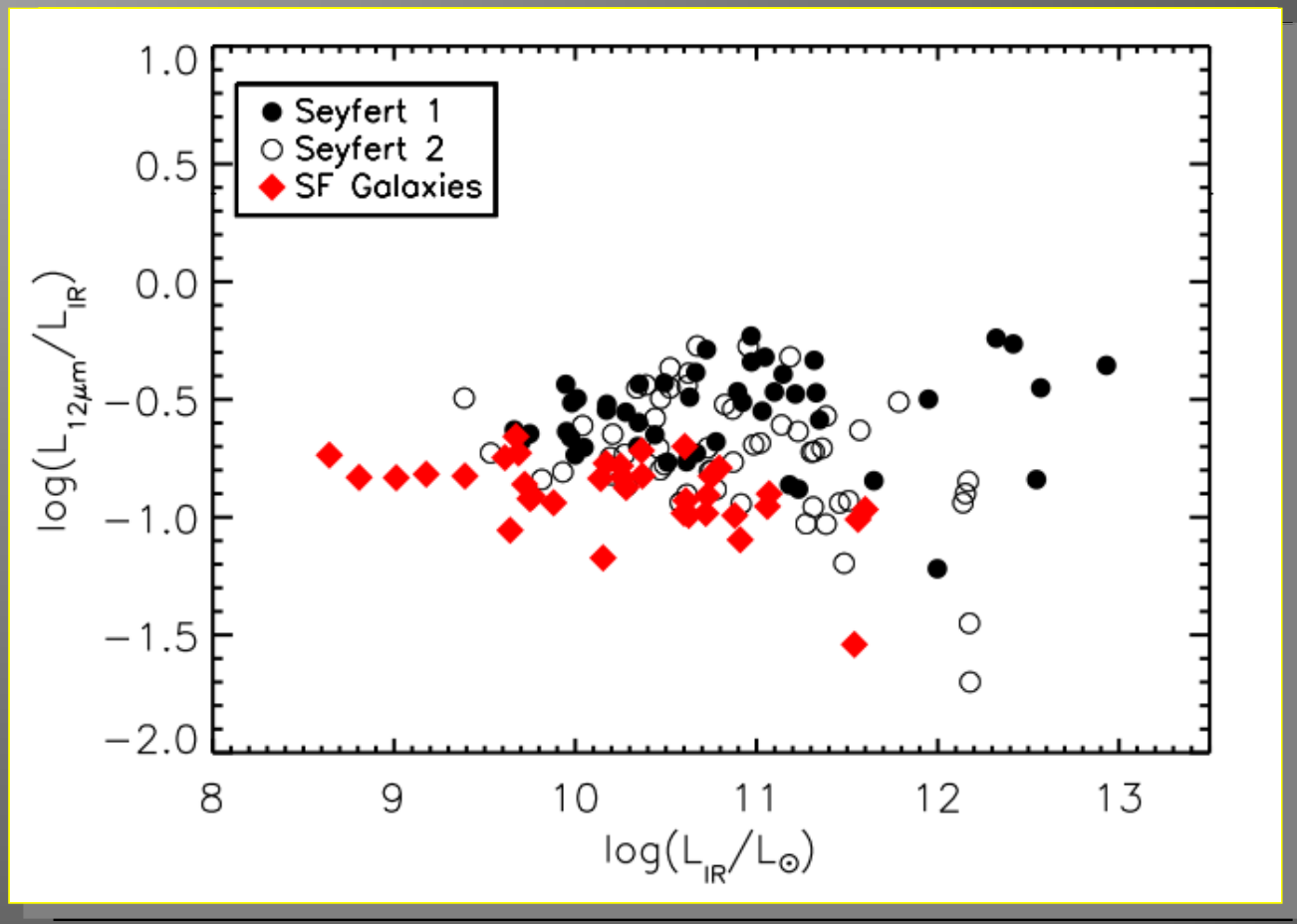

- AGN emission reveals its presence clearly at ~6μm (dust at ~800 K)
- Can it be seen and estimated at 12μm?
- At IRAS 12μm Seyferts contribute ~15% Lbol, compared to ~7% for starforming galaxies (Spinoglio et al. 1995)

The IRAS 12μm and PAH 11.2μm luminosities

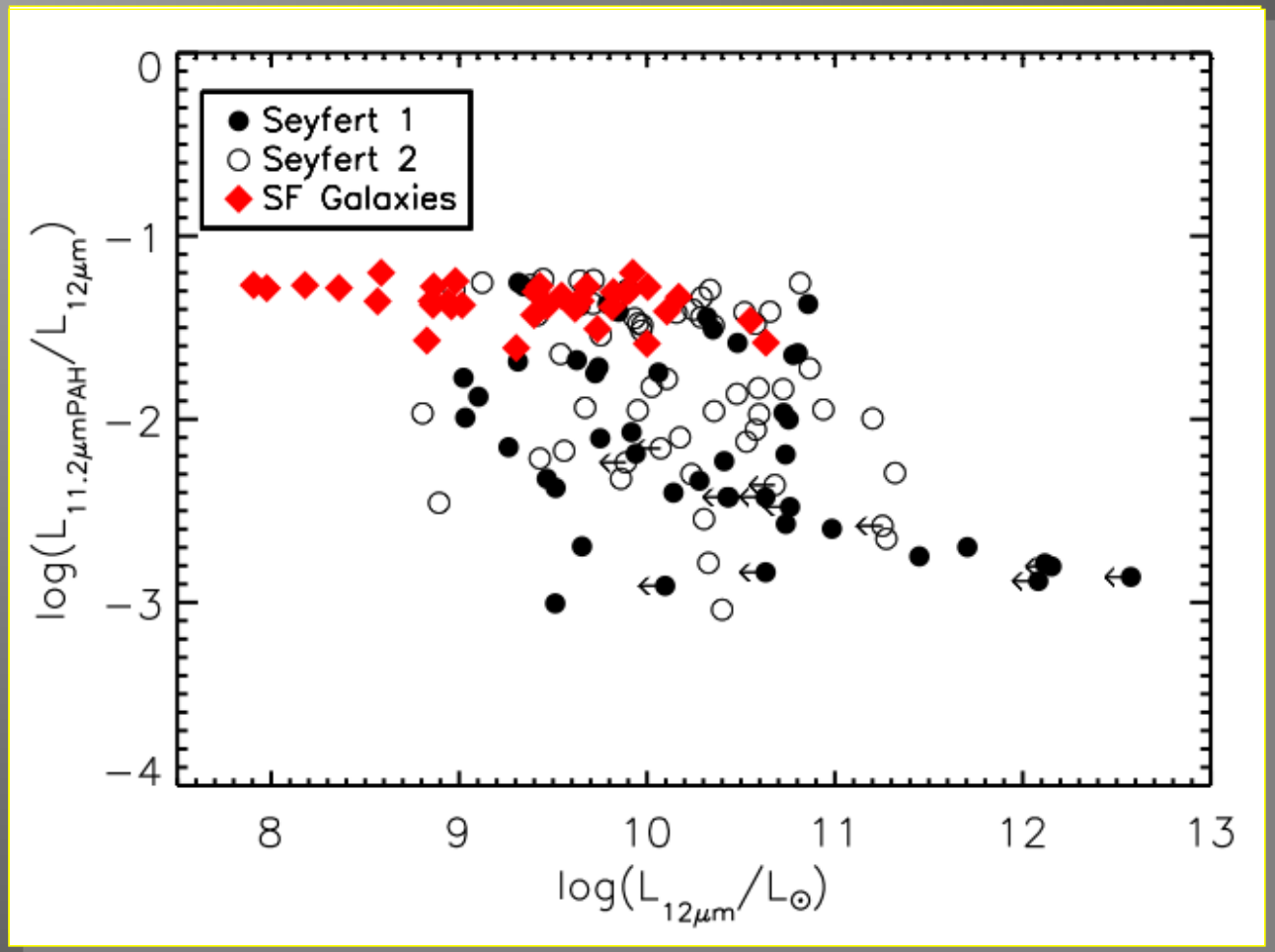

- In starbursts the 11.2μm PAH flux correlates with the IRAS 12μm continuum
- In Seyferts there is an extra contribution due to the AGN warm dust emission
- Can we quantify this in a statistical manner?

The 12μm "AGN fraction"

- Let's define as R the fraction of the mean 11.2μm PAH luminosity due to star formation (SF) to the 12μm luminosity

$$R = < L_{PAH\_SF} / L_{12\mu m\_SF} >$$

- Assuming that for every Seyfert the starburst contribution at 12μm scales with the 11.2μm flux then the total 12μm luminosity is

$$L_{12\mu m} = L_{SF} + L_{AGN} = (L_{PAH} / R) + L_{AGN}$$

- Consequently the AGN contribution ("AGN fraction") to the 12μm luminosity ($L_{12\mu m}$) is:

$$\text{"AGN fraction"} = (L_{12\mu m} - L_{SF}) / L_{12\mu m}$$

The 12μm "AGN" fraction (2): a sanity check

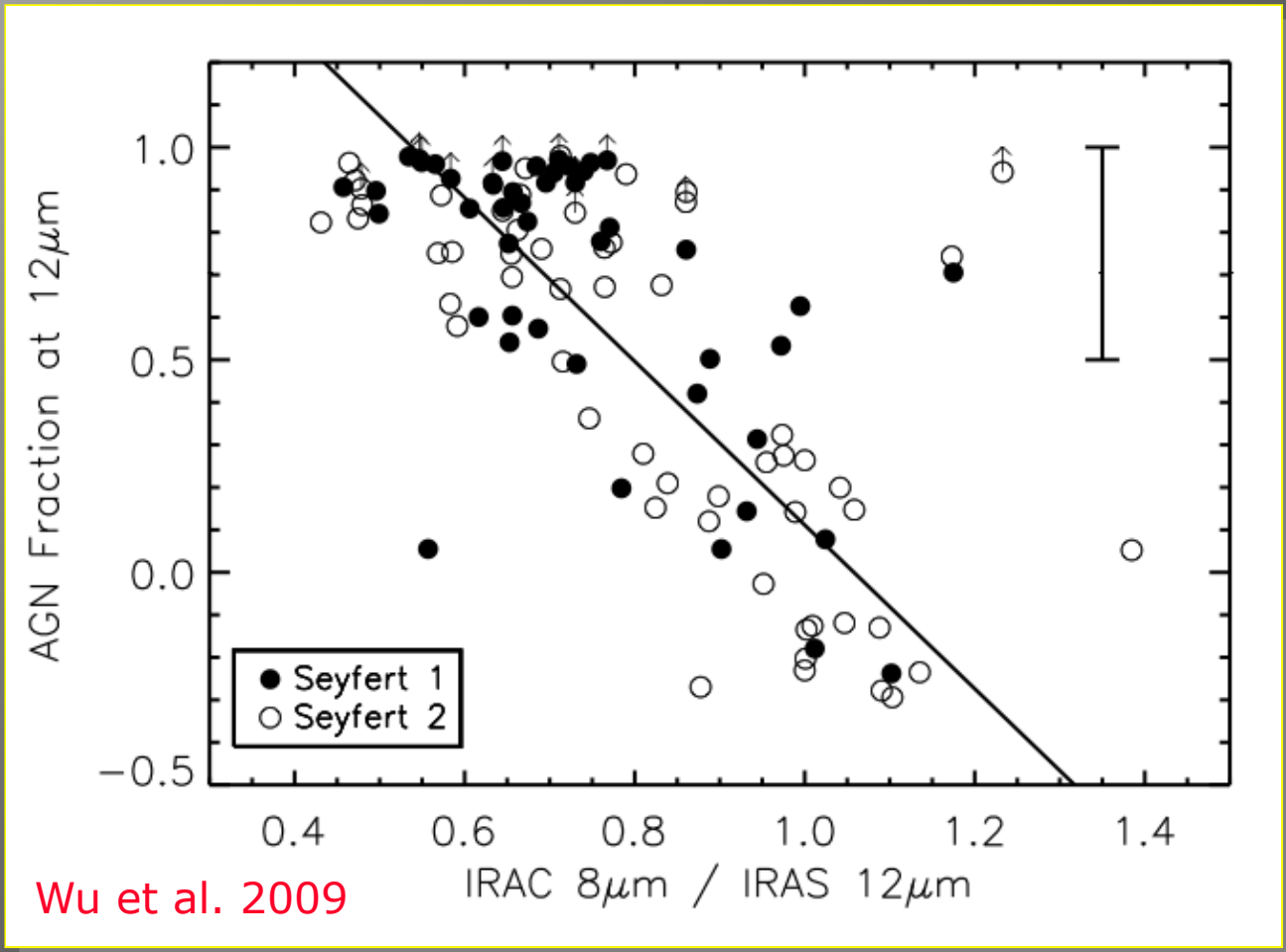

In starbursts the IRAC 8μm flux is dominated by the 7.7μm PAH (Smith et al. 2007)

Note that when the 7.7μm PAH contribution increases the AGN decreases as it should!

Conclusions

- The Infrared wavelength range has enabled us to develop a number of new tools to study the physics of the energy production in galaxies
- A number of superb facilities are in operation (Spitzer, Herschel, WISE) and more are planned (JWST/MIRI, Spica)
- The future is bright in the infrared

References

- Soifer et al. 2008, ARA&A, 46, 201
- Verma et al. 2005, Space Science Reviews, 119, 355
- Genzel et al. 1998, ApJ, 498, 579

IRS/NDWFS optically faint sources

31 optically faint sources with f_{24} > 0.75 mJy selected for IRS follow-up

(17 have R > 26 mag - no optical ID)

- *17 have redshifts measured with IRS (silicate and/or PAH)*
  16 with 1.7 < z < 2.8 (+/- 0.1-0.3 in z)
- *13 best fit with AGN-like templates (00183, Mrk 231)*
  4 best fit with SB-like templates (Arp 220, N7714)
- *16 have high q = log (f_{24} / f_{20cm}) > 0.8 (SB or radio quiet AGN)*
- *All have very large implied LIR: $1x10^{13} < L_{IR} < 5x10^{13} L_{\odot}$*

➢ MIR, optical selections bias initial IRS redshift survey in favor of dusty, warm, AGN-like ULIRGs with 1.6 < z < 3.

z < 1.6 ⇒ strong silicate reduces MIPS 24
z > 3 ⇒ silicate drop moves out of LL

IRS/NDWFS optically faint sources

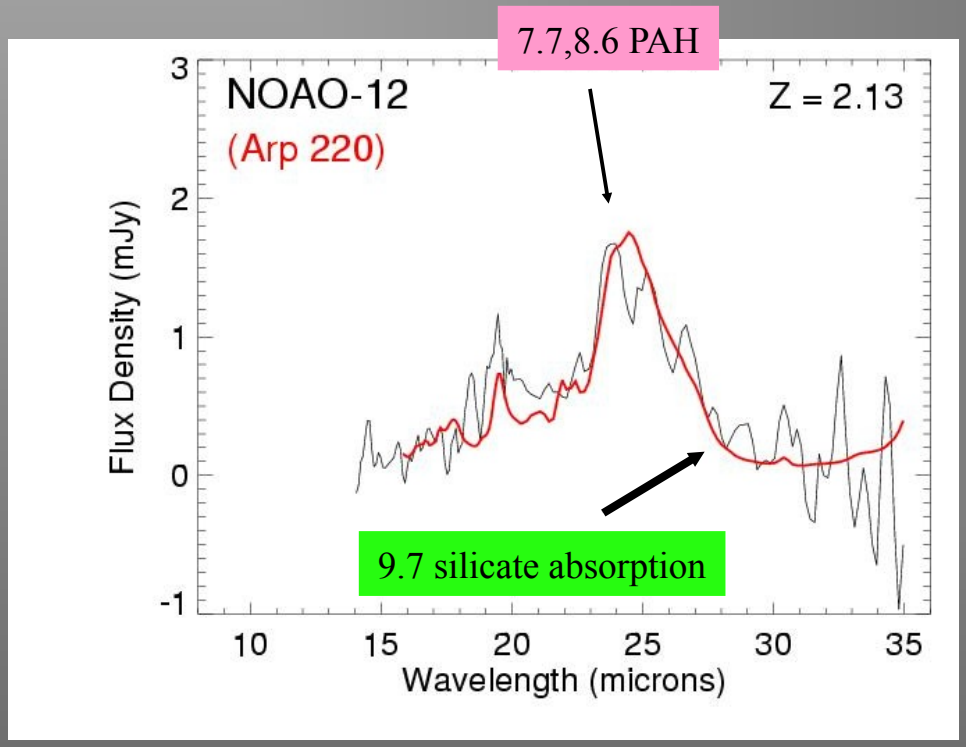

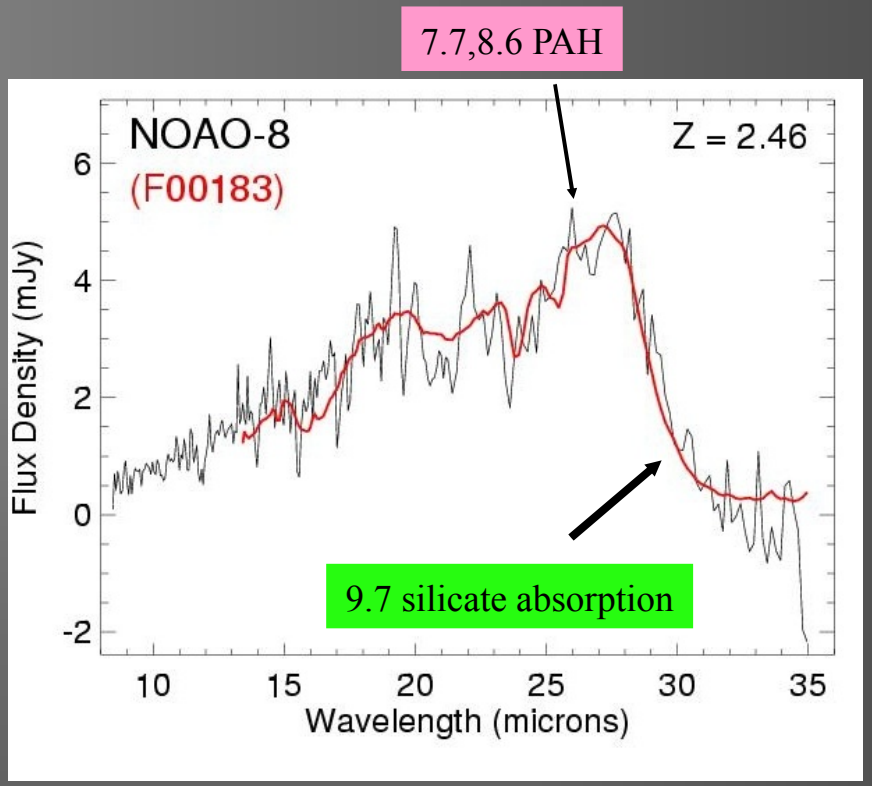

Houck, et al. (2005)

IRS ULIRG Summary

- *Composite (AGN+SB) spectra are common (Mrk 273, 05189, Mrk 1014, UGC 5101, etc.). There are a wide range of MIR spectra shapes among ULIRGs due to PAH emission, silicate and H_2O / hydrocarbon absorptions, and hot dust.*
  - Fitting number counts with 1-2 “templates” can be misleading.
- *Only 3/10 BGS sources have detectable [NeV]. Some (Arp 220, 14348 and 12112) are consistent with pure SB’s ([NeV]/[NeII] < 0.02-0.05). Arp 220 (low [NeV], low 6.2 PAH EQW, low 6.2 PAH/L_{IR}) may have both a heavily obscured SB and a buried AGN (*Spoon, et al. 2004; Iwasawa, et al. 2004*).*
  - The combination of fine structure line ratios, PAH strengths, and continuum fitting (hot dust) will provide an accurate assessment of the AGN/SB fraction. Comparison to HX data is critical.
- *High-luminosity ULIRGs tend to have smaller 6.2 PAH emission by 5-10x, and less silicate absorption, but there are obvious exceptions (e.g. 14537 and 00183). The high-luminosity ULIRGs are much more AGN-like in the MIR.*

Can the IRS Measure the Sub-mm Population ?

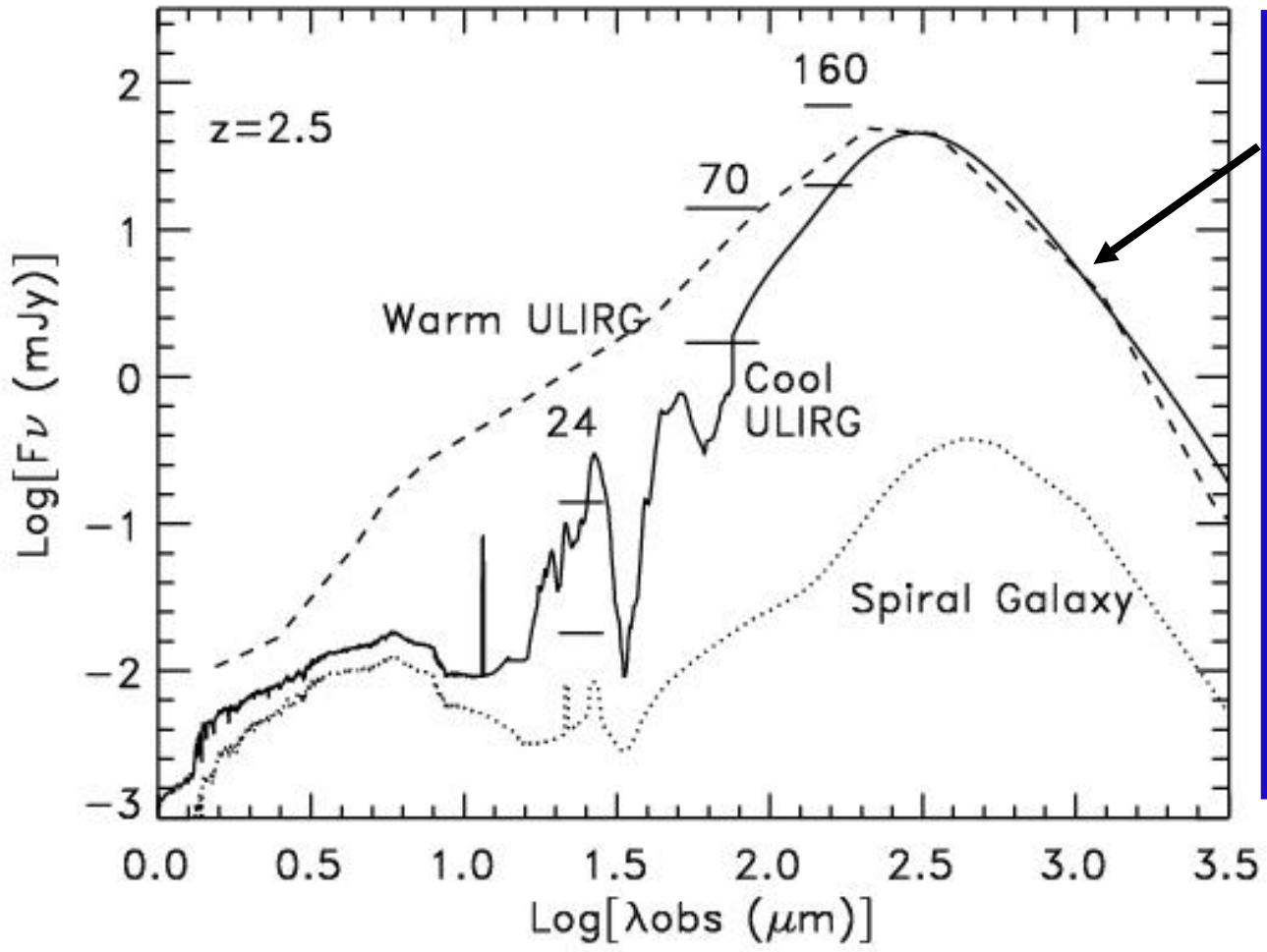

Normalized at 850μm to match bright SCUBA sample.

Cool source has L_{IR} ~ 5×10^{12} $L_{\odot}$ and S_{24} ~ 0.2-0.3 mJy

Would take ~4-5 hrs (per order) to get a 5σ detection with the IRS.

Courtesy of D. Frayer